

Bukti Korespondensi C-1

Nama Jurnal : Industrial & Engineering Chemistry Research
Volume : 61, 26, 9283-9299
No. ISSN : 0888-5885, 1520-5045
H-index : 231 (tahun 2021)
Impact Factor : 3,72 (tahun 2020)
SJR Index : 0,82 (tahun 2021)
Reputasi : Terindeks scopus, Q1 (tahun 2021)

Judul Artikel : Synthesis of Aminopropyl-Functionalized Mesoporous Silica Derived from Geothermal Silica for an Effective Slow-Release Urea Carrier

DOI : <https://doi.org/10.1021/acs.iecr.2c00424>

Riwayat Korespondensi

Item	Halaman
Submission of Original Manuscript (04 Februari 2022)	2-3
Original Manuscript	4-20
Revision Requested for Manuscript (11 Maret 2022)	21-23
Manuscript Formatting Request (11 Maret 2022)	24-25
Resubmission of the Revised Manuscript (28 April 2022)	26
Responses to Reviewer Comments	27-36
Revised Manuscript	37-53
Ready for Acceptance (25 Mei 2022)	54-55
Supplementary Journal Cover Invitation (25 Mei 2022)	56-57
Manuscript assigned to Editor (28 Mei 2022)	58-59
Resubmission of the Revised Manuscript 2 (28 Mei 2022)	60
Revised Manuscript 2	61-77
Decision on Manuscript (31 Mei 2022)	78

Submission of Original Manuscript (04 Februari 2022)

9/2/22, 11:52 AM

Department of Chemical Engineering, Diponegoro University Mail - Industrial & Engineering Chemistry Research - Manuscript...



Silviana Silviana <silviana@che.undip.ac.id>

Industrial & Engineering Chemistry Research - Manuscript ID ie-2022-004247

Industrial & Engineering Chemistry Research <onbehalfof@manuscriptcentral.com> Fri, Feb 4, 2022 at 8:08 PM

Reply-To: admin-journals@services.acs.org

To: silviana@che.undip.ac.id

Cc: eic@iecr.acs.org, silviana@che.undip.ac.id, atikahayujanitra@gmail.com, afr312000@gmail.com, dalanta@student.undip.ac.id

04-Feb-2022

Title: "Synthesis of aminopropyl-functionalized mesoporous silica derived from geothermal silica for effective slow-release urea carrier"

Authors: Silviana, S.; Janitra, Atikah; Sa'adah, Afriza; Dalanta, Febio

Manuscript ID: ie-2022-004247

Materials and Interfaces

Corresponding Author: Dr. S. Silviana

Corresponding Author's email: silviana@che.undip.ac.id

Manuscript Status: Submitted

Dear Dr. Silviana:

Your manuscript has been successfully submitted to Industrial & Engineering Chemistry Research.

Please reference the above manuscript ID in all future correspondence or when calling the office for questions. If there are any changes in your contact information, please log in to ACS Paragon Plus with your ACS ID at <http://acsparagonplus.acs.org/> and select "Edit Your Profile" to update that information.

You can view the status of your manuscript by checking your "Authoring Activity" tab on ACS Paragon Plus after logging in to <http://acsparagonplus.acs.org/>.

Journal Publishing Agreement and Copyright

Upon acceptance, ACS Publications will require the corresponding author to sign and submit a Journal Publishing Agreement. This agreement gives authors a number of rights regarding the use of their manuscripts. At acceptance, the corresponding author will receive an email linking through to the Journal Publishing Agreement Wizard, which helps you select the most appropriate license for your manuscript.

For more information please see:

https://pubs.acs.org/page/copyright/journals/jpa_faqs.html

ACS Authoring Services

Did you know that ACS provides authoring services to help scientists prepare their manuscripts and communicate their research more effectively? Trained chemists with field-specific expertise are available to edit your manuscript for grammar, spelling, and other language errors, and our figure services can help you increase the visual impact of your research.

Visit <https://authoringservices.acs.org> to see how we can help you! Please note that the use of these services does not guarantee that your manuscript will be accepted for publication.

Thank you for submitting your manuscript to Industrial & Engineering Chemistry Research.

Sincerely,

Industrial & Engineering Chemistry Research

PLEASE NOTE: This email message, including any attachments, contains confidential information related to peer review and is intended solely for the personal use of the recipient(s) named above. No part of this communication or any related attachments may be shared with or disclosed to any third party or organization without the explicit prior written consent of the journal Editor and ACS. If the reader of this message is not the intended recipient or is not

<https://mail.google.com/mail/u/0/?ik=ae189121fa&view=pt&search=all&permmsgid=msg-f%3A1723838066112508859&simpl=msg-f%3A1723838...> 1/2

9/2/22, 11:52 AM Department of Chemical Engineering, Diponegoro University Mail - Industrial & Engineering Chemistry Research - Manuscript...

responsible for delivering it to the intended recipient, you have received this communication in error. Please notify the sender immediately by e-mail, and delete the original message.

As an author or reviewer for ACS Publications, we may send you communications about related journals, topics or products and services from the American Chemical Society. Please email us at pubs-comms-unsub@acs.org if you do not want to receive these. Note, you will still receive updates about your manuscripts, reviews, or future invitations to review.

Thank you.

<https://mail.google.com/mail/u/0/?ik=ae189121fa&view=pt&search=all&permmsgid=msg-f%3A1723838066112508859&simpl=msg-f%3A1723838...> 2/2

Synthesis of aminopropyl-functionalized mesoporous silica derived from geothermal silica for effective slow-release urea carrier

S. Silviana*, Atikah A. Janitra, Afriza N. Sa'adah, Febio Dalanta

Department of Chemical Engineering, Faculty of Engineering, Diponegoro University, Tembalang, Semarang, 50275, Indonesia

Keywords: slow-release urea, mesoporous silica, aminopropyl-functionalized material, modified silica, urea.

ABSTRACT: Prominent slow-release urea was developed with aminopropyl-functionalized mesoporous silica to enhance urea adsorption and slow-release property. As novelty study, mesoporous silica was developed using treated geothermal silica as silica source, CTAB surfactant, and APTMS surface modification agent. The most desirable mesoporous silica with uniform micromorphology containing 38.55 %wt silica particles, 668.85 m²/g surface area, 149.33 – 353.28 mL/g adsorption-desorption range, 0.26 mL/g adsorption pore volume were achieved using 0.05 mole CTAB. Synthesized mesoporous silicas showed type-IV hysteresis, which corresponds to mesoporous material. DSC-TGA thermograms showed that mesoporous silica becomes more reactive with peaks at 82.3 °C and 159.5 °C, having good thermal stability, only experienced 17.61% weight loss until 124 °C. SEM showed functionalization and urea adsorption to mesoporous silica resulted in no significant microstructure changes. From FTIR spectra, MS/APTMS/U26.74 was observed to have higher C=O, N-H, C-N, C-H groups intensity among other samples. Cumulative urea release during seven days was 184.5 ppm for commercial urea and 124.6 ppm for MS/APTMS/U26.74. Higuchi kinetic model performed the best fit predicting MS/APTMS/U26.74 release kinetics with R² 0.9979 and Higuchi constant 24.4964 %day^{1/2}. Finally, synthesized MS/APTMS/U26.74 using geothermal silica, CTAB, APTMS can be noted as potential composition for slow-release urea to enhance efficiency.

INTRODUCTION

Nowadays, urea has been widely used as fertilizer ^{1,2}, source of nitrogen in ruminants ^{3,4}, pesticides ^{5,6}, microbial growth ^{7,8}, and various agriculture activities due to its rich nitrogen content, abundance, and cost-effectiveness. However, several studies reported that the high content of urea fertilizer is lost caused by leaching and ammonium volatilization upon application in soil, eventually generating severe environmental pollution, especially in soil and water sources ⁹⁻¹¹. Therefore, slow-release urea (SRU) development becomes a manner to improve urea efficiency, controllable usage and minimize the environmental drawbacks. Recently, SRUs are commonly prepared by encapsulating or adsorbing saturated urea solution to a porous matrix medium such as zeolites ¹²⁻¹⁴, porous polymer composites ¹⁵⁻¹⁷, or mesoporous materials ¹⁸⁻²³ in order to control the urea release. Several polymers have been performed for SRU matrix media, such as polyacrylonitrile ^{24,25}, polysulfone ⁹, poly (vinyl chloride) ²⁶, polyacrylic-rubber ²⁷, poly (vinyl acetate) ²⁸, and polyurethane ²⁹. However, those polymers generate additional environmental issues in terms of the remaining non-biodegradable polymer waste after they are used. Therefore, the application of biodegradable polymers has been carried out to solve the environmental issue of using conventional polymers on SRU. Natural polymers have been applied as the matrix medium for SRU, including cellulose ³⁰, chitosan ³¹, attapulgite ^{32,33}, algininate ^{34,35}, starch ³⁶, and lignin ²⁸. Nevertheless, due to their natural characteristics, those natural polymers are easily attacked by fungi, bacteria, and other microorganisms, causing a lack of performance. Therefore, further investigations to develop the prominent matrix material for enhancing SRU characteristics and

performance are still needed, and there remains big room to be studied.

Mesoporous silica (MS) has gained high attention caused by their potential in various utilizations, including drug delivery ³⁷⁻³⁹, catalysis ⁴⁰, adsorbent ⁴¹, sensing ⁴², and antibiotic-free antibacterial applications ⁴³. Due to the silica chemistry, MS has an ease to be functionalized and controllable tailoring, which allows it to be designed for the desired applications, including as the matrix medium for SRU. Many works have been conducted to synthesize MS with different structures, compositions, and pore properties to achieve desired and tunable characteristics ^{22,40,44,45}. Type of precursor, pH, reaction time, temperature, type and concentration of catalyst, co-solvent, and surfactant are the main influencers of the final properties of synthesized MS ^{37,40,42}. Several synthesis procedures have been reported in order to have tunable and controllable MS properties, generally conducted in acid and basic media ^{37,44,46}. On both conditions, the effect of reaction temperature, surfactant, co-solvent, and additives concentrations was observed, and numerous MS properties have been clearly explained ^{37,44,46}. The high specific surface area, high porosity, tunable network framework structure can enable the massive binding sites for urea in this matrix medium. However, it has also been reported that thickness, hydrophilicity, and layer structure of matrix medium strongly affect the release rate of SRU ^{27,29,31,46}. Consequently, to achieve the maintainable rate of urea from the slow-release urea, further modification and/or functionalization of the SRU matrix medium is highly required.

Aminopropyl-functionalized materials have gained high interest due to their strong absorption against several chemicals such as

amine, phosphate, and nitrate. The presence of an amine group on aminopropyl-functionalized silica, which has a similar amine functional group as urea, caused the crystallization of urea by hydrogen bonding with other amine groups. It acts as a seed to initiate crystallization of the urea network, thus enhancing the absorption of urea on the surface of an aminopropyl-functionalized silica^{23,47,48}. Various organometallic groups have been utilized to functionalize adsorption-based materials and enhance the capacity of adsorption and produce controllable kinetics^{49,50}. Currently, the most investigated aminopropyl-functionalized material is biochar or activated carbon. Nevertheless, those materials preferably have developed surface microstructures, but the micropores domination alters adsorbate diffusion into the pores generating a decrease in adsorption capacity. Compared to the biochar or activated carbon, MS has a high specific surface area, ordered pores, and relatively high pore volumes indicating a potential material for adsorbent with controllable diffusion behavior^{23,37}. Therefore, it was hypothesized that functionalization of MS for SRU matrix medium to enhance the performance of SRU in terms of high urea adsorption capacity and controllable diffusion of urea from the synthesized SRU to the soil.

In this study, the synthesis of SRU with MS as the matrix medium was prepared from geothermal silica. Geothermal silica can be applied as the silica source to synthesize MS due to its high content of SiO₂, which has been applied in numerous applications^{51–55}. The geothermal silica was purified using acid leaching treatment before it was used. The purified silica was converted to sodium silicate as the precursor of silica source in MS preparation. Cetyltrimethylammonium bromide (CTAB) was used as the surfactant, and the mole amounts of CTAB were varied to investigate the impacts on the synthesized MS properties. The synthesized MS was further functionalized by covalently grafting the aminopropyl groups on the MS surface using a 10% 3-Aminopropyl trimethoxy silane (APTMS) solution to enhance the sorption capacity and slow-release properties of the synthesized slow-release urea. The essentials analysis, including microstructures, chemical groups and compositions, surface area involving gas sorption, hysteresis behaviors, pore characteristics, and thermal properties, were comprehensively characterized using scanning electron microscopy (SEM), energy dispersive x-ray (EDX), x-ray fluorescence (XRF), x-ray diffraction (XRD), Fourier-transform infrared (FTIR), Brunauer-Emmet-Teller and Barrett-Joyner-Halenda (BET-BJH) analysis, thermogravimetric analysis (TGA), and differential scanning calorimetry (DSC). The synthesized slow-release urea was experimentally tested in the soil to investigate the release characteristics and its comparison to the commercial urea. The release kinetics of the synthesized slow-release urea were also studied by applying several appropriate kinetic models. As a novelty, the study of slow-release urea synthesis using aminopropyl-functionalized MS as the matrix derived from geothermal silica as the silica source and CTAB as the surfactant has not yet been reported in other previous studies.

MATERIALS AND METHODS

Materials

The geothermal silica sample as the primary raw material for mesoporous silica synthesis was supplied from the geothermal power plant of PT. Geo Dipa Energi, Dieng, Indonesia. Cetyltri-

thylammonium bromide (CTAB, 99–101%) and 3-Aminopropyl trimethoxy silane (APTMS, 99.8%) were purchased from Himedia and Sigma Aldrich, Germany, respectively. Sulfuric acid (H₂SO₄, 98%), sodium hydroxide (NaOH, 95%), and hydrochloric acid (HCl, 36.5–38%) that was used in purification treatments of geothermal silica were supplied from Mallinckrodt, USA. Ammonium hydroxide (NH₄OH, 25%) and ethanol (C₂H₅OH, 96%) utilized in the preparation were purchased from Merck, Germany. Commercial urea (Nitrogen ≥ 46%) was supplied from PT. Petrokimia Gresik, Indonesia. Distilled (DI) water was utilized in all experiments.

Methods

Purification treatments of geothermal silica samples

Geothermal silica contains contaminants. Therefore, it required purification treatment to produce high purity of silica as the primary material to synthesize mesoporous silica^{57–61}. There were two steps of purification treatments, i.e., acid leaching and sodium silicate process. Firstly, 250 g of geothermal silica sample was dried in an oven at 110 °C for 12 h to reduce its moisture content. Then, the dried sample was crushed into fine powder. This sample was then checked by X-ray Fluorescence (XRF, Thermo Fisher Scientific, USA) and X-ray Diffraction (XRD, Thermo Fisher Scientific, USA) instruments to reveal its chemical composition and the amorphous structure. Next, acid leaching treatment was conducted based on the methods recently reported^{57,58}. Such amounts of 125 g of treated geothermal silica were carefully dispersed and constantly mixed in 500 mL of 20% H₂SO₄ solution at 100 °C for 105 min. The acid processing by H₂SO₄ is intended to remove the residual impurities on the sample, specifically the metal oxides content. After that, repeated washing and rinsing were done to the residue to remove any unspent acid until achieving a neutral pH. The residue was then placed in an oven at a temperature of 110 °C until completely dried. The treated silica from this step was analyzed using XRF and XRD.

The second purification step was the sodium silicate process to further purify the treated silica. This procedure was conducted based on the method previously reported^{54,58}. It was started by mixing 125 g of treated silica sample with 600 mL of 4 M NaOH solution and was stirred and maintained at 90 °C for 60 min. After that, the mixture was filtered through a filter paper (Whatman No.42) using a vacuum filter. The generated filtrate was sodium silicate that was further applied as the precursor to synthesize mesoporous silica.

Synthesis of mesoporous silica

This step followed the modified Stöber method that was previously reported^{58–60}. Firstly, the primary solution was made of 10 moles of ethanol, 22.4 moles of water, and 5.2 moles of NH₄OH. The solution was constantly mixed at low speed (80–100 rpm) for 15 min. After that, CTAB as a surfactant was slowly added into the solution with variations of 0.015, 0.03, and 0.05 moles. Sodium silicate was prepared by dissolving 10 g treated silica in 82.5 mL of NaOH 4 M. Next, 100 mL of prepared sodium silicate solution was slowly added to the solution. The solution turned opaque immediately, indicating the reaction has started. The solution was continuously mixed and maintained for 2h at room condition. After that, the solution was filtered to separate the solids as the generated mesoporous silica from the mixture through a filter paper (Whatman No. 42) using a vacuum filter. Subsequently, the solids were washed to remove any unspent solution. The solid was then calcined using a furnace

burner at 550 °C to remove the remaining organic compounds, creating mesoporous structure throughout the surface of the silica. The prepared mesoporous silica was characterized using a Scanning Electron Microscopy Energy Dispersive X-ray (Thermo Fisher Scientific, USA), Brunauer-Emmet-Teller Barrett-Joyner-Halenda (BET-BJH) (autosorb IQ Quantachrome Instruments from Anton Paar Switzerland AG), Thermal Analysis of TG/DTA/DSC (Linseis STA 1600 Premium Series, USA), and Fourier Transform Infrared (IRPrestige21, Shimadzu Japan by transmittance mode of acquisition).

Purification treatments of geothermal silica samples

This procedure was based on previously reported studies^{48,49}. In this method, APTMS was utilized as a silane coupling agent to modify the surface characteristic of mesoporous silica. Firstly, calcined mesoporous silica was carefully mixed at 150 rpm with 10% APTMS

solution at room temperature for 8 h. This step was conducted to perform the surface modification reaction on the surface of mesoporous silica for a slow-release urea. It was then dried in an atmospheric pressure drying at 40 °C. Finally, the modified mesoporous silica with APTMS was characterized using BET-BJH analysis and FTIR.

Next, a gram of modified mesoporous silica/APTMS was added to the urea solution (U) with certain concentrations (6.74, 16.74, 26.74, and 36.74 %-wt) on the basis of 100 ml aquadest. The mesoporous silica/APTMS with different urea compositions is represented in Table 1. The mixture was constantly stirred for 24 h at room temperature to perform the adsorption of urea into the mesoporous silica by hydrogen bonding³⁷. Afterward, it was filtered, and the solids were dried in an oven with a temperature of 40 °C. Finally, the generated solids were characterized using FTIR.

Table 1. Contents of CTAB, APTMS, and Urea in Preparation of the Slow-release Urea

Sample code	CTAB (mole)	APTMS solution (%)	Urea solution (%-wt)
MS	0.05	0	0
MS/APTMS	0.05	10	0
MS/APTMS/U6.74	0.05	10	6.74
MS/APTMS/U16.74	0.05	10	16.74
MS/APTMS/U26.74	0.05	10	26.74
MS/APTMS/U36.74	0.05	10	36.74

Performance test of the prepared slow-release urea

The slow-release urea performance was experimentally assessed by measuring the value of urea carried out in overflow liquid. The test was applied for determining the dissolved urea content in groundwater. Figure 1. depicts the schematic illustration of the respective experiment. Initially, a gram of slow-release urea was immersed in 25 g of soil in a plastic vase. Subsequently, 25 mL of DI water was used for watering the sample every day for seven days of observation and the overflow water from the vase was carefully collected. This test was repeated for three replications. The urea content in the overflow liquid was measured using a UV-vis spectrophotometer (Thermo Scientific™ GENESYS 10S, USA). The measurement was performed at an optimum wavelength of 195 nm, while this wavelength closed to previous research i.e., 190 nm⁵¹.



Figure 1. Schematic illustration of the apparatus for slow-release urea performance test.

Study of urea release kinetics

The mechanism of urea release from the slow-release urea was theoretically evaluated by applying some kinetic models, which were pseudo-first order, pseudo-second order, Higuchi, and Hixson-Crowell models. The mathematical expressions of the pseudo-first order, pseudo-second order, Higuchi, and Hixson-Crowell are represented by Eq. (1)-(4).

Pseudo-first order model⁶²:

$$\ln Q_t = \ln Q_0 - k_1 t \quad (1)$$

Pseudo-second order model⁶³:

$$\frac{t}{Q_t} = \frac{1}{k_2 Q_0^2} + \frac{t}{Q_0} \quad (2)$$

Higuchi model⁶⁴:

$$Q_t = K_H t^{1/2} \quad (3)$$

Hixson-Crowell model⁶²:

$$Q_0^{1/3} - Q_t^{1/3} = K_{HC} t \quad (4)$$

Where Q_t is the released amount of urea at a certain time (%), Q_0 is the initial amount of urea in the slow-release urea (%), k_1 is the pseudo-first order rate constant, k_2 is the pseudo-second order rate constant, K_H is the Higuchi constant, K_{HC} is the Hixson-Crowell constant, and t is time (day).

RESULTS AND DISCUSSION

Properties of purified silica after acid leaching treatment

The sample of geothermal silica was treated using acid leaching treatment to remove the impurities, especially the metal oxides. Figure 2(a), depicts the XRF results of geothermal silica and the purified silica after acid leaching. The chemical composition of geothermal silica was found that consist of 86.3 %-wt of SiO_2 , with fairly high metal oxides including CaO, Fe_2O_3 , Cr_2O_3 , K_2O , and MnO with compositions of 3.21, 3.59, 0.07, 5.67, and 0.09 %-wt, respectively. This sample of geothermal silica was treated in 500 mL of 20% H_2SO_4 solution at 100 °C for 105 min to dissolve the metal oxides into the sulfuric acid. The XRF analysis of silica product after acid leaching revealed that the sample consists of 95 %-wt of SiO_2 and leaving the minor amount of metal oxides such as CaO, Cr_2O_3 , K_2O , and MnO with compositions of 0.43, 0.42, 0.22, and 2.00 %-wt, respectively. Based on this analysis, the acid leaching process significantly removed the metal oxides from the geothermal silica resulting in a higher purity of silica. The influence of acid leaching treatment is further evaluated by XRD analysis.

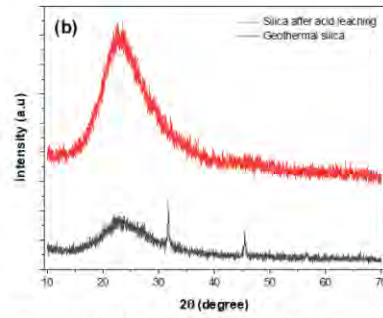
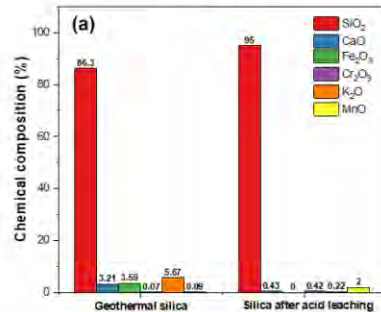


Figure 2. (a) XRF results of geothermal silica sample and purified silica after acid leaching process, and (b) XRD diffractograms of geothermal silica and purified silica after acid leaching.

Figure 2(b), represents the XRD diffractograms of geothermal silica and the purified silica after acid leaching. From the diffractogram pattern of geothermal silica, it can be seen a broad peak ranging from 2θ of $15^\circ - 30^\circ$, indicating the existence of amorphous SiO_2 . Three significant sharp peaks were found at 32.5° , 46.3° , and 49.8° , which correspond to Fe_2O_3 , K_2O , and Cr_2O_3 in the sample³⁷. The purified silica after acid leaching was also evaluated by XRD analysis. It can be clearly observed that the purified silica has a more significant broad peak at 2θ of $15^\circ - 30^\circ$, which indicates a higher amount of amorphous SiO_2 than the geothermal silica sample. Also, there are no other metal oxides peaks appearing in the diffractogram of the purified silica. Therefore, it can be reasonably concluded that the acid leaching treatment successfully removed the metal oxides content in the geothermal silica. Silica with higher purity ($\geq 95\%$) can be utilized as the main material for synthesizing mesoporous silica with higher Si content on its surface where surface modifying agents can react to.

Characterizations of synthesized mesoporous silica

Surface micrographs and chemical composition of synthesized mesoporous silica

In this study, the modified Stöber method was adapted in the synthesis of mesoporous silica. The reaction was conducted at room temperature using CTAB as a surfactant, aqueous NH_4OH as a catalyst, ethanol as a co-solvent, sodium silicate derived from geothermal silica as the silica source. For the different formulations of material synthesis, the amount of NH_4OH , ethanol, and sodium silicate were maintained fixed, while the amount of CTAB was varied at 0.015, 0.03, and 0.05 mole. Hence, the effects of CTAB mole amount in mesoporous silica synthesis were experimentally investigated. It was found that the different amount of CTAB as a surfactant in mesoporous silica synthesis has a significant effect on the micromorphology of the synthesized mesoporous silica, as clearly revealed by SEM-EDX analysis in Figure 3. with 10.000x and 20.000x magnifications. Figure 3(a), 3(b), and 3(c) depict the surface morphology images of mesoporous silica with 0.015, 0.03, and 0.05 mole of CTAB, respectively.

The different mole amounts of CTAB resulted in the different shapes of mesoporous silica particles. In using CTAB 0.015 mole (Figure 3(a).), the synthesized mesoporous silica has a randomized shape and is fairly similar to CTAB 0.03 mole (Figure 3(b).) and has a little development of the mesoporous silica particle. Meanwhile, in using CTAB 0.05 mole, the synthesized mesoporous silica has a

more uniform particle shape. These findings suggest that the addition of CTAB tends to produce mesoporous silica particles. This phenomenon agrees with the previous study that an increasing

amount of surfactant produces the abundant interaction of two-counter charge surfactant resulting in the growing silicates particle

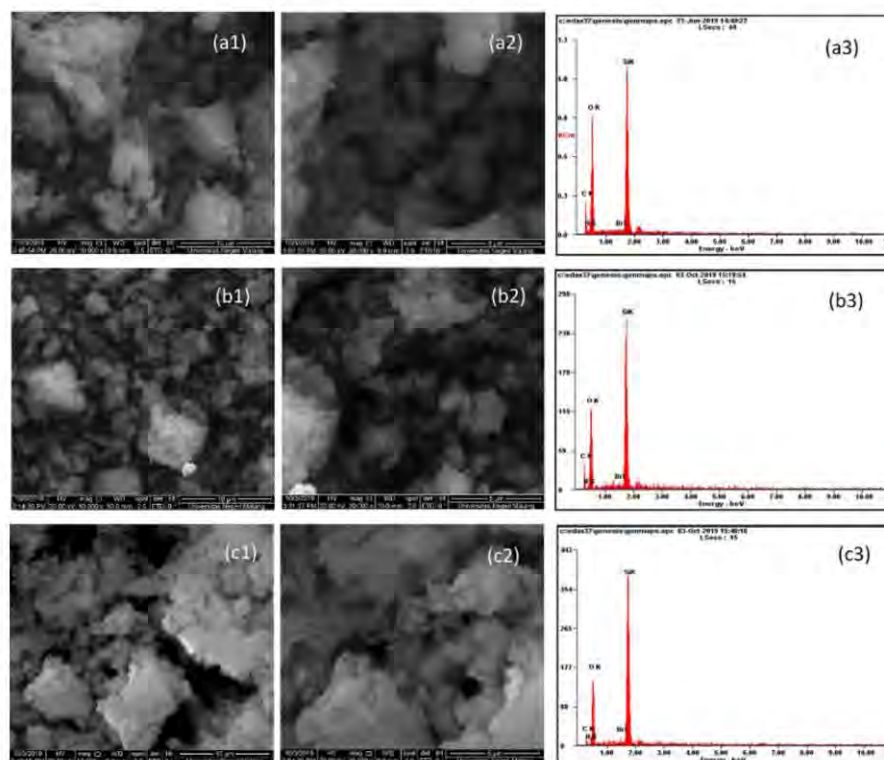


Figure 3. SEM-EDX micrographs of modified mesoporous silica using (a) 0.015 mole of CTAB, (b) 0.03 mole of CTAB, and (c) 0.05 mole of CTAB.

For further analysis, SEM-EDX analysis was carried out to reveal the chemical composition of synthesized mesoporous silica with different loaded amounts of CTAB. Figure 3. shows the EDX spectra for synthesized mesoporous silica with CTAB of 0.015 mole (Figure 3(a3).), 0.03 mole (Figure 3(b3).), and 0.05 mole (Figure 3(c3).). The quantification of EDX results is shown in Table 2, providing information about the chemical composition of the tested samples. Synthesized mesoporous silica with 0.015 mole, 0.03 mole, and 0.05 mole was recorded, consisting of 20.11, 23.70, and 35.88 %-wt of Si, respectively. The micrograph analysis resulted in the mesoporous silica from 0.05 mole CTAB visualized in white solid. According to previous research⁴⁵, CTAB surfactant can interact polarly with silica precursor. It can be observed that the hydrophilic head of CTAB can attach on the surface of silica, while the tail can be oriented to the polymer matrix. The phenomena of this interaction can be guessed by interaction between OH- ion on the silica surface and N⁺ ion of the CTAB; also a strong repulsion force between ion Si⁺ and N⁺ due

to Si⁺ ion having high positive charge ratio per volume. At a low concentration of CTAB, the repulsion force between ion Si⁺ and N⁺ is so dominant that the surfactant cannot be accessed. At this step, the ion exchange and aggregate formation can occur simultaneously. Furthermore, more mesoporous silica aggregates are released with higher CTAB. The aggregation of mesoporous silica is likely rectangular, detected by SEM analysis. Based on BET-BJH analysis, a higher amount of CTAB resulted in higher quality of mesoporous silica in terms of physical properties such as specific surface area, pore volume, and pore radius. Moreover, Si content as mesoporous silica can be detected higher at CTAB mole. Meanwhile, the components of C, N, and Br in EDX results were found as the remaining rest amount of CTAB in the synthesized mesoporous silica after calcination to remove the CTAB. It can be assumed that the calcination operation condition (at 550 °C for 3 h) did not completely decompose all the CTAB. It can be concluded that using 0.05 mole of CTAB provided the best mesoporous silica with high content of Si and lower content of unreacted CTAB. These findings from EDX

results are confirmed with SEM micrographs, as previously discussed.

Table 2. Chemical composition data extracted from EDX spectra for mesoporous silica using three different amounts of CTAB

Element	EDX recorded	MS-0.015 ^a		MS-0.03 ^b		MS-0.05 ^c	
		Weight (%)	Atomic (%)	Weight (%)	Atomic (%)	Weight (%)	Atomic (%)
Carbon	C K	25.16	33.59	27.94	27.66	11.42	17.36
Nitrogen	N K	4.08	4.67	2.59	3.00	2.72	3.54
Oxygen	O K	50.02	50.13	44.99	45.52	48.60	55.45
Bromine	Br K	0.64	0.13	0.78	0.16	1.38	0.32
Silicon	Si K	20.11	11.48	23.70	13.66	35.88	23.32

a) MS-0.015 represents the mesoporous silica with CTAB 0.015

b) MS-0.03 represents the mesoporous silica with CTAB 0.03

c) MS-0.05 represents the mesoporous silica with CTAB 0.05

Sorption isotherm and pore properties of synthesized mesoporous silica

The pore properties and sorption isotherm of several samples were analyzed using BET-BJH analysis by N₂ adsorption/desorp-

tion patterns. Figure 4. represents the sorption isotherm of geothermal silica (Figure 4(a).), purified silica by acid leaching (Figure 4(b).), synthesized mesoporous silica with CTAB 0.015 mole (Figure 4(c).), 0.03 mole (Figure 4(d).), and 0.05 mole (Figure 4(e).). Type IV of sorption isotherms class were developed for all samples indicating mesoporous materials⁵⁶.

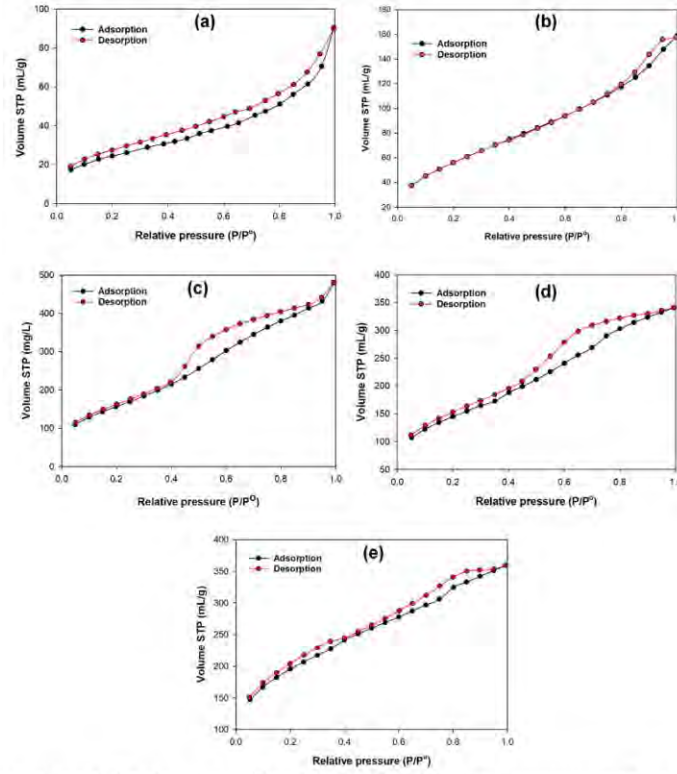


Figure 4. The sorption isotherm of (a) geothermal silica, (b) purified silica after acid leaching, and mesoporous silica products with CTAB variations (c) 0.015 mole, (d) 0.03 mole and (e) 0.05 mole.

The values of specific surface area, adsorbed-desorbed volume range, pore volume, and pore radius are completely summarized in Table 3, while pore size distribution of mesoporous silica product before and after APTMS introduction can be seen in Figure 5. They showed the variation of measured values upon increased CTAB. The specific surface area of geothermal silica was significantly increased from 40.89 m²/g to 178.06 m²/g in purified silica after acid leaching. It can be possibly due to the removal of metal oxide from the bulk body of silica that produces more empty sites resulting in higher measured surface area and higher adsorption ability. It was also found that the specific surface area considerably increased upon an increase of mole of CTAB, which are 582.45, 511.95, and 668.85 m²/g for synthesized mesoporous silica with the amounts of CTAB 0.015, 0.03, and 0.05 mole, respectively. This phenomenon indicates the higher construction of mesoporous structures upon an increase of CTAB loading, resulting in a higher estimated surface area. It is in agreement with the SEM results that in an increased loading of CTAB, it produces a more uniform shaped particle which possibly generates a higher surface area. At the same time, an increase of initial intake adsorption-desorption volume was also found, from 18.61

mL/g (geothermal silica) to 102.35, 103.47, 149.33 mL/g for synthesized mesoporous silica with moles of CTAB 0.015, 0.03, and 0.05 mole, respectively. However, the observed adsorption pore volume was decreased down upon the addition of CTAB, which is from 0.62 mL/g for purified silica to 0.62, 0.39, and 0.26 mL/g for synthesized mesoporous silica with moles of CTAB 0.015, 0.03, and 0.05 mole, respectively. It can be explainable by the increased growth of particles when the higher amount of CTAB was introduced, as evident by SEM images previously discussed. The uniform particle distribution can possibly produce smaller void volume in the bulk body due to the closer gaps between the particles. Further, the measured pore radii were 19.83, 17.07, 19.11, 15.31, 17.04 Å for geothermal silica, purified silica, mesoporous silica with 0.015, 0.03, and 0.05 mole of CTAB, respectively. All of those pore radius values indicate that all of them are in a group of mesoporous materials⁶⁶. Therefore, from these findings, synthesized mesoporous silica with 0.05 mole of CTAB showed the most desirable characteristics in terms of adsorption isotherm specific surface area, adsorbed-desorbed volume, and pore radius, suggesting a preferable matrix material for slow-release urea.

Table 3. BET analysis results, including specific surface area, pore volume, and pore radius (adsorption isotherm) of geothermal silica, purified silica after acid leaching, and modified mesoporous silica with different amounts of CTAB

Sample	Specific surface area (m ² /g)	Adsorbed-desorbed volume range (mL/g)	Pore volume (mL/g)	Pore radius (Å)
Geothermal silica	40.89	18.61 – 86.79	0.11	19.83
Purified silica after acid leaching	178.06	37.62 – 158.62	0.62	17.07
Mesoporous silica with CTAB 0.015 mole	582.45	102.35 – 485.75	0.62	19.11
Mesoporous silica with CTAB 0.03 mole	511.95	103.47 – 346.11	0.39	15.31
Mesoporous silica with CTAB 0.05 mole	668.85	149.33 – 353.28	0.26	17.04

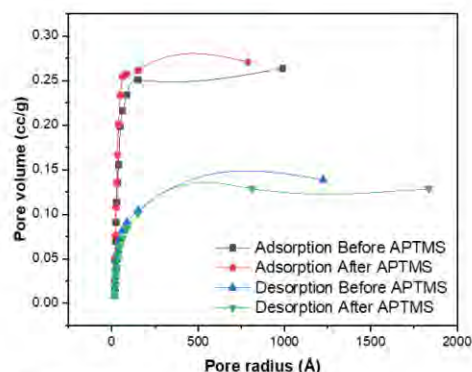


Figure 5. BJH pore size distribution of mesoporous silica products with CTAB 0.05 mole before and after treatment using APTMS.

Thermal analysis of synthesized mesoporous silica

To investigate the thermal characteristics of synthesized mesoporous silica, DSC and TGA analyses were performed. Figure 6. shows DSC thermograms of three different samples, i.e., geothermal silica, mesoporous silica (best formulation using CTAB 0.05 mole), and pure CTAB. The DSC thermogram of geothermal silica shows no sufficient peaks that indicate the melting behavior of the sample. DSC was carried out by comparing the temperature of the sample and reference material during temperature changes. The temperature and reference material will be the same if there are no changes. Thermal phenomena such as melting can cause the decomposition or changes in the amorphous structure of the sample. The DSC curve in Figure 6. shows two endothermic steps in mesoporous silica. The enthalpies measured were -69.2175 J/g (at 82.3 °C) and -10.0796 J/g (at 159.5 °C). The measured enthalpies in pure CTAB were -141.8772 J/g (at 115.4 °C) and -19.6368 J/g (at 272.4 °C).

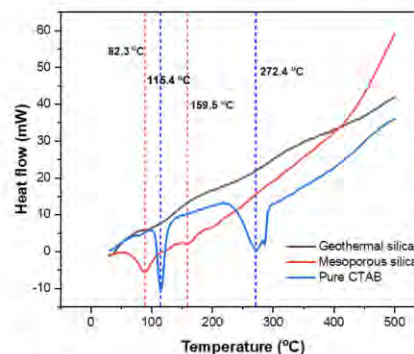


Figure 6. DSC thermogram of geothermal silica, mesoporous silica, and pure CTAB.

TGA analysis confirmed the weight loss behavior of geothermal silica, mesoporous silica, and pure CTAB on temperatures ranging from 30 – 500 °C. TGA thermograms of the three samples and a summary of the weight loss and degradation temperature are shown in Figure 7. and Table 4, respectively. All samples experienced a gradual weight loss as a function of temperature. Generally, the degradation occurred with four steps for geothermal silica and mesoporous silica and three steps for pure CTAB. The most significant weight loss in geothermal silica (Figure 7(a).) occurred at temperatures ranging from 30 – 135 °C with 11.59% weight loss. This condition is possibly due to the evaporation of trapped and bonded water in the sample. Meanwhile, based on the TGA thermogram of mesoporous silica (Figure 7(b).) shows four regions of weight loss which were 17.61% at 30 – 124 °C, 45.56% at 125 – 227 °C, 14.40% at 228 – 294 °C, and 5.72% at 295 – 500 °C. At the first step, the evaporation of trapped water molecules, the degradation of the organic compound at the second step, degradation of CTAB compound at the third step, and degradation of remaining long-chain organic compounds at the last step. In addition, the TGA thermogram of pure CTAB shows a significant weight loss of 87.45% at 227 – 287 °C, which was due to the degradation of organic chains in the CTAB. This condition was also experienced similarly in the TGA thermogram of mesoporous silica. This finding explains that the presence of

CTAB in mesoporous silica interfered with the intermolecular interaction of CTAB and silica, and this interaction led to a change in the thermal degradation behavior of synthesized mesoporous silica.

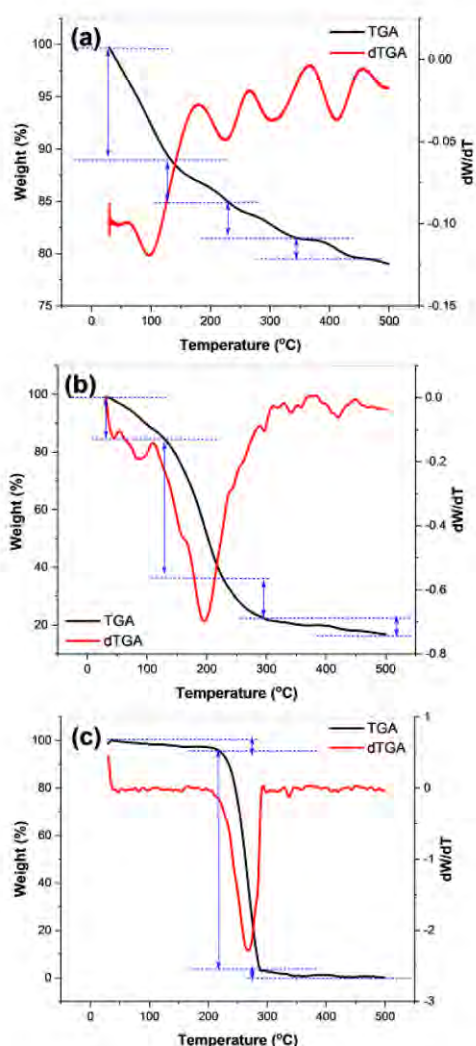


Figure 7. TGA thermograms of (a) Geothermal silica, (b) Mesoporous silica, (c) Pure CTAB.

Table 4. TGA data including weight losses at certain temperatures of geothermal silica, mesoporous silica, and pure CTAB

Sample	Temperature range (°C)	Weight loss (%)
Geothermal silica	30 – 135	11.59
	136 – 236	4.32
	237 – 347	1.86
	348 – 453	1.05
Mesoporous silica	30 – 124	17.61
	125 – 227	45.56
	228 – 294	14.40
	295 – 500	5.72
Pure CTAB	30 – 226	6.75
	227 – 287	87.45
	288 – 500	5.45

Characteristics of slow-release urea with APTMS as a surface modifying agent

Based on previous discussions, synthesized mesoporous silica with 0.05 mole of CTAB shows the prominent characteristic to be utilized as the matrix material for slow-release urea. Furthermore, to develop a desirable slow-release characteristic, surface modification of mesoporous silica was performed using a solution containing 10% of 3-Aminopropyl trimethoxy silane (APTMS). APTMS possibly performs an intermolecular interaction with the molecules of urea⁴⁷. This interaction provides strong bonding between urea and the matrix of (mesoporous silica); therefore, they can be combined to produce a slow-release urea. However, introduction of APTMS also created cross-linking between the APTMS molecules, which led to vertical polymerization and possibly pore blocking. This phenomenon affected the properties of mesoporous silica, especially its porosity, resulting in lower value of surface area, pore volume, and pore radius as seen in Table 5.

Table 5. BET analysis results, including specific surface area, pore volume, and pore radius (adsorption isotherm) of modified mesoporous silica using 0.05 moles CTAB before and after introduction of APTMS

Sample	Specific surface area (m ² /g)	Adsorbed-desorbed volume range (mL/g)	Pore volume (mL/g)	Pore radius (Å)
Mesoporous silica with CTAB 0.05 mole before introduction of APTMS	668.85	149.33 – 353.28	0.26	17.04

Mesoporous silica with CTAB 0.05 mole after introduction of APTMS	103.05	4.62 – 93.18	0.14	15.30
---	--------	--------------	------	-------

Figure 8. represents the SEM micrographs and the EDX spectra of synthesized slow-release urea. Based on Figure 8., it can be observed that all samples had similar surface micromorphology with MS/APTMS. No significant changes in terms of microstructure occurred upon an increase of urea introduction to the slow-release urea. It can be reasonably concluded that the introduction of urea to the MS/APTMS as the matrix did not influence the microstructure of the generated slow-release urea. In addition, EDX results in Figure 8. reveal the spectra of recorded elementals in the tested samples. It was found that the major elementals that appeared in all samples were Si, C, and O. The complete summary of the chemical composition of synthesized slow-release urea is shown in Table 6. From Table 6, increasing urea concentration to the slow-release urea generates higher composition of N, corresponding to the quantity of urea in the slow-release urea. MS/APTMS has 2.81%-wt of nitrogen, and gradually increased upon increasing introduction of urea which are 4.02, 4.63, 5.17, and 6.36 %wt for MS/APTMS/U6.74, MS/APTMS/U16.74, MS/APTMS/U26.74, and MS/APTMS/U36.74, respectively. Therefore, the initial urea concentration introduced to the slow-release urea significantly influenced the generated urea concentration in the synthesized slow-release urea.

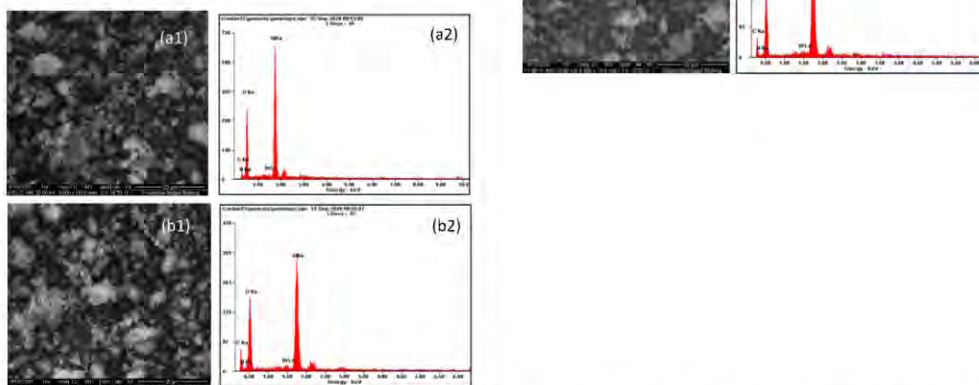


Figure 8. SEM-EDX micrographs and spectra of (a) MS/APTMS, and synthesized slow-release urea: (b) MS/APTMS/U6.74, (c) MS/APTMS/U16.74, (d) MS/APTMS/U26.74, and (e) MS/APTMS/U36.74.

Table 6. Chemical composition from EDX analysis of synthesized slow-release urea

Sample code		C K	N K	O K	Br K	Si K
MS/APTMS	Weight (%)	18.50	5.71	48.12	1.03	26.64
	Atomic (%)	26.03	6.89	50.83	0.22	16.03
MS/APTMS/U6.74	Weight (%)	25.93	4.02	47.91	1.06	21.07
	Atomic (%)	34.80	4.63	48.26	0.21	12.09
MS/APTMS/U16.74	Weight (%)	14.90	4.63	46.71	0.36	33.40
	Atomic (%)	21.82	5.81	51.36	0.08	20.92
MS/APTMS/U26.74	Weight (%)	21.51	5.17	47.03	0.83	25.82

	Atomic (%)	29.35	6.15	49.00	0.17	15.32
MS/APTMS/U36.74	Weight (%)	25.70	6.36	44.66	0.91	22.37
	Atomic (%)	34.55	7.33	45.08	0.18	12.86

FTIR analysis was performed to examine the formation of interaction bonding of urea in a matrix structure and the effect of APTMS on the synthesized slow-release urea. Figure 9. represents the FTIR spectra of different tested samples at wavenumbers of 4000 – 500 cm^{-1} (Figure 9(a).) and 2300 – 1300 cm^{-1} (Figure 9(b).) ⁴⁹. From Figure 9(a)., it can be found that all tested samples experienced an intense broad peak ranging from 1250 – 900 cm^{-1} indicating the vibration of Si-O-Si groups ⁴⁸. Figure 9(b). was developed to further analyze the formation of new functional groups upon the application of APTMS and the introduction of urea to the matrix. It can be seen that the application of APTMS to the mesoporous silica generated slightly higher recorded absorbance at 1556 and 1495 cm^{-1} that correspond to the vibrations of N-H and C-N groups, respectively ²³. This is explainable by the formation of abundant N-H and C-N groups from APTMS on the mesoporous silica structure during the surface modification process.

On the other hand, the varied concentrations of urea introduction to the MS/APTMS were also found, resulting in higher recorded absorbance intensity at several wavenumbers. Absorption bands at 2100 and 1636 cm^{-1} indicate the stretching vibrations of N=C=O and C=O groups, attributed to the natural composition and cyanate

impurities inside the urea. Intense peaks recorded at 1556, 1495, and 1340 cm^{-1} are related to the vibrations of N-H, C-N, and C-H groups ^{48,49}. By comparing the relative absorbance intensity of the tested samples, a sample of MS/APTMS/U26.74 generates the higher intensity of C=O, N-H, C-N, and C-H groups. The higher intensity means the higher content of respective groups in the MS/APTMS/U26.74 than other samples, suggesting the best formulation for the slow-release urea. Figure 9(c). depicts the proposed bonding formations of grafted aminopropyl groups from APTMS to the siloxane groups on the surface of the mesoporous silica resulting in the aminopropyl-functionalized mesoporous silica. This functionalization is needed to effectively adsorb the urea and control its release. The amine groups from urea bonded with amine sites of aminopropyl groups. This amine bonding formation (N-H) was recorded and explained on FTIR spectra. Furthermore, hydrogen bonding as another attractive intermolecular force can occur due to the abundance of highly electronegative atoms such as oxygen (O), nitrogen (N), and hydrogen (H). Therefore, it can provide a stronger bonding of urea groups on the surface of the functionalized mesoporous silica thus, resulting in the effective slow-release property.

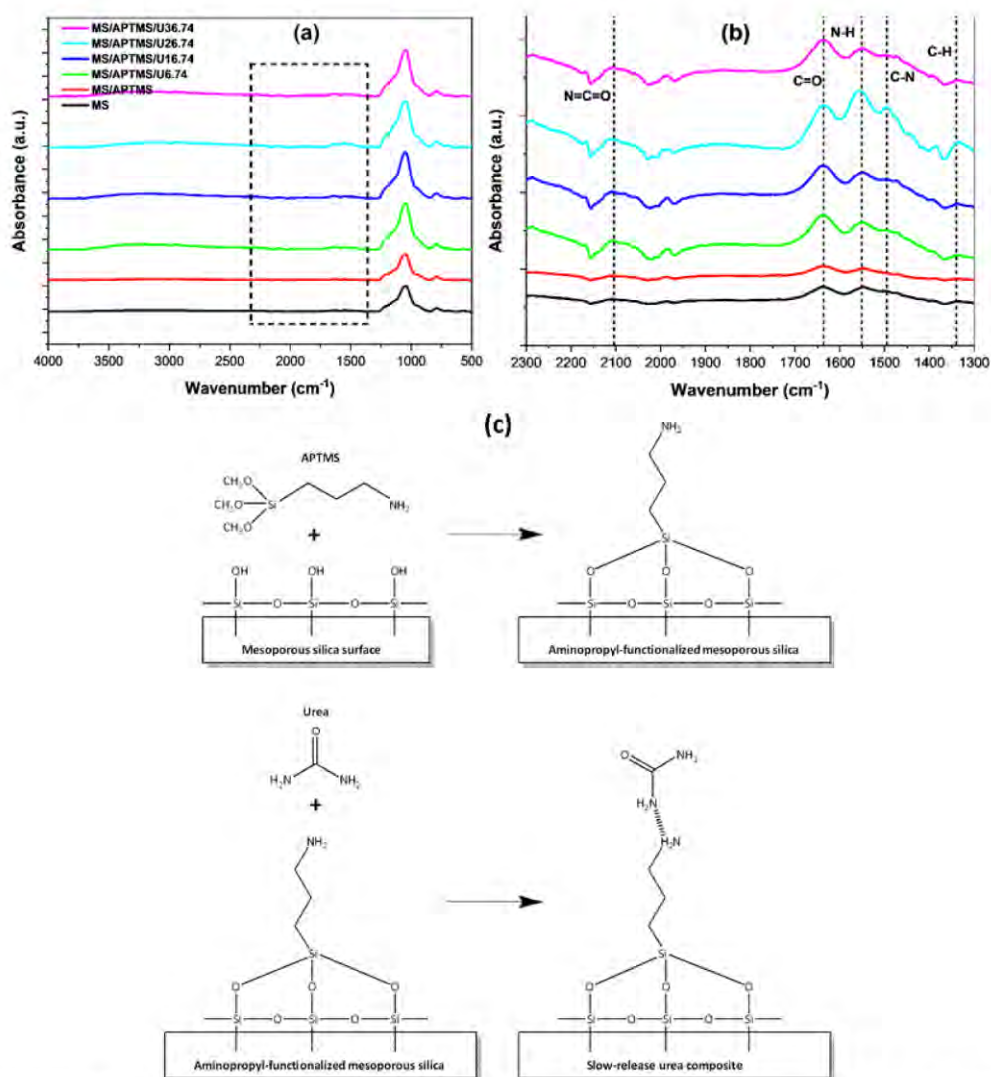


Figure 9. FTIR results of slow-release urea with different formulations (a) FTIR results with wavenumber 4000-500 cm⁻¹, (b) Further evaluation of FTIR spectra at wavenumber 2300-1300 cm⁻¹, and (c) Proposed bonding formation mechanisms of aminopropyl and urea groups on synthesized slow-release urea.

Study of release kinetics of synthesized slow-release urea

The performance of slow-release urea was executed by measuring urea content in overflow liquid (see section 2.2.4.). The observed samples were MS/APTMS/U26.74 as the best formulation for slow-release urea previously discussed and the commercial silica as the control variable. Figure 10(a). depicts the amount (ppm) of urea released during seven days of observation from the sample to the

overflow liquid. The highest overflow urea concentration was recorded on the second day for MS/APTMS/U26.74 with a value of 28.55 ppm, and nearly constant on the next days. On the other hand, the highest overflow urea content was found on the third day with a value of 52.65 ppm and gradually decreased on the next few days. Subsequently, the performance of synthesized slow-release urea was also evaluated by measuring the cumulative urea release, as presented in Figure 10(b). MS/APTMS/U26.74 shows the linear trend of cumulative urea release profile with total release urea of 124.6

ppm on the last day. In contrast, the commercial urea shows an exponential trend of cumulative urea release profile with a value of 184.5 ppm in total. This result indicates that APTMS/U26.74 can release the urea slower than the commercial urea. It can be partially due to the abundance of solid interaction bonding between urea molecules and the MS/APTMS as the matrix of this slow-release urea resulting in a relatively slower release of urea molecules.

To further understand the behavior of urea release, kinetic modeling of urea release was evaluated using several models, i.e., pseudo-first order (Figure 10(c).), pseudo-second order (Figure 10(d).), Higuchi (Figure 10(e).), and Hixson-Crowell (Figure 10(f).). The fitted kinetic parameters and the correlation coefficients are completely listed in Table 7. The pseudo-first order model provided a reasonably good fit for commercial urea and MS/APTMS/U26.74 with R^2 values of 0.8528 and 0.8395, respectively. The pseudo-first order rate kinetic constant values were 0.3502 day^{-1} for commercial urea and 0.2654 day^{-1} for MS/APTMS/U26.74. In addition, the k_1 value of commercial urea was recorded higher than MS/APTMS/U26.74, indicating that the commercial urea has a higher urea release per day than MS/APTMS/U26.74. This result indicates that the modified slow-release urea had a significant impact on reducing its release rate. On the other hand, in this study, the pseudo-second order kinetic model was seemingly unsuitable for modeling the urea release behavior. It is evident with the low number of correlation coefficients with just only 0.3258 for commercial

urea and 0.5703 for MS/APTMS/U26.74. The low value of R^2 indicates that the model is less capable of being used for data predictions. The Higuchi kinetic model performed the best fit of urea release among other fitted models, which had the highest R^2 values of 0.9901 for commercial urea and 0.9979 for MS/APTMS/U26.74. The Higuchi constants were measured $54.0668 \text{ \% day}^{1/2}$ for commercial urea and $24.4964 \text{ \% day}^{1/2}$ for MS/APTMS/U26.74. The higher Higuchi constant represents the higher diffusion rate of urea release from the sample⁶². Thus, the modification of MS/APTMS as the matrix medium has significantly improved the urea release rate by reducing the diffusivity of urea release from the slow-release urea due to solid interaction bonding between modified mesoporous silica and the urea molecules. The Hixson-Crowell model was also showed the excellent urea release fit for both samples with R^2 values of 0.9617 and 0.9772 for commercial urea and MS/APTMS/U26.74, respectively, with Hixson-Crowell constants of $4.8308 \text{ \%}^{1/3} \text{ day}^1$ and $2.3678 \text{ \%}^{1/3} \text{ day}^1$ for commercial urea and MS/APTMS/U26.74, respectively. This result suggests that the primary mechanism of urea release is a diffusion-controlled mechanism⁶⁶, a similar indication from the Higuchi model previously discussed. Based on the studies and results, it can be reasonably suggested that the modification of mesoporous silica with APTMS has a significant impact on reducing urea release rate by lowering the diffusivity of urea from the slow-release urea. Based on the findings and explanation, it can be reasonably concluded that the slow-release urea has been successfully synthesized.

Table 7. Model parameter and correlation coefficient of commercial urea and MS/APTMS/U26.74 to evaluate urea release kinetics using pseudo-first order, Higuchi, and Hixson-Crowell models

Sample	Kinetic models							
	Pseudo-first order		Pseudo-second order		Higuchi		Hixson-Crowell	
	k_1 (day^{-1})	R^2	k_2 (\% day^{-1})	R^2	K_H ($\text{\%}^{1/2} \text{ day}^{-1}$)	R^2	K_{HC} ($\text{\%}^{1/3} \text{ day}^{-1}$)	R^2
Commercial urea	0.3502	0.8528	0.0037	0.3286	54.0668	0.9901	4.8308	0.9617
MS/APTMS/U26.74	0.2654	0.8395	0.0046	0.5703	24.4964	0.9979	2.3678	0.9772

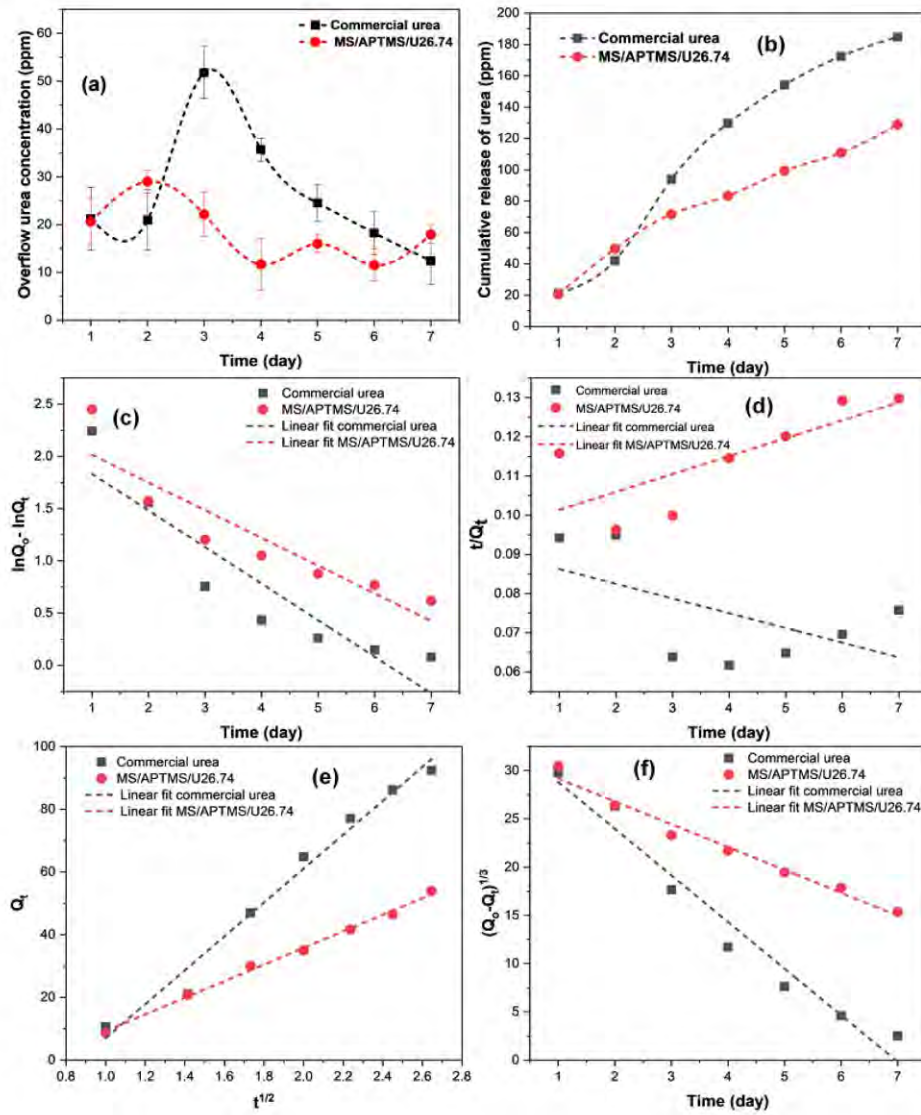


Figure 10. Performance test results of slow-release urea: (a) Result of measured urea concentration in overflow liquid and (b) Cumulative release of urea for commercial urea and MS/APTMS/U26.74. Curve fittings of urea release kinetics for commercial urea and MS/APTMS/U26.74 using (c) Pseudo-first order model, (d) Pseudo-second order model, (e) Higuchi model, and (f) Hixson-Crowell model.

CONCLUSION

In this work, a prominent slow-release urea fertilizer was developed with aminopropyl-functionalized mesoporous silica as the matrix to enhance the urea adsorption and slow-release property. It was developed by utilizing geothermal silica as the silica source, CTAB

as the surfactant, and APTMS as the surface modification agent. The acid leaching treatment using H_2SO_4 was conducted to purify the geothermal silica sample and increase SiO_2 content from 86.30% to 96.00%, which is feasible for mesoporous silica synthesis. The synthesized mesoporous silica was formulated with different mole

amounts of CTAB. It showed the most desirable mesoporous silica with fairly uniform surface micromorphology containing particles with 38.55 %wt of silica content, surface area of 668.85 m²/g, adsorption-desorption range of 149.33 – 353.28 mL/g, and adsorption pore volume of 0.26 mL/g were achieved with addition of 0.05 mole of CTAB. All synthesized mesoporous silicas showed type IV hysteresis which correspond to mesoporous type material, signaling the successful development of the mesoporous structure. The DSC results showed that the mesoporous silica becomes more reactive with recorded enthalpies of 69.2175 J/g and -10.0796 J/g at temperatures of 82.3 °C and 159.5 °C due to the addition of CTAB in the synthesis process. TGA thermograms showed that the mesoporous silica has quite good thermal stability and only experienced 17.61% of weight loss at a temperature of up to 124 °C. These findings suggest the excellent potential of the synthesized mesoporous silica for prominent matrix material. Further, the functionalization of the aminopropyl group to the mesoporous silica using APTMS was done. SEM results showed that the functionalization process and the adsorption of urea to the mesoporous silica resulted in no significant changes in the microstructure of mesoporous silica. Meanwhile, significant changes were observed in generated chemical functional groups after the APTMS functionalization resulting in some new groups including C=O, N-H, and C-N. From the FTIR spectra, MS/APTMS/U26.74 was observed to have a relatively higher intensity of C=O, N-H, C-N, and C-H groups among the other samples, suggesting the higher content of respective groups in the MS/APTMS/U26.74. The comparison experiment and the kinetic study regarding the release property and kinetic between MS/APTMS/U26.74 as the best slow-release urea and the commercial urea was investigated. The cumulative urea release during seven days of observation was 184.5 ppm for commercial urea and 124.6 ppm for MS/APTMS/U26.74. The abundance of strong interaction bonding between urea molecules and the MS/APTMS as the matrix of relatively slower release of urea molecules. The Higuchi kinetic model performed the best fit among the other models to predict the release kinetics of MS/APTMS/U26.74 with generated R² of 0.9979 and Higuchi constant of 24.4964 % day^{-1/2}. The Higuchi constant of MS/APTMS/U26.74 was smaller than commercial urea (54.0668 % day^{-1/2}), indicating the synthesized slow-release urea has a lower urea diffusivity out from the sample, thus resulting in the slower and controllable urea release. Finally, the synthesized MS/APTMS/U26.74 by utilizing geothermal silica, CTAB, and APTMS can be noted as a potential composition for the slow-release urea fertilizer to enhance the usage efficiency of urea.

Author Contributions

S. Silviana: Conceptualization, Methodology, Supervision, Funding acquisition, Resources, Writing – original draft. Atikah Ayu Janitra: Methodology, Investigation, Writing – original draft. Afriza Ni'matus Sa'adah: Project administration, Software, Formal analysis. Febio Dalanta: Data curation, Software, Visualization, Formal analysis, Writing – review and editing.

Funding Sources

This project was financially supported by the Ministry of Education, Culture, Research and Technology of the Republic of Indonesia through grant No. 225-S4/UN7.6.1/PP/2020.

ACKNOWLEDGMENT

The authors would also like to show their gratitude to the community of AMaL (Advanced Material Laboratory) of Diponegoro University for all support and discussion throughout the research.

ABBREVIATIONS

SRU, slow-release urea; MS, mesoporous silica; CTAB, Cetyltrimethylammonium bromide; APTMS, (3-Aminopropyl)trimethoxysilane; SEM: scanning electron microscopy; XRF: x-ray fluorescence, XRD: x-ray diffraction; FTIR: fourier-transform infrared; BET-BJH: barrett-joyner-halenda; TGA: thermogravimetric analysis; DSC: differential scanning calorimetry; HCl: hydrochloric acid; U6.74: urea 6.74 %wt; U16.74: urea 16.74 %wt; U26.74: urea 26.74 %wt; U36.74: urea 36.74 %wt.

REFERENCES

- (1) Kay-Shoemaker, J. L.; Watwood, M. E.; Kilpatrick, L.; Harris, K. Exchangeable ammonium and nitrate from different nitrogen fertilizer preparations in polyacrylamide-treated and untreated agricultural soils. *Biol. Fertil. Soils* **2000**, *31* (3–4), 245–248. <https://doi.org/10.1007/s003740050652>.
- (2) Saha, B. K.; Rose, M. T.; Wong, V.; Cavagnaro, T. R.; Patti, A. F. Hybrid brown coal-urea fertiliser reduces nitrogen loss compared to urea alone. *Sci. Total Environ.* **2017**, *601–602*, 1496–1504. <https://doi.org/10.1016/j.scitotenv.2017.05.270>.
- (3) Getahun, D.; Alemneh, T.; Akebergn, D.; Getabalew, M.; Zewdie, D. Urea Metabolism and Recycling in Ruminants. *Biomed. J. Sci. Tech. Res.* **2019**, *20* (1). <https://doi.org/10.26717/BJSTR.2019.20.003401>.
- (4) Hailemariam, S.; Zhao, S.; He, Y.; Wang, J. Urea transport and hydrolysis in the rumen: A review. *Anim. Nutr.* **2021**, *7* (4), 989–996. <https://doi.org/10.1016/j.aninu.2021.07.002>.
- (5) Mehta, R.; Brahmabhatt, H.; Saha, N. K.; Bhattacharya, A. Removal of substituted phenyl urea pesticides by reverse osmosis membranes: Laboratory scale study for field water application. *Desalination* **2015**, *358*, 69–75. <https://doi.org/10.1016/j.desal.2014.12.019>.
- (6) Berrada, H.; Font, G.; Moltó, J. C. Determination of Urea Pesticide Residues in Vegetable, Soil, and Water Samples. *Crit. Rev. Anal. Chem.* **2003**, *33* (1), 19–41. <https://doi.org/10.1080/713609152>.
- (7) Sasmal, S.; Roy Chowdhury, S.; Podder, D.; Haldar, D. Urea-Appended Amino Acid To Vitalize Yeast Growth, Enhance Fermentation, and Promote Ethanol Production. *ACS Omega* **2019**, *4* (8), 13172–13179. <https://doi.org/10.1021/acsomega.9b01260>.
- (8) Santos, A. S.; Ferreira, L. M. M.; Martin-Rosset, W.; Cotovio, M.; Silva, F.; Bennett, R. N.; Cone, J. W.; Bessa, R. J. B.; Rodrigues, M. A. M. The influence of casein and urea as nitrogen sources on in vitro equine caecal fermentation. *Animal* **2012**, *6* (7), 1096–1102. <https://doi.org/10.1017/S1751731111002527>.
- (9) Azeem, B.; KuShaari, K.; Man, Z. B.; Basit, A.; Thanh, T. H. Review on materials & methods to produce controlled release coated urea fertilizer. *J. Control. Release* **2014**, *181* (12), 11–21. <https://doi.org/10.1016/j.jconrel.2014.02.020>.
- (10) Jie, C.; Jing-zhang, C.; Man-zhi, T.; Zi-tong, G. Soil degradation: a global problem endangering sustainable development. *J. Geogr. Sci.* **2002**, *12* (2), 243–252. <https://doi.org/10.1007/BF02837480>.
- (11) Liu, L.; Kost, J.; Fishman, M. L.; Hicks, K. B. A Review: Controlled Release Systems for Agricultural and Food Applications; 2008; hal 265–281. <https://doi.org/10.1021/bk-2008-0992.ch014>.
- (12) Espécie Bueno, S. C.; Filho, M. B.; de Almeida, P. S. G.; Polidoro, J. C.; Olivares, F. L.; Sthel, M. S.; Vargas, H.; Mota, L.; da Silva, M. G. Cuban zeolite as ammonium carrier in urea-based fertilizer pellets: Photoacoustic-based sensor for monitoring N-ammonia losses by volatilization in aqueous solutions. *Sensors Actuators B Chem.* **2015**, *212*, 35–40. <https://doi.org/10.1016/j.snb.2015.01.114>.
- (13) Mihok, F.; Macko, J.; Oriňák, A.; Oriňáková, R.; Koval, K.; Sisáková, K.; Petruš, O.; Kostecká, Z. Controlled nitrogen release fertilizer based on zeolite clinoptilolite: Study of preparation process and release properties using molecular dynamics. *Curr. Res. Green Sustain.*

- Chem. **2020**, *3*, 100030. <https://doi.org/10.1016/j.crgsc.2020.100030>.
- (14) Maghsoodi, M. R.; Najafi, N.; Reyhanitabar, A.; Oustan, S. Hydroxyapatite nanorods, hydrochar, biochar, and zeolite for controlled-release urea fertilizers. *Geoderma* **2020**, *379*, 114644. <https://doi.org/10.1016/j.geoderma.2020.114644>.
- (15) Pereira, E. I.; da Cruz, C. C. T.; Solomon, A.; Le, A.; Cavigelli, M. A.; Ribeiro, C. Novel Slow-Release Nanocomposite Nitrogen Fertilizers: The Impact of Polymers on Nanocomposite Properties and Function. *Ind. Eng. Chem. Res.* **2015**, *54* (14), 3717–3725. <https://doi.org/10.1021/acs.iecr.5b00176>.
- (16) Yamamoto, C. F.; Pereira, E. I.; Mattoso, L. H. C.; Matsunaka, T.; Ribeiro, C. Slow release fertilizers based on urea/urea-formaldehyde polymer nanocomposites. *Chem. Eng. J.* **2016**, *287*, 390–397. <https://doi.org/10.1016/j.cej.2015.11.023>.
- (17) Shen, Y.; Zhou, J.; Du, C.; Zhou, Z. Hydrophobic modification of waterborne polymer slows urea release and improves nitrogen use efficiency in rice. *Sci. Total Environ.* **2021**, *794*, 148612. <https://doi.org/10.1016/j.scitotenv.2021.148612>.
- (18) Bortolin, A.; Aouada, F. A.; de Moura, M. R.; Ribeiro, C.; Longo, E.; Mattoso, L. H. C. Application of polysaccharide hydrogels in adsorption and controlled-extended release of fertilizers processes. *J. Appl. Polym. Sci.* **2012**, *123* (4), 2291–2298. <https://doi.org/10.1002/app.34742>.
- (19) Li, L.; Sun, Y.; Cao, B.; Song, H.; Xiao, Q.; Yi, W. Preparation and performance of polyurethane/mesoporous silica composites for coated urea. *Mater. Des.* **2016**, *99*, 21–25. <https://doi.org/10.1016/j.matdes.2016.03.043>.
- (20) de Silva, M.; Siriwardena, D. P.; Sandaruwan, C.; Priyadarshana, G.; Karunaratne, V.; Kottegoda, N. Urea-silica nanohybrids with potential applications for slow and precise release of nitrogen. *Mater. Lett.* **2020**, *272*, 127839. <https://doi.org/10.1016/j.matlet.2020.127839>.
- (21) Elhassani, C. E.; Essamlali, Y.; Aqili, M.; Nzenguet, A. M.; Ganetri, I.; Zahouily, M. Urea-impregnated HAP encapsulated by lignocellulosic biomass-extruded composites: A novel slow-release fertilizer. *Environ. Technol. Innov.* **2019**, *15*, 100403. <https://doi.org/10.1016/j.eti.2019.100403>.
- (22) Vanichvattanadecha, C.; Singhapong, W.; Jaroenworuluck, A. Different sources of silicon precursors influencing on surface characteristics and pore morphologies of mesoporous silica nanoparticles. *Appl. Surf. Sci.* **2020**, *513*, 145568. <https://doi.org/10.1016/j.apsusc.2020.145568>.
- (23) Yang, Y.; Wang, J.; Qian, X.; Shan, Y.; Zhang, H. Aminopropyl-functionalized mesoporous carbon (APTMS-CMK-3) as effective phosphate adsorbent. *Appl. Surf. Sci.* **2018**, *427*, 206–214. <https://doi.org/10.1016/j.apsusc.2017.08.213>.
- (24) Ghobashy, M. M.; Mousaa, I. M.; El-Sayyad, G. S. Radiation synthesis of urea/hydrogel core shells coated with three different natural oils via a layer-by-layer approach: An investigation of their slow release and effects on plant growth-promoting rhizobacteria. *Prog. Org. Coatings* **2021**, *151*, 106022. <https://doi.org/10.1016/j.porgcoat.2020.106022>.
- (25) Guo; Liu; Zhan; Wu, L. Preparation and Properties of a Slow-Release Membrane-Encapsulated Urea Fertilizer with Superabsorbent and Moisture Preservation. *Ind. Eng. Chem. Res.* **2005**, *44* (12), 4206–4211. <https://doi.org/10.1021/ie0489406>.
- (26) Abdelghany, A. M.; Meikhaile, M. S.; Asker, N. Synthesis and structural-biological correlation of PVC/PVAc polymer blends. *J. Mater. Res. Technol.* **2019**, *8* (5), 3908–3916. <https://doi.org/10.1016/j.jmrt.2019.06.053>.
- (27) Cui, Y.; Xiang, Y.; Xu, Y.; Wei, J.; Zhang, Z.; Li, L.; Li, J. Poly-acrylic acid grafted natural rubber for multi-coated slow release compound fertilizer: Preparation, properties and slow-release characteristics. *Int. J. Biol. Macromol.* **2020**, *146*, 540–548. <https://doi.org/10.1016/j.jbiomac.2020.01.051>.
- (28) dos Santos, A. C. S.; Henrique, H. M.; Cardoso, V. L.; Reis, M. H. M. Slow release fertilizer prepared with lignin and poly(vinyl acetate) bioblend. *Int. J. Biol. Macromol.* **2021**, *185*, 543–550. <https://doi.org/10.1016/j.jbiomac.2021.06.169>.
- (29) Liu, J.; Yang, Y.; Gao, B.; Li, Y. C.; Xie, J. Bio-based elastic polyurethane for controlled-release urea fertilizer: Fabrication, properties, swelling and nitrogen release characteristics. *J. Clean. Prod.* **2019**, *209*, 528–537. <https://doi.org/10.1016/j.jclepro.2018.10.263>.
- (30) Pang, L.; Gao, Z.; Zhang, S.; Li, Y.; Hu, S.; Ren, X. Preparation and anti-UV property of modified cellulose membranes for biopesticides controlled release. *Ind. Crops Prod.* **2016**, *89*, 176–181. <https://doi.org/10.1016/j.indcrop.2016.05.014>.
- (31) Sathisaran, L.; Balasubramanian, M. Physical characterization of chitosan/gelatin-alginate composite beads for controlled release of urea. *Heliyon* **2020**, *6* (11), e05495. <https://doi.org/10.1016/j.heliyon.2020.e05495>.
- (32) Ni, B.; Liu, M.; Lü, S.; Xie, L.; Wang, Y. Multifunctional Slow-Release Organic-Inorganic Compound Fertilizer. *J. Agric. Food Chem.* **2010**, *58* (23), 12373–12378. <https://doi.org/10.1021/jf1029306>.
- (33) Ni, B.; Liu, M.; Lü, S.; Xie, L.; Wang, Y. Environmentally Friendly Slow-Release Nitrogen Fertilizer. *J. Agric. Food Chem.* **2011**, *59* (18), 10169–10175. <https://doi.org/10.1021/jf102131z>.
- (34) Shan, L.; Gao, Y.; Zhang, Y.; Yu, W.; Yang, Y.; Shen, S.; Zhang, S.; Zhu, L.; Xu, L.; Tian, B.; Yun, J. Fabrication and Use of Alginate-Based Cryogel Delivery Beads Loaded with Urea and Phosphates as Potential Carriers for Bioremediation. *Ind. Eng. Chem. Res.* **2016**, *55* (28), 7655–7660. <https://doi.org/10.1021/acs.iecr.6b01256>.
- (35) Wang, Y.; Liu, M.; Ni, B.; Xie, L. κ-Carrageenan–Sodium Alginate Beads and Superabsorbent Coated Nitrogen Fertilizer with Slow-Release, Water-Retention, and Anticompaction Properties. *Ind. Eng. Chem. Res.* **2012**, *51* (3), 1413–1422. <https://doi.org/10.1021/ie2020526>.
- (36) Qiao, D.; Liu, H.; Yu, L.; Bao, X.; Simon, G. P.; Petinakis, E.; Chen, L. Preparation and characterization of slow-release fertilizer encapsulated by starch-based superabsorbent polymer. *Carbohydr. Polym.* **2016**, *147*, 146–154. <https://doi.org/10.1016/j.carbpol.2016.04.010>.
- (37) Wanyika, H.; Gatebe, E.; Kioni, P.; Tang, Z.; Gao, Y. Mesoporous Silica Nanoparticles Carrier for Urea: Potential Applications in Agrochemical Delivery Systems. *J. Nanosci. Nanotechnol.* **2012**, *12* (3), 2221–2228. <https://doi.org/10.1166/jnn.2012.5801>.
- (38) He, H.; Xiao, H.; Kuang, H.; Xie, Z.; Chen, X.; Jing, X.; Huang, Y. Synthesis of mesoporous silica nanoparticle-oxaliplatin conjugates for improved anticancer drug delivery. *Colloids Surfaces B Biointerfaces* **2014**, *117*, 75–81. <https://doi.org/10.1016/j.colsurfb.2014.02.014>.
- (39) Yan, E.; Ding, Y.; Chen, C.; Li, R.; Hu, Y.; Jiang, X. Polymer/silica hybrid hollow nanospheres with pH-sensitive drug release in physiological and intracellular environments. *Chem. Commun.* **2009**, No. 19, 2718. <https://doi.org/10.1039/b900751b>.
- (40) Yang, D.; Fan, R.; Luo, F.; Chen, Z.; Gerson, A. R. Facile and green fabrication of efficient Au nanoparticles catalysts using plant extract via a mesoporous silica-assisted strategy. *Colloids Surfaces A Physicochem. Eng. Asp.* **2021**, *621*, 126580. <https://doi.org/10.1016/j.colsurfa.2021.126580>.
- (41) Yin, F.; Xu, F.; Zhang, K.; Yuan, M.; Cao, H.; Ye, T.; Wu, X.; Xu, F. Synthesis and evaluation of mesoporous silica/mesoporous molecularly imprinted nanoparticles as adsorbents for detection and selective removal of imidacloprid in food samples. *Food Chem.* **2021**, *364*, 130216. <https://doi.org/10.1016/j.foodchem.2021.130216>.
- (42) Huang, R.; Shen, Y.-W.; Guan, Y.-Y.; Jiang, Y.-X.; Wu, Y.; Rahman, K.; Zhang, L.-J.; Liu, H.-J.; Luan, X. Mesoporous silica nanoparticles: facile surface functionalization and versatile biomedical applications in oncology. *Acta Biomater.* **2020**, *116*, 1–15. <https://doi.org/10.1016/j.actbio.2020.09.009>.
- (43) Kaya, S.; Cresswell, M.; Boccaccini, A. R. Mesoporous silica-based bioactive glasses for antibiotic-free antibacterial applications. *Mater. Sci. Eng. C* **2018**, *83*, 99–107. <https://doi.org/10.1016/j.msec.2017.11.003>.
- (44) dos Santos, S. M. L.; Nogueira, K. A. B.; de Souza Gama, M.; Lima, J. D. F.; da Silva Júnior, I. J.; de Azevedo, D. C. S. Synthesis and characterization of ordered mesoporous silica (SBA-15 and SBA-16) for adsorption of biomolecules. *Microporous Mesoporous Mater.* **2013**, *180*, 284–292.

- <https://doi.org/10.1016/j.micromeso.2013.06.043>.
- (45) Policcichio, A.; Conte, G.; Stelitano, S.; Bonaventura, C. P.; Putz, A.-M.; Ianaşi, C.; Almásy, L.; Horváth, Z. E.; Agostino, R. G. Hydrogen storage performances for mesoporous silica synthesized with mixed tetraethoxysilane and methyltriethoxysilane precursors in acidic condition. *Colloids Surfaces A Physicochem. Eng. Asp.* **2020**, *601*, 125040. <https://doi.org/10.1016/j.colsurfa.2020.125040>.
 - (46) Gil-Ortiz, R.; Naranjo, M. Á.; Ruiz-Navarro, A.; Caballero-Molada, M.; Atares, S.; García, C.; Vicente, O. New Eco-Friendly Polymeric-Coated Urea Fertilizers Enhanced Crop Yield in Wheat. *Agronomy* **2020**, *10* (3), 438. <https://doi.org/10.3390/agronomy10030438>.
 - (47) Cheah, W.-K.; Sim, Y.-L.; Yeoh, F.-Y. Amine-functionalized mesoporous silica for urea adsorption. *Mater. Chem. Phys.* **2016**, *175*, 151–157. <https://doi.org/10.1016/j.matchemphys.2016.03.007>.
 - (48) Luechinger, M.; Prins, R.; Pirngruber, G. D. Functionalization of silica surfaces with mixtures of 3-aminopropyl and methyl groups. *Microporous Mesoporous Mater.* **2005**, *85* (1–2), 111–118. <https://doi.org/10.1016/j.micromeso.2005.05.031>.
 - (49) Hicks, J. C.; Dabestani, R.; Buchanan, A. C.; Jones, C. W. Assessing site-isolation of amine groups on aminopropyl-functionalized SBA-15 silica materials via spectroscopic and reactivity probes. *Inorganica Chim. Acta* **2008**, *361* (11), 3024–3032. <https://doi.org/10.1016/j.jica.2008.01.002>.
 - (50) Burkett, S. L.; Sims, S. D.; Mann, S. Synthesis of hybrid inorganic-organic mesoporous silica by co-condensation of siloxane and organosiloxane precursors. *Chem. Commun.* **1996**, No. 11, 1367–1368. <https://doi.org/10.1039/CC9960001367>.
 - (51) Purnomo, A.; Dalanta, F.; Oktaviani, A. D.; Silviana, S. Superhydrophobic coatings and self-cleaning through the use of geothermal scaling silica in improvement of material resistance; 2018; hal 020077. <https://doi.org/10.1063/1.5065037>.
 - (52) Silviana, S.; Darmawan, A.; Subagio, A.; Dalanta, F. Statistical Approaching for Superhydrophobic Coating Preparation using Silica Derived from Geothermal Solid Waste. *ASEAN J. Chem. Eng.* **2020**, *19* (2), 91. <https://doi.org/10.22146/ajche.51178>.
 - (53) Silviana, S.; Darmawan, A.; Dalanta, F.; Subagio, A.; Hermawan, F.; Milen Santoso, H. Superhydrophobic Coating Derived from Geothermal Silica to Enhance Material Durability of Bamboo Using Hexadimethylsilazane (HMDS) and Trimethylchlorosilane (TMCS). *Materials (Basel)* **2021**, *14* (3), 530. <https://doi.org/10.3390/ma14030530>.
 - (54) Silviana, S.; Darmawan, A.; Janitra, A. A.; Ma'ruf, A.; Triesty, I. Silicon preparation derived from geothermal silica by reduction using magnesium. *Int. J. Emerg. Trends Eng. Res.* **2020**, *8* (8), 4861–4866. <https://doi.org/10.30534/ijeter/2020/126882020>.
 - (55) Silviana, S.; Sanyoto, G. J.; Darmawan, A. Preparation of Geothermal Silica Glass Coating Film Through Multi-factor Optimization. *J. Teknol.* **2021**, *83* (4), 41–49. <https://doi.org/10.11113/jurnalteknologi.v83.16377>.
 - (56) Tut Hakkıdır, F. S.; Şengün, R.; Aydın, H. Characterization and Comparison of geothermal fluids geochemistry within the Kızıldere Geothermal Field in Turkey: New findings with power capacity expanding studies. *Geothermics* **2021**, *94*, 102110. <https://doi.org/10.1016/j.geothermics.2021.102110>.
 - (57) Silviana, S.; Anggoro, D. D.; Salsabila, C. A.; Aprilio, K. Utilization of geothermal waste as a silica adsorbent for biodiesel purification. *Korean J. Chem. Eng.* **2021**, *38* (10), 2091–2105. <https://doi.org/10.1007/s11814-021-0827-z>.
 - (58) Silviana, S.; Bayu, W. J. Silicon Conversion From Bamboo Leaf Silica By Magnesiothermic Reduction for Development of Li-ion Battery Anode. *MATEC Web Conf.* **2018**, *156*, 05021. <https://doi.org/10.1051/mateconf/201815605021>.
 - (59) Silviana, S.; Purbasari, A.; Siregar, A.; Rochyati, A. F.; Papra, T. Synthesis of mesoporous silica derived from geothermal waste with cetyl trimethyl ammonium bromide (CTAB) surfactant as drug delivery carrier. *AIP Conf. Proc.* **2020**, 2296. <https://doi.org/10.1063/5.0030487>.
 - (60) Silviana, S.; Sagala, E. A. P. P.; Sari, S. E.; Siagian, C. T. M. Preparation of mesoporous silica derived from geothermal silica as precursor with a surfactant of cetyltrimethylammonium bromide; 2019; hal 020070. <https://doi.org/10.1063/1.5141683>.
 - (61) Silviana, S.; Sanyoto, G. J.; Darmawan, A.; Sutanto, H. GEOTHERMAL SILICA WASTE AS SUSTAINABLE AMORPHOUS SILICA SOURCE FOR THE SYNTHESIS OF SILICA XEROGELS. *Rasayan J. Chem.* **2020**, *13* (03), 1692–1700. <https://doi.org/10.31788/RJC.2020.1335701>.
 - (62) Silviana, S.; Dalanta, F.; Sanyoto, G. J. Utilization of bamboo leaf silica as a superhydrophobic coating using trimethylchlorosilane as a surface modification agent. *J. Phys. Conf. Ser.* **2021**, *1943* (1), 012180. <https://doi.org/10.1088/1742-6596/1943/1/012180>.
 - (63) Silviana, S.; Ma'ruf, A. Synthesized Silica Mesoporous from Silica Geothermal Assisted with CTAB and Modified by APTMS. *Int. J. Emerg. Trends Eng. Res.* **2020**, *8* (8), 4854–4860. <https://doi.org/10.30534/ijeter/2020/125882020>.
 - (64) Travaglini, L.; Picchetti, P.; Del Giudice, A.; Galantini, L.; De Cola, L. Tuning and controlling the shape of mesoporous silica particles with CTAB/sodium deoxycholate catanionic mixtures. *Microporous Mesoporous Mater.* **2019**, *279*, 423–431. <https://doi.org/10.1016/j.micromeso.2019.01.030>.
 - (65) Che Ismail, N. H.; Ahmad Bakhtiar, N. S. A.; Md. Akil, H. Effects of cetyltrimethylammonium bromide (CTAB) on the structural characteristic of non-expandable muscovite. *Mater. Chem. Phys.* **2017**, *196*, 324–332. <https://doi.org/10.1016/j.matchemphys.2017.05.007>.
 - (66) Khoeni, M.; Najafi, A.; Rastegar, H.; Amani, M. Improvement of hollow mesoporous silica nanoparticles synthesis by hard-templating method via CTAB surfactant. *Ceram. Int.* **2019**, *45* (10), 12700–12707. <https://doi.org/10.1016/j.ceramint.2019.03.125>.

Revision Requested for Manuscript (11 Maret 2022)

9/2/22, 11:47 AM

Department of Chemical Engineering, Diponegoro University Mail – Revision Requested for Manuscript ID ie-2022-004247



Silviana Silviana <silviana@che.undip.ac.id>

Revision Requested for Manuscript ID ie-2022-004247

Industrial & Engineering Chemistry Research <onbehalf@manuscriptcentral.com>

Fri, Mar 11, 2022 at 3:42 AM

Reply-To: nenoff-office@iecr.acs.org

To: silviana@che.undip.ac.id

10-Mar-2022

Journal: Industrial & Engineering Chemistry Research

Manuscript ID: ie-2022-004247

Title: "Synthesis of aminopropyl-functionalized mesoporous silica derived from geothermal silica for effective slow-release urea carrier"

Author(s): Silviana, S.; Janitra, Atikah; Sa'adah, Afriza; Dalanta, Febio

COVID-19 Support: Please visit the following website to access important information for ACS authors and reviewers during the COVID-19 crisis: <https://axial.acs.org/2020/03/25/chemists-covid-19-coronavirus/>

We are flexible in these unprecedented times affecting the global research community. If you need more time to complete authoring or reviewing tasks, please contact the editorial office and request an extension.

Dear Dr. Silviana:

The reviews for your manuscript are attached. The reviewers have raised points that require consideration and revision of the manuscript before it is suitable for publication. However, with adequate response and revision, the manuscript should be acceptable for publication in Industrial & Engineering Chemistry Research. Please address all the reviewers' comments in both the revised manuscript and in the letter back to the editor. The editor in particular would like a revision to this: the rationale for developing the material (p. 1-2) needs to be improved, as does their basic interpretation of their performance test results. Specifically, with the information provided the reader can't be sure that their new material actually performs better than the "commercial urea." We would like to receive your revision as soon as possible, by 09-Apr-2022 at the latest.

To revise your manuscript, log into ACS Paragon Plus with your ACS ID at <http://acsparagonplus.acs.org/> and select "My Authoring Activity". There you will find your manuscript title listed under "Revisions Requested by Editorial Office." With the exception of your main text file, all of your original files will be available to you for review or replacement during the revision process. If you need to replace a file, please be sure to remove the original before uploading a new one. In all circumstances you must upload a new manuscript text file.

When submitting your revised manuscript through ACS Paragon Plus, you will be able to respond to the comments made by the reviewer(s) in the text box provided or by attaching a file containing your detailed responses to all of the points raised by the reviewers.

Please note that you may receive a follow-up message within 24 hours describing the non-scientific changes you must also make to your manuscript before you submit the revision.

Prior to submitting the manuscript, ensure that the manuscript addresses the following points:

Funding Sources: Authors are required to report ALL funding sources and grant/award numbers relevant to this manuscript. Enter all sources of funding for ALL authors relevant to this manuscript in BOTH the Open Funder Registry tool in ACS Paragon Plus and in the manuscript to meet this requirement. See http://pubs.acs.org/page/4authors/funder_options.html for complete instructions.

ORCID: Authors submitting manuscript revisions are required to provide their own validated ORCID iDs before completing the submission, if an ORCID iD is not already associated with their ACS Paragon Plus user profiles. This iD may be provided during original manuscript submission or when submitting the manuscript revision. You can provide only your own ORCID iD, a unique researcher identifier. If your ORCID iD is not already validated and associated with your ACS Paragon Plus user profile, you may do so by following the ORCID-related links in the Email/Name section of your ACS Paragon Plus account. All authors are encouraged to register for and associate their own ORCID iDs with their ACS Paragon Plus profiles. The ORCID iD will be displayed in the published article for any author on a manuscript who has a validated ORCID iD associated with ACS Paragon Plus when the manuscript is accepted. Learn more at <http://www.orcid.org>.

<https://mail.google.com/mail/u/0/?ik=ae189121fa&view=pt&search=all&permmsgid=msg-f%3A1726946975314236136&simpl=msg-f%3A1726946...> 1/3

ACS Publications uses Crossref Similarity Check Powered by iThenticate to detect instances of similarity in submitted manuscripts. In publishing only original research, ACS is committed to deterring plagiarism, including self-plagiarism. Your manuscript may be screened for similarity to published material.

We look forward to seeing your paper in Industrial & Engineering Chemistry Research.

Sincerely,

Dr. Tina M. Nenoff
Associate Editor
Industrial & Engineering Chemistry Research
Sandia National Laboratories
Phone: 919-967-7730
Email: nenoff-office@iecr.acs.org

Please click the link below to view the Industrial & Engineering Chemistry Research Author Guidelines:

<http://pubs.acs.org/page/iecred/submission/index.html>

Reviewer(s) Comments to Author:

Reviewer: 1

Comments to the Author

Page 1, left column. Reference is made to a number of slow release materials. Do the authors know how much they slow the release of urea, and how it compares to what was developed here? It would also be helpful if the authors could provide some idea of how long in actual field applications the slow release of urea needs to be controlled? Is this length of time longer than one would expect that the "natural Materials" (cellulose, chitosan, attapulgite, alginates, starch 36, and lignin 28,) would survive degradation by microbes. Note also, Attapulgite is a "clay mineral" and like the silica base developed here it is not likely to degrade, except over "geologic" spans of time. Finally it seems likely the deterioration of concern relates to the impact of microbes on the complex organic coatings used to enhance performance, and not the deterioration of the bulk substrate itself.

Page 1, left column, line 38: The authors investigated comparative leaching behaviors – would they care to comment on ammonium volatilization.

Page 2, paragraph 2. The procedure outlined for purifying the geothermal silica seems a trifle cumbersome; why not just use a commercial sodium silicate solution as a starting material?

Page 5. Line 56: Point out that the selection of "0.05 mole" CTAB as having the best response to calcination is based only on carbon and silicon, neither the nitrogen or bromine contents support this contention.

Page 8, "Thermal analysis of synthesized mesoporous silica" Were the TGA and DSC studies performed using air or an inert gas (Ar or N₂)?

Page 10, line 18, column 1: "MS/APTMS has 2.81%-wt of nitrogen" - this is not the same value as appears in the first entry (5.71 wt %) of Table 6.

Page 3 (Performance test of the prepared slow-release urea) and Page 13 (Study of release kinetics of synthesized slow-release urea): First of all the authors need to say how much commercial urea was put into the leaching test apparatus for comparison. Table 6 states that MS/APTMS/U26.74 contains 5.17 weight % N while Page 2 line 11, column 2 states that commercial urea contains around 46% urea. If similar weights of the two materials were included in leaching tests then it would be expected that the releases from commercial urea would be greater than the urea loaded on the mesoporous silica simply because there was much more on the commercial urea to start with. And, more importantly, one cannot make the case that the MS/APTMS/U26.74 was effective at retarding urea releases unless one knows the relative amounts of urea put into the two leach tests.

Page 14, Fig. 10-B: It would be highly informative if the data in Fig. 10-B were used to determine what fraction of the total urea initially added to the experiments (as either commercial urea or as 1 gram of MS/APTMS/U26.74) was released during the relatively short term of the leaching tests.

Reviewer: 2

Comments to the Author

This manuscript entitled "Synthesis of aminopropyl-functionalized mesoporous silica derived from geothermal silica

<https://mail.google.com/mail/u/0/?ik=ae189121fa&view=pt&search=all&permmsgid=msg-f%3A1726946975314236136&siml=msg-f%3A1726946...> 2/3

for effective slow-release urea carrier" deals on the preparation and characterization of an amino-functionalized silica for slow release of urea. The subject is original and into the scope of the journal. However, this paper contains many basic mistakes and cannot be considered as publishable. Some comments are indicated as follows:

- 1.- It is not admissible to give surface area values with one or two decimal digits. Even in the abstract section.
- 2.- This sentence "SEM showed functionalization and urea adsorption to mesoporous silica resulted in no significant microstructure changes" is confused and must be rewritten
- 3.- The cost of the prepared silica is very high due to the use of a high cost surfactant and the amino compound, and the purification of the geothermal silica. For this reason, the possible application of this materials as potential slow release fertilizer is not viable from the economic viewpoint.
- 4.- Please, it a mistake to write Ammonium hydroxide (NH₄OH, 25%). This is a non-existent compound. Write aqueous ammonia.
- 5.- The presence of Cr₂O₃ is another drawback for using this silica. This point must be indicated.
- 6.- The discussion contains sentences that include errors in basic chemical concepts. For example, in this sentence "the repulsion force between ion Si⁺ and N⁺ is so dominant that the surfactant cannot be accessed."
- 7.- There are many other basic mistakes along the text.

FOR ASSISTANCE WITH YOUR MANUSCRIPT SUBMISSION PLEASE CONTACT:

ACS Publications Customer Services & Information (CSI)

Email: support@services.acs.org

Phone: 202-872-4357

Toll Free Phone: 800-227-9919 (USA/Canada only)

PLEASE NOTE: This email message, including any attachments, contains confidential information related to peer review and is intended solely for the personal use of the recipient(s) named above. No part of this communication or any related attachments may be shared with or disclosed to any third party or organization without the explicit prior written consent of the journal Editor and ACS. If the reader of this message is not the intended recipient or is not responsible for delivering it to the intended recipient, you have received this communication in error. Please notify the sender immediately by e-mail, and delete the original message.

As an author or reviewer for ACS Publications, we may send you communications about related journals, topics or products and services from the American Chemical Society. Please email us at pubs-comms-unsub@acs.org if you do not want to receive these. Note, you will still receive updates about your manuscripts, reviews, or future invitations to review.

Thank you.

Manuscript Formatting Request (11 Maret 2022)

9/2/22, 12:02 PM

Department of Chemical Engineering, Diponegoro University Mail - Silviana, S. ie-2022-004247 -- Manuscript Formatting Req...



Silviana Silviana <silviana@che.undip.ac.id>

Silviana, S. ie-2022-004247 -- Manuscript Formatting Request - Non-scientific changes

Industrial & Engineering Chemistry Research <onbehalfof@manuscriptcentral.com>

Fri, Mar 11, 2022 at 3:42 PM

Reply-To: iecr-admin@services.acs.org

To: silviana@che.undip.ac.id

11-Mar-2022

Manuscript ID: ie-2022-004247

Manuscript Type: Article

Title: "Synthesis of aminopropyl-functionalized mesoporous silica derived from geothermal silica for effective slow-release urea carrier"

Author(s): Silviana, S.; Janitra, Atikah; Sa'adah, Afriza; Dalanta, Febio

Dear Dr. Silviana:

You recently received a Revision Request from Dr. Tina Nenoff. In addition to addressing the Editor's concerns and the requests of the reviewers, please complete the following before submitting your revision:

- An email address is required for each corresponding author identified on the manuscript file. Please add the corresponding author email(s) to any page of the manuscript.
- Please include author names, article titles, journal name, publication year, and at least the first page for each reference citation for the following incomplete journal references: 3.
- A Table of Contents graphic must be included on the last page of your manuscript file. Guidelines for creating a successful graphic can be found at: http://pubs.acs.org/paragonplus/submission/toc_abstract_graphics_guidelines.pdf
- Please include your longest and least essential tables in a separate document uploaded with the file designation 'Supporting Information for Publication' and remove them from your manuscript file. Your figures/tables should be labeled S1, S2, etc. Also, include a title page on your Supporting Information file and a Supporting Information paragraph at the end of your manuscript. The last line of the paragraph should read as follows: This information is available free of charge via the Internet at <http://pubs.acs.org/>. If you choose not to make this change, please note why in your response letter.

We look forward to receiving your revised manuscript, so that processing of your manuscript may proceed without further delay.

Be sure that the final versions of your manuscript file and any Supporting Information files intended for publication (including the pdf versions, if provided) are free of all markup elements, such as track changes, comments, colored text, highlights, and sticky notes.

Please include an annotated copy of the manuscript to show revisions and track changes for the benefit of the reviewers. This marked manuscript should be uploaded electronically in the File Upload section as "Supporting Information for Review Only" during submission of your revision.

Thank you for considering Industrial & Engineering Chemistry Research as a forum for the publication of your work.

Sincerely,

Jelena Pavlovic
Industrial & Engineering Chemistry Research

FOR ASSISTANCE WITH YOUR MANUSCRIPT SUBMISSION PLEASE CONTACT:

ACS Publications Customer Services & Information (CSI)

Email: support@services.acs.org

Phone: 202-872-4357

Toll Free Phone: 800-227-9919 (USA/Canada only)

<https://mail.google.com/mail/u/0/?ik=ae189121fa&view=pt&search=all&permmsgid=msg-f%3A1726992279052633016&siml=msg-f%3A1726992...> 1/2

9/2/22, 12:02 PM

Department of Chemical Engineering, Diponegoro University Mail - Silviana, S. ie-2022-004247 -- Manuscript Formatting Req...

PLEASE NOTE: This email message, including any attachments, contains confidential information related to peer review and is intended solely for the personal use of the recipient(s) named above. No part of this communication or any related attachments may be shared with or disclosed to any third party or organization without the explicit prior written consent of the journal Editor and ACS. If the reader of this message is not the intended recipient or is not responsible for delivering it to the intended recipient, you have received this communication in error. Please notify the sender immediately by e-mail, and delete the original message.

As an author or reviewer for ACS Publications, we may send you communications about related journals, topics or products and services from the American Chemical Society. Please email us at pubs-comms-unsub@acs.org if you do not want to receive these. Note, you will still receive updates about your manuscripts, reviews, or future invitations to review.

Thank you.

<https://mail.google.com/mail/u/0/?ik=ae189121fa&view=pt&search=all&permmsgid=msg-f%3A1726992279052633016&simpl=msg-f%3A1726992...> 2/2

Resubmission of the Revised Manuscript (28 April 2022)

9/2/22, 12:20 PM

Department of Chemical Engineering, Diponegoro University Mail - Industrial & Engineering Chemistry Research - Manuscript...



Silviana Silviana <silviana@che.undip.ac.id>

Industrial & Engineering Chemistry Research - Manuscript ID ie-2022-004247.R1

Industrial & Engineering Chemistry Research <onbehalf@manuscriptcentral.com> Thu, Apr 28, 2022 at 11:04 PM
Reply-To: support@services.acs.org
To: silviana@che.undip.ac.id
Cc: nenoff-office@iecr.acs.org, silviana@che.undip.ac.id, atikahayujanita@gmail.com, afr312000@gmail.com, dalanta@student.undip.ac.id

28-Apr-2022

Title: "Synthesis of aminopropyl-functionalized mesoporous silica derived from geothermal silica for effective slow-release urea carrier"
Authors: Silviana, S.; Janitra, Atikah; Sa'adah, Afriza; Dalanta, Febio
Manuscript ID: ie-2022-004247.R1
Materials and Interfaces
Manuscript Status: Submitted

Dear Dr. Silviana:

Your manuscript has been successfully submitted to Industrial & Engineering Chemistry Research.

Please reference the above manuscript ID in all future correspondence or when calling the office for questions. If there are any changes in your contact information, please log in to ACS Paragon Plus with your ACS ID at <http://acsparagonplus.acs.org/> and select "Edit Your Profile" to update that information.

You can view the status of your manuscript by checking your "Authoring Activity" tab on ACS Paragon Plus after logging in to <http://acsparagonplus.acs.org/>.

ACS Authoring Services

Did you know that ACS provides authoring services to help scientists prepare their manuscripts and communicate their research more effectively? Trained chemists with field-specific expertise are available to edit your manuscript for grammar, spelling, and other language errors, and our figure services can help you increase the visual impact of your research.

Visit <https://authoringservices.acs.org> to see how we can help you! Please note that the use of these services does not guarantee that your manuscript will be accepted for publication.

Thank you for submitting your manuscript to Industrial & Engineering Chemistry Research.

Sincerely,

Industrial & Engineering Chemistry Research

PLEASE NOTE: This email message, including any attachments, contains confidential information related to peer review and is intended solely for the personal use of the recipient(s) named above. No part of this communication or any related attachments may be shared with or disclosed to any third party or organization without the explicit prior written consent of the journal Editor and ACS. If the reader of this message is not the intended recipient or is not responsible for delivering it to the intended recipient, you have received this communication in error. Please notify the sender immediately by e-mail, and delete the original message.

As an author or reviewer for ACS Publications, we may send you communications about related journals, topics or products and services from the American Chemical Society. Please email us at pubs-comms-unsub@acs.org if you do not want to receive these. Note, you will still receive updates about your manuscripts, reviews, or future invitations to review.

Thank you.

Responses to Reviewer Comments

Reviewers' Comments Responses

Synthesis of aminopropyl-functionalized mesoporous silica derived from geothermal silica for effective slow-release urea carrier

Reviewer #1

No	Comments	Response
1	Page 1, left column. Reference is made to a number of slow release materials. Do the authors know how much they slow the release of urea, and how it compares to what was developed here? It would also be helpful if the authors could provide some idea of how long in actual field applications the slow release of urea needs to be controlled? Is this length of time longer than one would expect that the "natural Materials" (cellulose, chitosan, attapulgite, algininate, starch 36, and lignin 28.) would survive degradation by microbes. Note also, Attapulgite is a "clay mineral" and like the silica base developed here it is not likely to degrade, except over "geologic" spans of time. Finally it seems likely the deterioration of concern relates to the impact of microbes on the complex organic coatings used to enhance performance, and not the deterioration of the bulk substrate itself.	<p>Thank you for the comment.</p> <p>Slow-release urea synthesized in this study released about 64.4% urea on the seventh day, comparable with lower release rate compared to referred studies.</p> <p>Some referred studies:</p> <p>- Azeem, B.; KuShaari, K.; Man, Z. B.; Basit, A.; Thanh, T. H. (2014): Review on materials & methods to produce controlled release coated urea fertilizer <i>J. Control. Release</i> 2014, <i>181</i> (12), 11–21. https://doi.org/10.1016/j.jconrel.2014.02.020 <u>Sulfur-only coated urea: 83% release after 7 days.</u></p> <p>- Maghsoodi, M. R.; Najafi, N.; Reyhanitabar, A.; Oustan, S. (2020) Hydroxyapatite nanorods, hydrochar, biochar, and zeolite for controlled-release urea fertilizers. <i>Geoderma</i> 2020, <i>379</i>, 114644. https://doi.org/10.1016/j.geoderma.2020.114644 <u>Impregnation of urea using hydroxyapatite (HAP): 88% urea release after 460s.</u></p> <p>- Pereira, E. I.; da Cruz, C. C. T.; Solomon, A.; Le, A.; Cavigelli, M. A.; Ribeiro, C. (2015) Novel Slow-Release Nanocomposite Nitrogen Fertilizers: The Impact of Polymers on Nanocomposite Properties and Function. <i>Ind. Eng. Chem. Res.</i> 2015, <i>54</i> (14), 3717–3725. https://doi.org/10.1021/acs.iecr.5b00176</p>

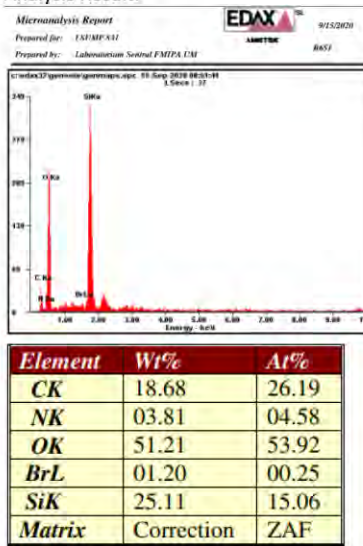
	<p><u>Bentonite in polycaprolactone or polyacrylamide hydrogel: 75% urea release after 30 or 60h.</u></p> <p>- Guo ; Liu; Zhan; Wu, L. (2005) Preparation and Properties of a Slow-Release Membrane-Encapsulated Urea Fertilizer with Superabsorbent and Moisture Preservation. <i>Ind. Eng. Chem. Res.</i> 2005, <i>44</i> (12), 4206–4211. https://doi.org/10.1021/ie0489406 <u>Slow-release membrane encapsulated urea with Superabsorbent and Moisture Preservation (SMUSMP) : 90% nitrogen release after fifth day.</u></p> <p>- Wang, Y. , Y.; Liu, M.; Ni, B.; Xie, L. (2012) Carrageenan–Sodium Alginate Beads and Superabsorbent Coated Nitrogen Fertilizer with Slow-Release, Water-Retention, and Anticompaction Properties. <i>Ind. Eng. Chem. Res.</i> 2012, <i>51</i> (3), 1413–1422. https://doi.org/10.1021/ie2020526 <u>Double-coated slow-release fertilizer using ethyl cellulose (EC and starch-based superabsorbent polymer: 70% urea release at 96h.</u></p> <p>As for organic coatings degradation, similar compounds studied by Emily Asenath Smith and Wei Chen (2008) <i>How to Prevent the Loss of Surface Functionality Derived from Aminosilanes</i> DOI: 10.1021/la802234x can be referred to. Smith and Chen studied degradation of silane agents by simulating biological media in a slightly accelerated manner.</p> <p>APTES incorporated with APTMS used in the study is susceptible to hydrolysis after 24h, but shows hydrolytically stable results after 48h. While the study was not conducted in actual field application, it shows that silane agent such as APTMS can reach hydrolytically stability from biological degradation. Please do note that the study was conducted by</p>
--	---

		<p>simulating in a slightly accelerated manner. Therefore, deterioration concern regarding complex organic compound might be minimized.</p> <p>As of our study, field application was done every 7 days, which is the time when the farmers in Indonesia monitor the effect of their fertilizer on their plants. By analyzing the plants condition at the 7th until the 14th day, they determine whether to add more fertilizer or not. From the experimental results, it was shown that commercial urea almost completely leached out after seven days, thus more fertilizer should be added every seventh day. Compared to slow release urea, with around 30% less release rate, fertilizer addition can be executed every nine to ten days, therefore the product can reduce the total amount of required fertilizer prior harvesting.</p>
2	Page 1, left column, line 38: The authors investigated comparative leaching behaviors – would they care to comment on ammonium volatilization.	<p>Thank you for your comment.</p> <p>It looks like that we've made a mistake in phrasing the words "ammonium volatilization". It should be "ammonia volatilization" which is a process that occurs when ammonium-fertilized soil lost its nitrogen content due to environmental factors (in the form of ammonia).</p> <p>We have revised the term accordingly.</p>
3	Page 2, paragraph 2. The procedure outlined for purifying the geothermal silica seems a trifle cumbersome; why not just use a commercial sodium silicate solution as a starting material?	<p>Thank you for your comment.</p> <p>While it's possible to use commercial sodium silicate, we did this research not solely based on economical reason, but also as a waste management method. Our raw material (geothermal solid silica waste) is considered as waste and become one of main problems of geothermal power plant in Dieng, Java, Indonesia. Currently, it is just stored in waste disposal area such as a big landfill area without any further treatment and its quantity increases up to 10 tons/day.</p>

		<p>Moreover, commercial silica (95%-99%) in Indonesia costs about US\$ 200 per ton while sodium silicate costs about US\$ 4,000 per ton. It also needs to be transported from the mining and processing industry (Bangka, Sumatera) to agriculture-based area in Indonesia (Java).</p> <p>By utilizing this geothermal silica, we not only cut the costs for raw material and transportation, but also minimizing waste problem and fulfilling the need of waste management in the geothermal power plant itself.</p>
4	<p>Page 5. Line 56: Point out that the selection of "0.05 mole" CTAB as having the best response to calcination is based only on carbon and silicon, neither the nitrogen or bromine contents support this contention.</p>	<p>Thank you for the comment.</p> <p>CTAB $[(C_{16}H_{33})N(CH_3)_3]Br$ itself contains C (carbon), N (nitrogen), and Br (bromine) with C element having the most atom numbers compared to N and Br. Thus, we determined the best calcination respond based only on carbon and silicon. However, we did analyze N, O, and Br since silica and CTAB contains those elements.</p> <p>Nevertheless, we have revised the sentence by adding "based on C content" to point out our best response selection.</p>
5	<p>Page 8, "Thermal analysis of synthesized mesoporous silica" Were the TGA and DSC studies performed using air or an inert gas (Ar or N₂)?</p>	<p>Thank you for the question.</p> <p>TGA and DSC studies were done using inert N₂ (nitrogen) gas.</p> <p>We have also revised and added this information in the paper.</p> <p>Thank you.</p>
6	<p>Page 10, line 18, column 1: "MS/APTMS has 2.81%-wt of nitrogen" - this is not the same value as appears in the first entry (5.71 wt %) of Table 6.</p>	<p>Thank you for notifying us about this problem.</p> <p>We made a mistake when inserting the value of MS/APTMS nitrogen weight, we do apologize about this mistake. The values have been revised accordingly. Weight percentage of nitrogen should be 3.81%-wt instead of 2.81 %-wt and 5.71 %-wt. Please do note that the revised</p>

values are not only nitrogen but also the other detected elements.

Analysis Result:



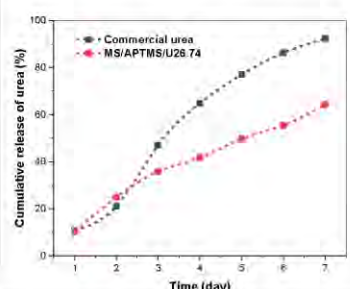
Thank you.

Thank you for the comment.



7 Page 3 (Performance test of the prepared slow-release urea) and Page 13 (Study of release kinetics of synthesized slow-release urea): First of all the authors need to say how much commercial urea was put into the leaching test apparatus for comparison. Table 6 states that MS/APTMS/U26.74 contains 5.17 weight % N while Page 2 line 11, column 2 states that commercial urea contains around 46% urea. If similar weights of the two materials were included in leaching tests then it would be expected that the releases from commercial urea would be greater than the urea loaded on the mesoporous silica simply because there was much more on the commercial urea to start with. And, more importantly, one cannot make the case that the MS/APTMS/U26.74 was effective at retarding urea releases unless one knows the relative amounts of urea put into the two leach tests.

Initial total urea content of each sample (commercial urea and slow-release fertilizers) was set to be 200 ppm. Therefore, the samples are not having the same weights, but the same initial urea content. In addition, commercial urea having 46% of nitrogen, not urea (urea is a compound by itself).

Commercial urea used in the study was 200 ppm. While the samples are immersed in different concentrations of urea but with the absorbed urea controlled at 200 ppm. By looking at the leach test results, commercial silica released more urea (at 184.5 ppm (92.4%)) compared to sample

		<p>MS/APTMS/U26.74 (124.6 ppm (64.4%)) on the seventh day.</p> <p>However, we do realize that this initial urea content was not stated in the manuscript and created misunderstanding. We have revised the "Study of release kinetics of synthesized slow-release urea" section by adding the sentence "Initial urea content in each sample was set to be 200 ppm".</p>																								
8	<p>Page 14, Fig. 10-B: It would be highly informative if the data in Fig. 10-B were used to determine what fraction of the total urea initially added to the experiments (as either commercial urea or as 1 gram of MS/APTMS/U26.74) was released during the relatively short term of the leaching tests.</p>	<p>Thank you for the suggestion.</p> <p>Since initial urea content inside the samples were 200 ppm, we have revised Fig. 10-B as fraction per total urea added.</p>  <table border="1"> <caption>Data points estimated from Fig. 10-B</caption> <thead> <tr> <th>Time (day)</th> <th>Commercial urea (%)</th> <th>MS/APTMS/U26.74 (%)</th> </tr> </thead> <tbody> <tr><td>1</td><td>10</td><td>10</td></tr> <tr><td>2</td><td>25</td><td>20</td></tr> <tr><td>3</td><td>45</td><td>35</td></tr> <tr><td>4</td><td>65</td><td>45</td></tr> <tr><td>5</td><td>80</td><td>55</td></tr> <tr><td>6</td><td>90</td><td>60</td></tr> <tr><td>7</td><td>95</td><td>65</td></tr> </tbody> </table>	Time (day)	Commercial urea (%)	MS/APTMS/U26.74 (%)	1	10	10	2	25	20	3	45	35	4	65	45	5	80	55	6	90	60	7	95	65
Time (day)	Commercial urea (%)	MS/APTMS/U26.74 (%)																								
1	10	10																								
2	25	20																								
3	45	35																								
4	65	45																								
5	80	55																								
6	90	60																								
7	95	65																								

Reviewer #2

No	Comments	Responses
1	It is not admissible to give surface area values with one or two decimal digits. Even in the abstract section.	<p>Thank you for the comment.</p> <p>We have revised surface area values to three decimal digits, the values we obtained from BET-BJH analysis report. We do round the values to two decimal digits previously.</p> <p>Geothermal silica</p>  <p>Purified silica after leaching</p>  <p>CTAB 0.015 mole</p>

		<div data-bbox="869 336 1244 627"> <p>Quantachrome Autosorb™ Automated Gas Sorption Data Adsorption and Desorption v18m-2015, Quantachrome Instruments version 3.01</p> <p>Analysis Sample ID: LAC2P Sample Name: 20150117 Sample Weight: 0.0000 g Sample Temp: 25.00 °C Analysis Date: 2/13/2015 Analysis Time: 10:00:00 Analysis Mode: Static Analysis Mode: Air/Water</p> <p>Report Date: 2/13/2015 Filename: 20150117 LAC2P Sample ID: LAC2P Sample Name: 20150117 Sample Weight: 0.0000 g Sample Temp: 25.00 °C Analysis Date: 2/13/2015 Analysis Time: 10:00:00 Analysis Mode: Static Analysis Mode: Air/Water</p> <p>Multi-Point BET</p> <p>Data Reduction Parameters Data</p> <p>Adsorption</p> <p>Multi-Point BET Data</p> <p>BET Analysis</p> </div> <p>CTAB 0.03 mole</p> <div data-bbox="869 683 1244 974"> <p>Quantachrome Autosorb™ Automated Gas Sorption Data Adsorption and Desorption v18m-2015, Quantachrome Instruments version 3.01</p> <p>Analysis Sample ID: LAC2P Sample Name: 20150117 Sample Weight: 0.0000 g Sample Temp: 25.00 °C Analysis Date: 2/13/2015 Analysis Time: 10:00:00 Analysis Mode: Static Analysis Mode: Air/Water</p> <p>Report Date: 2/13/2015 Filename: 20150117 LAC2P Sample ID: LAC2P Sample Name: 20150117 Sample Weight: 0.0000 g Sample Temp: 25.00 °C Analysis Date: 2/13/2015 Analysis Time: 10:00:00 Analysis Mode: Static Analysis Mode: Air/Water</p> <p>Multi-Point BET</p> <p>Data Reduction Parameters Data</p> <p>Adsorption</p> <p>Multi-Point BET Data</p> <p>BET Analysis</p> </div> <p>CTAB 0.05 mole</p> <div data-bbox="869 1030 1244 1321"> <p>Quantachrome Autosorb™ Automated Gas Sorption Data Adsorption and Desorption v18m-2015, Quantachrome Instruments version 3.01</p> <p>Analysis Sample ID: LAC2P Sample Name: 20150117 Sample Weight: 0.0000 g Sample Temp: 25.00 °C Analysis Date: 2/13/2015 Analysis Time: 10:00:00 Analysis Mode: Static Analysis Mode: Air/Water</p> <p>Report Date: 2/13/2015 Filename: 20150117 LAC2P Sample ID: LAC2P Sample Name: 20150117 Sample Weight: 0.0000 g Sample Temp: 25.00 °C Analysis Date: 2/13/2015 Analysis Time: 10:00:00 Analysis Mode: Static Analysis Mode: Air/Water</p> <p>Multi-Point BET</p> <p>Data Reduction Parameters Data</p> <p>Adsorption</p> <p>Multi-Point BET Data</p> <p>BET Analysis</p> </div>
2	<p>This sentence “SEM showed functionalization and urea adsorption to mesoporous silica resulted in no significant microstructure changes” is confused and must be rewritten</p>	<p>Thank you for the comment.</p> <p>By “no significant microstructure changes”, we refer to “no changes in its morphology when viewed using SEM”. Nevertheless, we do agree that the term “microstructure” might be confusing, therefore, we have revised</p>

		“microstructure” to “morphology” as a more general term.
3	The cost of the prepared silica is very high due to the use of a high cost surfactant and the amino compound, and the purification of the geothermal silica. For this reason, the possible application of this materials as potential slow release fertilizer is not viable from the economic viewpoint.	<p>Thank you for the comment.</p> <p>This study was conducted not only for economic reasons but also as a waste treatment method. Our raw material (geothermal solid silica waste) is considered waste and is one of the major problems with the geothermal power plant in Dieng, Java, Indonesia. Currently, it is dumped in landfills without further treatment, and the amount has increased to 10 tons per day.</p> <p>In addition, in Indonesia, commercially available silica (95%-99%) costs about US \$ 0.2 / kg, while sodium silicate (purified silica precursor) costs about US \$ 4 / kg. It also needs to be transported from the mining and processing industries (Bangka, Sumatra) to the agricultural areas of Indonesia (Java).</p> <p>This geothermal silica not only reduces raw material and transportation costs, but also minimizes waste problems and addresses the waste disposal needs of the geothermal power plant itself.</p> <p>As for the surfactant (i.e. CTAB and APTMS), it is unfortunate that those compounds are not produced locally and need to be ordered overseas. Still, their usages are merely around 0.05% of sodium silica weight.</p> <p>Amino compound used in this study is locally available commercial urea, which is absorbed into the mesoporous silica. Looking at the results that cumulative urea release of slow-release fertilizer is 30% slower than commercial urea, it can increase efficiency in urea usage (by preventing ammonia volatilization and minimizing leached urea) as an advantage in determining its value.</p>

4	Please, it a mistake to write Ammonium hydroxide (NH ₄ OH, 25%). This is a non-existent compound. Write aqueous ammonia.	<p>Thank you for the suggestion.</p> <p>We do sorry about our mistake, it seems like that aqueous ammonia is indeed the correct way to address NH₄OH, 25%. We have revised the chemical name accordingly.</p>
5	The presence of Cr ₂ O ₃ is another drawback for using this silica. This point must be indicated.	<p>Thank you for the comment.</p> <p>We do agree that geothermal silica waste contains Cr₂O₃ which is one of the drawbacks in using this material since this compound is not very reactive. However, it dissolves in acid as hydrated chromium ions [Cr(H₂O)₆]³⁺.</p> <p>We have revised the manuscript to indicate this drawback.</p>
6	The discussion contains sentences that include errors in basic chemical concepts. For example, in this sentence "the repulsion force between ion Si ⁺ and N ⁺ is so dominant that the surfactant cannot be accessed."	<p>Thank you for the comment.</p> <p>We do apologize for our error. It seems that we did some mistakes in assessing the attraction/repulsion force between the ions. We have revised the manuscript by omitting this sentence to prevent any misunderstanding.</p>
7	There are many other basic mistakes along the text.	<p>Thank you for your comment.</p> <p>We have done our best to revise some basic mistakes and revised some errors.</p>

Synthesis of aminopropyl-functionalized mesoporous silica derived from geothermal silica for effective slow-release urea carrier

S. Silviana*, Atikah A. Janitra, Afriza N. Sa'adah, Febio Dalanta

Department of Chemical Engineering, Faculty of Engineering, Diponegoro University, Tembalang, Semarang, 50275, Indonesia

Keywords: slow-release urea, mesoporous silica, aminopropyl-functionalized material, modified silica, urea.

ABSTRACT: Prominent slow-release urea was developed with aminopropyl-functionalized mesoporous silica to enhance urea adsorption and slow-release property. As novelty study, mesoporous silica was developed using treated geothermal silica as silica source, CTAB surfactant, and APTMS surface modification agent. The most desirable mesoporous silica with uniform micromorphology containing 38.55 %-wt silica particles, 668.849 m²/g surface area, 149.33 – 353.28 mL/g adsorption-desorption range, 0.26 mL/g adsorption pore volume were achieved using 0.05 mole CTAB. Synthesized mesoporous silicas showed type-IV hysteresis, which corresponds to mesoporous material. DSC-TGA thermograms showed that mesoporous silica becomes more reactive with peaks at 82.3 °C and 159.5 °C, having good thermal stability, only experienced 17.61% weight loss until 124 °C. SEM showed functionalization and urea adsorption to mesoporous silica resulted in no significant morphological changes. From FTIR spectra, MS/APTMS/U26.74 was observed to have higher C=O, N-H, C-N, C-H groups intensity among other samples. Cumulative urea release during seven days was 184.5 ppm (92.4%) for commercial urea and 124.6 ppm (64.4%) for MS/APTMS/U26.74. Higuchi kinetic model performed the best fit predicting MS/APTMS/U26.74 release kinetics with R² 0.9979 and Higuchi constant 24.4964 %day^{1/2}. Finally, synthesized MS/APTMS/U26.74 using geothermal silica, CTAB, APTMS can be noted as potential composition for slow-release urea to enhance efficiency.

INTRODUCTION

Nowadays, urea has been widely used as fertilizer^{1,2}, source of nitrogen in ruminants^{3,4}, pesticides^{5,6}, microbial growth^{7,8}, and various agriculture activities due to its rich nitrogen content, abundance, and cost-effectiveness. However, several studies reported that the high content of urea fertilizer is lost caused by leaching and ammonia volatilization⁹ upon application in soil, eventually generating severe environmental pollution, especially in soil and water sources.¹⁰⁻¹² Therefore, slow-release urea (SRU) development becomes a manner to improve urea efficiency, controllable usage and minimize the environmental drawbacks. Recently, SRUs are commonly prepared by encapsulating or adsorbing saturated urea solution to a porous matrix medium such as zeolites¹³⁻¹⁵, porous polymer composites¹⁶⁻¹⁸, or mesoporous materials¹⁹⁻²⁴ in order to control the urea release. Several polymers have been performed for SRU matrix media, such as polyacrylonitrile^{25,26}, polysulfone¹⁰, poly (vinyl chloride)²⁷, polyacrylic-rubber²⁸, poly (vinyl acetate)²⁹, and polyurethane³⁰. Sulfur-only coated urea releases 83% urea after 7 days³¹, while using impregnation using hydroxyapatite having release rate of 88% after 460s¹⁴. Another study using bentonite in polycaprolactone or polyacrylamide hydrogel yields 75% urea release after 30 or 60h¹⁵. Slow-release membrane encapsulated urea yields 90% nitrogen release after fifth day²⁵ and double-coated slow-release fertilizer using ethyl cellulose (EC and starch-based superabsorbent polymer) yields 70% urea release at 96h³¹. However, those polymers generate additional environmental issues in terms of the remaining non-biodegradable polymer waste after they are used. Therefore, the application of bio-

degradable polymers has been carried out to solve the environmental issue of using conventional polymers on SRU. Natural polymers have been applied as the matrix medium for SRU, including inorganics such as attapulgite^{31,31} and organics such as cellulose³³, chitosan³⁴, alginate^{35,36}, starch³⁷, and lignin³⁸. Nevertheless, due to their natural characteristics, those natural polymers are easily attacked by fungi, bacteria, and other microorganisms, causing a lack of performance. Therefore, further investigations to develop the prominent matrix material for enhancing SRU characteristics and performance are still needed, and there remains big room to be studied.

Mesoporous silica (MS) has gained high attention caused by their potential in various utilizations, including drug delivery³⁹⁻⁴⁰, catalysis⁴¹, adsorbent⁴², sensing⁴³, and antibiotic-free antibacterial applications⁴⁴. Due to the silica chemistry, MS has an ease to be functionalized and controllable tailoring, which allows it to be designed for the desired applications, including as the matrix medium for SRU. Many works have been conducted to synthesize MS with different structures, compositions, and pore properties to achieve desired and tunable characteristics^{23,41,45,46}. Type of precursor, pH, reaction time, temperature, type and concentration of catalyst, co-solvent, and surfactant are the main influencers of the final properties of synthesized MS^{39,41,43}. Several synthesis procedures have been reported in order to have tunable and controllable MS properties, generally conducted in acid and basic media^{45,45,47}. On both conditions, the effect of reaction temperature, surfactant, co-solvent, and additives concentrations was observed, and numerous MS properties have been clearly explained^{39,45,47}. The high specific surface area, high porosity, tunable network framework structure can enable the massive binding sites

for urea in this matrix medium. However, it has also been reported that thickness, hydrophilicity, and layer structure of matrix medium strongly affect the release rate of SRU^{28,30,34,47}. Consequently, to achieve the maintainable rate of urea from the slow-release urea, further modification and/or functionalization of the SRU matrix medium is highly required.

Aminopropyl-functionalized materials have gained high interest due to their strong absorption against several chemicals such as amine, phosphate, and nitrate. The presence of an amine group on aminopropyl-functionalized silica, which has a similar amine functional group as urea, caused the crystallization of urea by hydrogen bonding with other amine groups. It acts as a seed to initiate crystallization of the urea network, thus enhancing the absorption of urea on the surface of an aminopropyl-functionalized silica^{34,48,49}. Various organometallic groups have been utilized to functionalize adsorption-based materials and enhance the capacity of adsorption and produce controllable kinetics^{50,51}. Currently, the most investigated aminopropyl-functionalized material is biochar or activated carbon. Nevertheless, those materials preferably have developed surface morphology, but the micropores domination alters adsorbate diffusion into the pores generating a decrease in adsorption capacity. Compared to the biochar or activated carbon, MS has a high specific surface area, ordered pores, and relatively high pore volumes indicating a potential material for adsorbent with controllable diffusion behavior^{25,58}. Therefore, it was hypothesized that functionalization of MS for SRU matrix medium to enhance the performance of SRU in terms of high urea adsorption capacity and controllable diffusion of urea from the synthesized SRU to the soil.

In this study, the synthesis of SRU with MS as the matrix medium was prepared from geothermal silica. Geothermal silica can be applied as the silica source to synthesize MS due to its high content of SiO₂, which has been applied in numerous applications^{52–57}. The geothermal silica was purified using acid leaching treatment before it was used. The purified silica was converted to sodium silicate as the precursor of silica source in MS preparation. Cetyltrimethylammonium bromide (CTAB) was used as the surfactant, and the mole amounts of CTAB were varied to investigate the impacts on the synthesized MS properties. The synthesized MS was further functionalized by covalently grafting the aminopropyl groups on the MS surface using a 10% 3-Aminopropyl trimethoxy silane (APTMS) solution to enhance the sorption capacity and slow-release properties of the synthesized slow-release urea. The essentials analysis, including morphology, chemical groups and compositions, surface area involving gas sorption, hysteresis behaviors, pore characteristics, and thermal properties, were comprehensively characterized using scanning electron microscopy (SEM), energy dispersive x-ray (EDX), x-ray fluorescence (XRF), x-ray diffraction (XRD), Fourier-transform infrared (FTIR), Brunauer-Emmet-Teller and Barrett-Joyner-Halenda (BET-BJH) analysis, thermogravimetric analysis (TGA), and differential scanning calorimetry (DSC). The synthesized slow-release urea was experimentally tested in the soil to investigate the release characteristics and its comparison to the commercial urea. The release kinetics of the synthesized slow-release urea were also studied by applying several appropriate kinetic models. As a novelty, the study of slow-release urea synthesis using aminopropyl-functionalized MS as the matrix derived from geothermal silica as the silica source and CTAB as the surfactant has not yet been reported in other previous studies.

MATERIALS AND METHODS

Materials

The geothermal silica sample as the primary raw material for mesoporous silica synthesis was supplied from the geothermal power plant of PT. Geo Dipa Energi, Dieng, Indonesia. Cetyltrimethylammonium bromide (CTAB, 99–101%) and 3-Aminopropyl trimethoxy silane (APTMS, 99.8%) were purchased from Himedia and Sigma Aldrich, Germany, respectively. Sulfuric acid (H₂SO₄, 98%), sodium hydroxide (NaOH, 95%), and hydrochloric acid (HCl, 36.5–38%) that was used in purification treatments of geothermal silica were supplied from Mallinckrodt, USA. Aqueous ammonia (NH₄OH, 25%) and ethanol (C₂H₅OH, 96%) utilized in the preparation were purchased from Merck, Germany. Commercial urea (Nitrogen ≥ 46%) was supplied from PT. Petrokimia Gresik, Indonesia. Distilled (DI) water was utilized in all experiments.

Methods

Purification treatments of geothermal silica samples

Geothermal silica contains contaminants. Therefore, it required purification treatment to produce high purity of silica as the primary material to synthesize mesoporous silica^{58–62}. There were two steps of purification treatments, i.e., acid leaching and sodium silicate process. Firstly, 250 g of geothermal silica sample was dried in an oven at 110 °C for 12 h to reduce its moisture content. Then, the dried sample was crushed into fine powder. This sample was then checked by X-ray Fluorescence (XRF, Thermo Fisher Scientific, USA) and X-ray Diffraction (XRD, Thermo Fisher Scientific, USA) instruments to reveal its chemical composition and the amorphous structure. Next, acid leaching treatment was conducted based on the methods recently reported^{58,59}. Such amounts of 125 g of treated geothermal silica were carefully dispersed and constantly mixed in 500 mL of 20% H₂SO₄ solution at 100 °C for 105 min. The acid processing by H₂SO₄ is intended to remove the residual impurities on the sample, specifically the metal oxides content. After that, repeated washing and rinsing were done to the residue to remove any unspent acid until achieving a neutral pH. The residue was then placed in an oven at a temperature of 110 °C until completely dried. The treated silica from this step was analyzed using XRF and XRD.

The second purification step was conducted by filtering out the sodium silicate to further purify the treated silica from insoluble impurities. This procedure was conducted based on the method previously reported^{55,59}. It was started by mixing 125 g of treated silica sample with 600 mL of 4 M NaOH solution and was stirred and maintained at 90 °C for 60 min. After that, the mixture was filtered through a filter paper (Whatman No.42) using a vacuum filter. The generated filtrate was sodium silicate that was further applied as the precursor to synthesize mesoporous silica.

Synthesis of mesoporous silica

This step followed the modified Stöber method that was previously reported^{59–61}. Firstly, the primary solution was made of 10 moles of ethanol, 22.4 moles of water, and 5.2 moles of NH₄OH. The solution was constantly mixed at low speed (80–100 rpm) for 15 min. After that, CTAB as a surfactant was slowly added into the solution with variations of 0.015, 0.03, and 0.05 moles. Sodium silicate was prepared by dissolving 10 g treated silica in 82.5 mL of NaOH 4 M. Next, 100 mL of prepared sodium silicate solution was slowly

added to the solution. The solution turned opaque immediately, indicating the reaction has started. The solution was continuously mixed and maintained for 2 h at room condition. After that, the solution was filtered to separate the solids as the generated mesoporous silica from the mixture through a filter paper (Whatman No. 42) using a vacuum filter. Subsequently, the solids were washed to remove any unspent solution. The solid was then calcined using a furnace burner at 550 °C to remove the remaining organic compounds, creating mesoporous structure throughout the surface of the silica. The prepared mesoporous silica was characterized using a Scanning Electron Microscopy Energy Dispersive X-ray (Thermo Fisher Scientific, USA), Brunauer-Emmet-Teller Barrett-Joyner-Halenda (BET-BJH) (autosorb IQ Quantachrome Instruments from Anton Paar Switzerland AG), Thermal Analysis of TG/DTA/DSC (Linseis STA 1600 Premium Series, USA), and Fourier Transform Infrared (IRPrestige21, Shimadzu Japan by transmittance mode of acquisition).

Purification treatments of geothermal silica samples

This procedure was based on previously reported studies^{49,50}. In this method, APTMS was utilized as a silane coupling agent to modify the surface characteristic of mesoporous silica. Firstly, calcined mesoporous silica was carefully mixed at 150 rpm with 10% APTMS solution at room temperature for 8 h. This step was conducted to perform the surface modification reaction on the surface of mesoporous silica for a slow-release urea. It was then dried in an atmospheric pressure drying at 40 °C. Finally, the modified mesoporous silica with APTMS was characterized using BET-BJH analysis and FTIR.

Next, a gram of modified mesoporous silica/APTMS was added to the urea solution (U) with certain concentrations (6.74, 16.74, 26.74, and 36.74 %-wt) on the basis of 100 ml aquadest. The mesoporous silica/APTMS with different urea compositions is represented in Table 1. The mixture was constantly stirred for 24 h at room temperature to perform the adsorption of urea into the mesoporous silica by hydrogen bonding³⁸. Afterward, it was filtered, and the solids were dried in an oven with a temperature of 40 °C. Finally, the generated solids were characterized using FTIR.

Table 1. Contents of CTAB, APTMS, and Urea in Preparation of the Slow-release Urea

Sample code	CTAB (mole)	APTMS solution (%)	Urea solution (%-wt)
MS	0.05	0	0
MS/APTMS	0.05	10	0
MS/APTMS/U6.74	0.05	10	6.74
MS/APTMS/U16.74	0.05	10	16.74
MS/APTMS/U26.74	0.05	10	26.74
MS/APTMS/U36.74	0.05	10	36.74

Performance test of the prepared slow-release urea

The slow-release urea performance was experimentally assessed by measuring the value of urea carried out in overflow liquid. The test was applied for determining the dissolved urea content in groundwater. Figure 1. depicts the schematic illustration of the respective experiment. Initially, a gram of slow-release urea was immersed in 25 g of soil in a plastic vase. Subsequently, 25 mL of DI water was used for watering the sample every day for seven days of observation and the overflow water from the vase was carefully collected. This test was repeated for three replications. The urea content in the overflow liquid was measured using a UV-vis spectrophotometer (Thermo Scientific[®] GENESYS 10S, USA). The measurement was performed at an optimum wavelength of 195 nm, while this wavelength closed to previous research i.e., 190 nm⁶².



Figure 1. Schematic illustration of the apparatus for slow-release urea performance test.

Study of urea release kinetics

The mechanism of urea release from the slow-release urea was theoretically evaluated by applying some kinetic models, which were pseudo-first order, pseudo-second order, Higuchi, and Hixson-Crowell models. The mathematical expressions of the pseudo-first order, pseudo-second order, Higuchi, and Hixson-Crowell are represented by Eq. (1)-(4).

Pseudo-first order model⁶²:

$$\ln Q_t = \ln Q_o - k_1 t \quad (1)$$

Pseudo-second order model⁶⁴:

$$\frac{t}{Q_t} = \frac{1}{k_2 Q_o^2} - \frac{t}{Q_o} \quad (2)$$

Higuchi model⁶⁵:

$$Q_t = K_H t^{1/2} \quad (3)$$

Hixson-Crowell model⁶³:

$$Q_o^{1/3} - Q_t^{1/3} = K_{HC} t \quad (4)$$

Where Q_t is the released amount of urea at a certain time (%), Q_o is the initial amount of urea in the slow-release urea (%), k_1 is the pseudo-first order rate constant, k_2 is the pseudo-second order rate constant, K_H is the Higuchi constant, K_{HC} is the Hixson-Crowell constant, and t is time (day).

RESULTS AND DISCUSSION

Properties of purified silica after acid leaching treatment

The sample of geothermal silica was treated using acid leaching treatment to remove the impurities, especially the metal oxides. Figure 2(a). depicts the XRF results of geothermal silica and the purified silica after acid leaching. The chemical composition of geothermal silica was found that consist of 86.3 %-wt of SiO_2 , with fairly high metal oxides including CaO , Fe_2O_3 , Cr_2O_3 , K_2O , and MnO with compositions of 3.21, 3.59, 0.07, 5.67, and 0.09 %-wt, respectively. The presence of Cr_2O_3 is one of the drawbacks in using this geothermal silica since this compound is not very reactive, but dissolves in acid as hydrated chromium ions $[\text{Cr}(\text{H}_2\text{O})_6]^{3+}$. This sample of geothermal silica was treated in 500 mL of 20% H_2SO_4 solution at 100 °C for 105 min to dissolve the metal oxides into the sulfuric acid. The XRF analysis of silica product after acid leaching revealed that the sample consists of 95 %-wt of SiO_2 and leaving the minor amount of metal oxides such as CaO , Cr_2O_3 , K_2O , and MnO with compositions of 0.43, 0.42, 0.22, and 2.00 %-wt, respectively. Based on this analysis, the acid leaching process significantly removed the metal oxides from the geothermal silica resulting in a higher purity of silica. The influence of acid leaching treatment is further evaluated by XRD analysis.

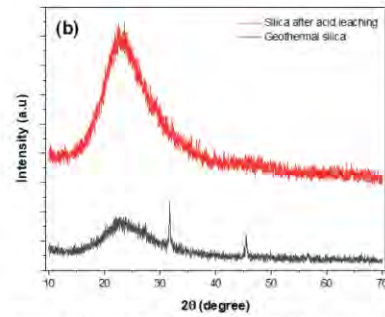
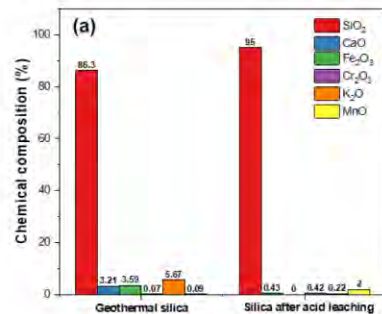


Figure 2. (a) XRF results of geothermal silica sample and purified silica after acid leaching process, and (b) XRD diffractograms of geothermal silica and purified silica after acid leaching.

Figure 2(b). represents the XRD diffractograms of geothermal silica and the purified silica after acid leaching. From the diffractogram pattern of geothermal silica, it can be seen a broad peak ranging from 2θ of $15^\circ - 30^\circ$, indicating the existence of amorphous SiO_2 . Three significant sharp peaks were found at 32.5° , 46.3° , and 49.8° , which correspond to Fe_2O_3 , K_2O , and Cr_2O_3 in the sample³⁸. The purified silica after acid leaching was also evaluated by XRD analysis. It can be clearly observed that the purified silica has a more significant broad peak at 2θ of $15^\circ - 30^\circ$, which indicates a higher amount of amorphous SiO_2 than the geothermal silica sample. Also, there are no other metal oxides peaks appearing in the diffractogram of the purified silica. Therefore, it can be reasonably concluded that the acid leaching treatment successfully removed the metal oxides content in the geothermal silica. Silica with higher purity ($\geq 95\%$) can be utilized as the main material for synthesizing mesoporous silica with higher Si content on its surface where surface modifying agents can react to.

Characterizations of synthesized mesoporous silica

Surface micrographs and chemical composition of synthesized mesoporous silica

In this study, the modified Stober method was adapted in the synthesis of mesoporous silica. The reaction was conducted at room temperature using CTAB as a surfactant, aqueous NH_4OH as a catalyst, ethanol as a co-solvent, sodium silicate derived from geothermal silica as the silica source. For the different formulations of material synthesis, the amount of NH_4OH , ethanol, and sodium silicate were maintained fixed, while the amount of CTAB was varied at 0.015, 0.03, and 0.05 mole. Hence, the effects of CTAB mole amount in mesoporous silica synthesis were experimentally investigated. It was found that the different amount of CTAB as a surfactant in mesoporous silica synthesis has a significant effect on the micromorphology of the synthesized mesoporous silica, as clearly revealed by SEM-EDX analysis in Figure 3. with 10.000x and 20.000x magnifications. Figure 3(a), 3(b), and 3(c) depict the surface morphology images of mesoporous silica with 0.015, 0.03, and 0.05 mole of CTAB, respectively.

The different mole amounts of CTAB resulted in the different shapes of mesoporous silica particles. In using CTAB 0.015 mole (Figure 3(a).), the synthesized mesoporous silica has a randomized shape and is fairly similar to CTAB 0.03 mole (Figure 3(b).) and has a little development of the mesoporous silica particle. Meanwhile, in using CTAB 0.05 mole, the synthesized mesoporous silica has a

more uniform particle shape. These findings suggest that the addition of CTAB tends to produce mesoporous silica particles. This phenomenon agrees with the previous study that an increasing

amount of surfactant produces the abundant interaction of two-counter charge surfactant resulting in the growing silicates particle⁶¹.

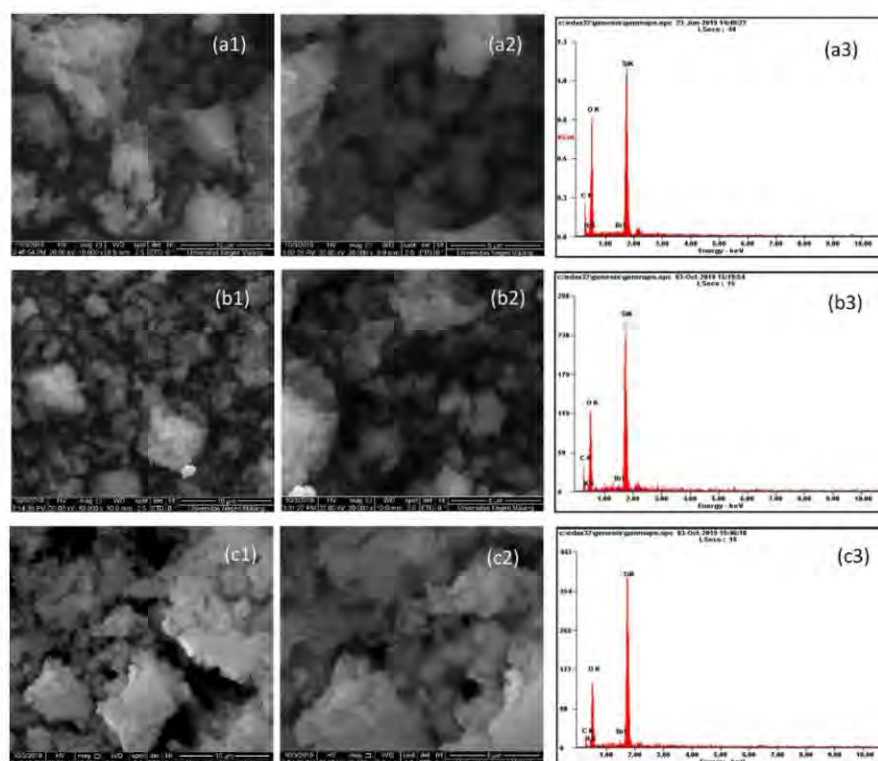


Figure 3. SEM-EDX micrographs of modified mesoporous silica using (a) 0.015 mole of CTAB, (b) 0.03 mole of CTAB, and (c) 0.05 mole of CTAB.

For further analysis, SEM-EDX analysis was carried out to reveal the chemical composition of synthesized mesoporous silica with different loaded amounts of CTAB. Figure 3. shows the EDX spectra for synthesized mesoporous silica with CTAB of 0.015 mole (Figure 3(a3).), 0.03 mole (Figure 3(b3).), and 0.05 mole (Figure 3(c3).). The quantification of EDX results is shown in Table 2, providing information about the chemical composition of the tested samples. Synthesized mesoporous silica with 0.015 mole, 0.03 mole, and 0.05 mole was recorded, consisting of 20.11, 23.70, and 35.88 %-wt of Si, respectively. The micrograph analysis resulted in the mesoporous silica from 0.05 mole CTAB visualized in white solid. According to previous research⁶⁶, CTAB surfactant can interact polarly with silica precursor. It can be observed that the hydrophilic head of CTAB can attach on the surface of silica, while the tail can be oriented to the polymer matrix. The phenomena of this interaction can be guessed by interaction between OH⁻ ion on the silica surface and N⁺ ion of the CTAB. At this step, the ion exchange and aggregate formation

can occur simultaneously. Furthermore, more mesoporous silica aggregates are released with higher CTAB. The aggregation of mesoporous silica is likely rectangular, detected by SEM analysis. Based on BET-BJH analysis, a higher amount of CTAB resulted in higher quality of mesoporous silica in terms of physical properties such as specific surface area, pore volume, and pore radius. Moreover, Si content as mesoporous silica can be detected higher at CTAB mole. Meanwhile, the components of C, N, and Br in EDX results were found as the remaining rest amount of CTAB in the synthesized mesoporous silica after calcination to remove the CTAB. It can be assumed that the calcination operation condition (at 550 °C for 3 h) did not completely decompose all the CTAB. It can be concluded that using 0.05 mole of CTAB provided the best mesoporous silica with high content of Si and lower content of unreacted CTAB (based on C content). These findings from EDX results are confirmed with SEM micrographs, as previously discussed.

Table 2. Chemical composition data extracted from EDX spectra for mesoporous silica using three different amounts of CTAB

Element	EDX recorded	MS-0.015 ^a		MS-0.03 ^b		MS-0.05 ^c	
		Weight (%)	Atomic (%)	Weight (%)	Atomic (%)	Weight (%)	Atomic (%)
Carbon	C K	25.16	33.59	27.94	27.66	11.42	17.36
Nitrogen	N K	4.08	4.67	2.59	3.00	2.72	3.54
Oxygen	O K	50.02	50.13	44.99	45.52	48.60	55.45
Bromine	Br K	0.64	0.13	0.78	0.16	1.38	0.32
Silicon	Si K	20.11	11.48	23.70	13.66	35.88	23.32

a) MS-0.015 represents the mesoporous silica with CTAB 0.015

b) MS-0.03 represents the mesoporous silica with CTAB 0.03

c) MS-0.05 represents the mesoporous silica with CTAB 0.05

Sorption isotherm and pore properties of synthesized mesoporous silica

The pore properties and sorption isotherm of several samples were analyzed using BET-BJH analysis by N₂ adsorption/desorp-

tion patterns. Figure 4. represents the sorption isotherm of geothermal silica (Figure 4(a).), purified silica by acid leaching (Figure 4(b).), synthesized mesoporous silica with CTAB 0.015 mole (Figure 4(c).), 0.03 mole (Figure 4(d).), and 0.05 mole (Figure 4(e).). Type IV of sorption isotherms class were developed for all samples indicating mesoporous materials⁶⁷.

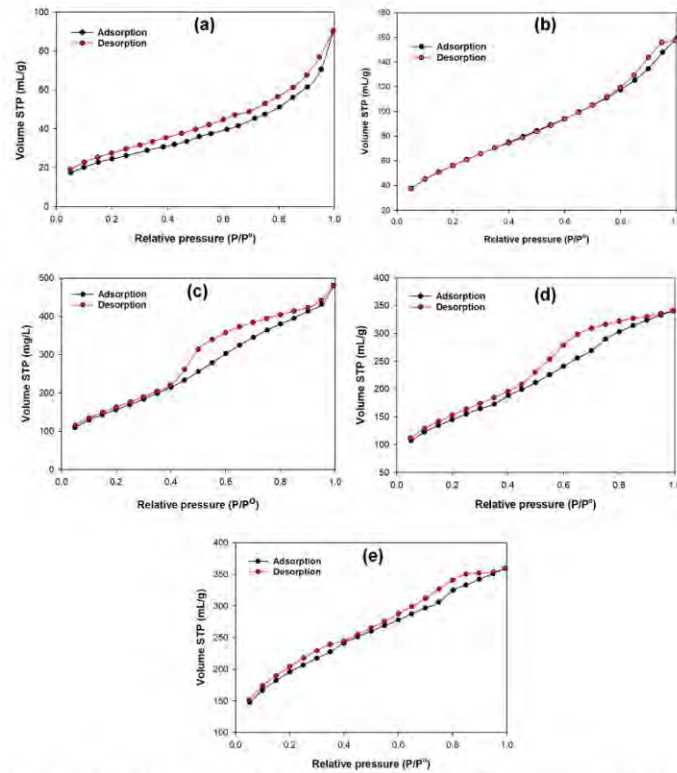


Figure 4. The sorption isotherm of (a) geothermal silica, (b) purified silica after acid leaching, and mesoporous silica products with CTAB variations (c) 0.015 mole, (d) 0.03 mole and (e) 0.05 mole.

The values of specific surface area, adsorbed-desorbed volume range, pore volume, and pore radius are completely summarized in Table 3, while pore size distribution of mesoporous silica product before and after APTMS introduction can be seen in Figure 5. They showed the variation of measured values upon increased CTAB. The specific surface area of geothermal silica was significantly increased from $40.899 \text{ m}^2/\text{g}$ to $178.063 \text{ m}^2/\text{g}$ in purified silica after acid leaching. It can be possibly due to the removal of metal oxide from the bulk body of silica that produces more empty sites resulting in higher measured surface area and higher adsorption ability. It was also found that the specific surface area considerably increased upon an increase of mole of CTAB, which are 582.454 , 511.946 , and $668.849 \text{ m}^2/\text{g}$ for synthesized mesoporous silica with the amounts of CTAB 0.015, 0.03, and 0.05 mole, respectively. This phenomenon indicates the higher construction of mesoporous structures upon an increase of CTAB loading, resulting in a higher estimated surface area. It is in agreement with the SEM results that in an increased loading of CTAB, it produces a more uniform shaped particle which possibly generates a higher surface area. At the same time, an increase of initial intake adsorption-desorption volume was also found, from 18.61

mL/g (geothermal silica) to 102.35, 103.47, 149.33 mL/g for synthesized mesoporous silica with moles of CTAB 0.015, 0.03, and 0.05 mole, respectively. However, the observed adsorption pore volume was decreased down upon the addition of CTAB, which is from 0.62 mL/g for purified silica to 0.62, 0.39, and 0.26 mL/g for synthesized mesoporous silica with moles of CTAB 0.015, 0.03, and 0.05 mole, respectively. It can be explainable by the increased growth of particles when the higher amount of CTAB was introduced, as evident by SEM images previously discussed. The uniform particle distribution can possibly produce smaller void volume in the bulk body due to the closer gaps between the particles. Further, the measured pore radii were 19.83, 17.07, 19.11, 15.31, 17.04 Å for geothermal silica, purified silica, mesoporous silica with 0.015, 0.03, and 0.05 mole of CTAB, respectively. All of those pore radius values indicate that all of them are in a group of mesoporous materials⁶⁷. Therefore, from these findings, synthesized mesoporous silica with 0.05 mole of CTAB showed the most desirable characteristics in terms of adsorption isotherm specific surface area, adsorbed-desorbed volume, and pore radius, suggesting a preferable matrix material for slow-release urea.

Table 3. BET analysis results, including specific surface area, pore volume, and pore radius (adsorption isotherm) of geothermal silica, purified silica after acid leaching, and modified mesoporous silica with different amounts of CTAB

Sample	Specific surface area (m ² /g)	Adsorbed-desorbed volume range (mL/g)	Pore volume (mL/g)	Pore radius (Å)
Geothermal silica	40.899	18.61 – 86.79	0.11	19.83
Purified silica after acid leaching	178.063	37.62 – 158.62	0.62	17.07
Mesoporous silica with CTAB 0.015 mole	582.454	102.35 – 485.75	0.62	19.11
Mesoporous silica with CTAB 0.03 mole	511.946	103.47 – 346.11	0.39	15.31
Mesoporous silica with CTAB 0.05 mole	668.849	149.33 – 353.28	0.26	17.04

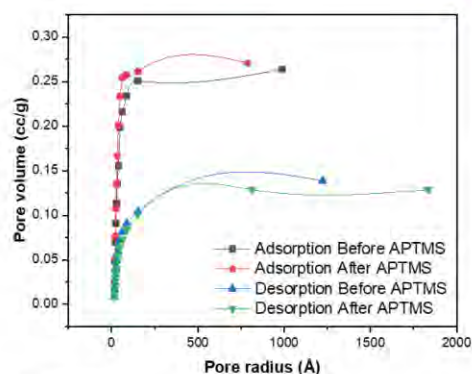


Figure 5. BJH pore size distribution of mesoporous silica products with CTAB 0.05 mole before and after treatment using APTMS.

Thermal analysis of synthesized mesoporous silica

To investigate the thermal characteristics of synthesized mesoporous silica, DSC and TGA analyses were performed using inert gas (nitrogen). Figure 6. shows DSC thermograms of three different samples, i.e., geothermal silica, mesoporous silica (best formulation using CTAB 0.05 mole), and pure CTAB. The DSC thermogram of geothermal silica shows no sufficient peaks that indicate the melting behavior of the sample. DSC was carried out by comparing the temperature of the sample and reference material during temperature changes. The temperature and reference material will be the same if there are no changes. Thermal phenomena such as melting can cause the decomposition or changes in the amorphous structure of the sample. The DSC curve in Figure 6. shows two endothermic steps in mesoporous silica. The enthalpies measured were -69.2175 J/g (at 82.3 °C) and -10.0796 J/g (at 159.5 °C). The measured enthalpies in pure CTAB were -141.8772 J/g (at 115.4 °C) and -19.6368 J/g (at 272.4 °C).

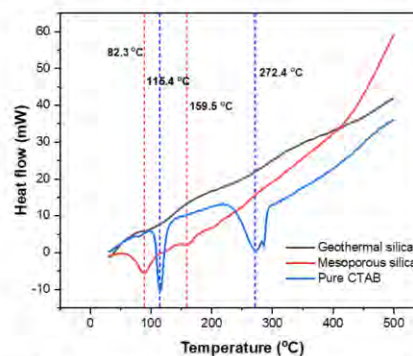


Figure 6. DSC thermogram of geothermal silica, mesoporous silica, and pure CTAB.

TGA analysis confirmed the weight loss behavior of geothermal silica, mesoporous silica, and pure CTAB on temperatures ranging from 30 – 500 °C. TGA thermograms of the three samples and a summary of the weight loss and degradation temperature are shown in Figure 7. and Table 4, respectively. All samples experienced a gradual weight loss as a function of temperature. Generally, the degradation occurred with four steps for geothermal silica and mesoporous silica and three steps for pure CTAB. The most significant weight loss in geothermal silica (Figure 7(a).) occurred at temperatures ranging from 30 – 135 °C with 11.59% weight loss. This condition is possibly due to the evaporation of trapped and bonded water in the sample. Meanwhile, based on the TGA thermogram of mesoporous silica (Figure 7(b).) shows four regions of weight loss which were 17.61% at 30 – 124 °C, 45.56% at 125 – 227 °C, 14.40% at 228 – 294 °C, and 5.72% at 295 – 500 °C. At the first step, the evaporation of trapped water molecules, the degradation of the organic compound at the second step, degradation of CTAB compound at the third step, and degradation of remaining long-chain organic compounds at the last step. In addition, the TGA thermogram of pure CTAB shows a significant weight loss of 87.45% at 227 – 287 °C, which was due to the degradation of organic chains in the CTAB. This condition was also experienced similarly in the TGA thermogram of mesoporous silica. This finding explains that the presence of

CTAB in mesoporous silica interfered with the intermolecular interaction of CTAB and silica, and this interaction led to a change in the thermal degradation behavior of synthesized mesoporous silica.

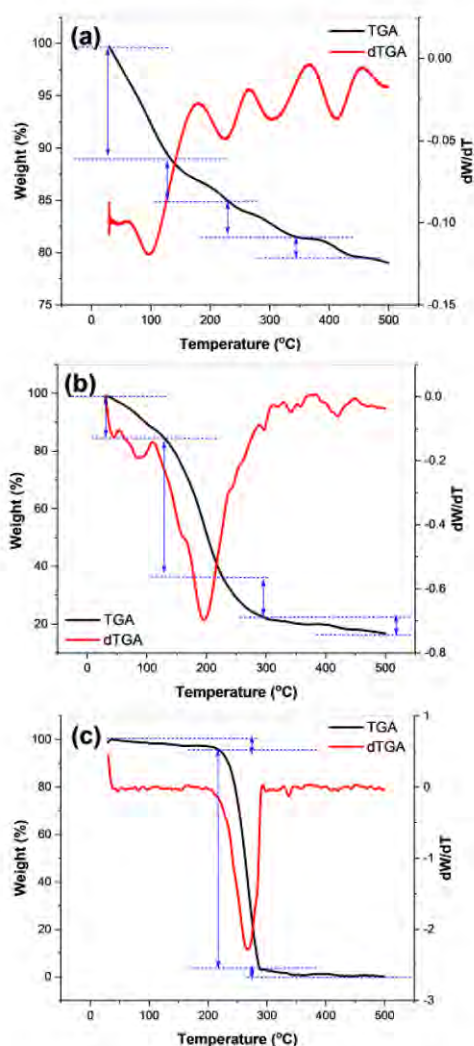


Figure 7. TGA thermograms of (a) Geothermal silica, (b) Mesoporous silica, (c) Pure CTAB.

Table 4. TGA data including weight losses at certain temperatures of geothermal silica, mesoporous silica, and pure CTAB

Sample	Temperature range (°C)	Weight loss (%)
Geothermal silica	30 – 135	11.59
	136 – 236	4.32
	237 – 347	1.86
	348 – 453	1.05
Mesoporous silica	30 – 124	17.61
	125 – 227	45.56
	228 – 294	14.40
	295 – 500	5.72
Pure CTAB	30 – 226	6.75
	227 – 287	87.45
	288 – 500	5.45

Characteristics of slow-release urea with APTMS as a surface modifying agent

Based on previous discussions, synthesized mesoporous silica with 0.05 mole of CTAB shows the prominent characteristic to be utilized as the matrix material for slow-release urea. Furthermore, to develop a desirable slow-release characteristic, surface modification of mesoporous silica was performed using a solution containing 10% of 3-Aminopropyl trimethoxy silane (APTMS). APTMS possibly performs an intermolecular interaction with the molecules of urea⁴⁸. This interaction provides strong bonding between urea and the matrix of (mesoporous silica); therefore, they can be combined to produce a slow-release urea. However, introduction of APTMS also created cross-linking between the APTMS molecules, which led to vertical polymerization and possibly pore blocking. This phenomenon affected the properties of mesoporous silica, especially its porosity, resulting in lower value of surface area, pore volume, and pore radius as seen in Table 5.

Table 5. BET analysis results, including specific surface area, pore volume, and pore radius (adsorption isotherm) of modified mesoporous silica using 0.05 moles CTAB before and after introduction of APTMS

Sample	Specific surface area (m ² /g)	Adsorbed-desorbed volume range (mL/g)	Pore volume (mL/g)	Pore radius (Å)
Mesoporous silica with CTAB 0.05 mole before introduction of APTMS	668.849	149.33 – 353.28	0.26	17.04

Mesoporous silica with CTAB 0.05 mole after introduction of APTMS	103.049	4.62 – 93.18	0.14	15.30
---	---------	--------------	------	-------

Figure 8. represents the SEM micrographs and the EDX spectra of synthesized slow-release urea. Based on Figure 8., it can be observed that all samples had similar surface micromorphology with MS/APTMS. No significant changes in terms of morphology occurred upon an increase of urea introduction to the slow-release urea. It can be reasonably concluded that the introduction of urea to the MS/APTMS as the matrix did not influence the morphology of the generated slow-release urea. In addition, EDX results in Figure 8. reveal the spectra of recorded elemental in the tested samples. It was found that the major elements that appeared in all samples were Si, C, and O. The complete summary of the chemical composition of synthesized slow-release urea is shown in Table 6. From Table 6, increasing urea concentration to the slow-release urea generates higher composition of N, corresponding to the quantity of urea in the slow-release urea. MS/APTMS has 3.81%-wt of nitrogen, and gradually increased upon increasing introduction of urea which are 4.02, 4.63, 5.17, and 6.36 %-wt for MS/APTMS/U6.74, MS/APTMS/U16.74, MS/APTMS/U26.74, and MS/APTMS/U36.74, respectively. Therefore, the initial urea concentration introduced to the slow-release urea significantly influenced the generated urea concentration in the synthesized slow-release urea.

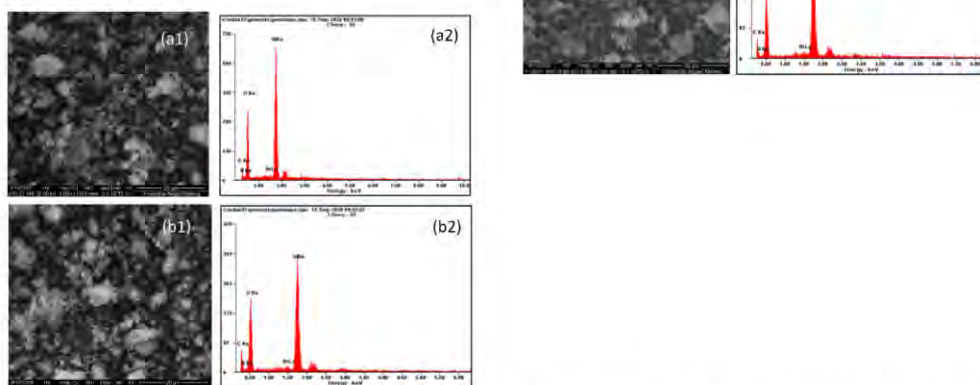


Figure 8. SEM-EDX micrographs and spectra of (a) MS/APTMS, and synthesized slow-release urea: (b) MS/APTMS/U6.74, (c) MS/APTMS/U16.74, (d) MS/APTMS/U26.74, and (e) MS/APTMS/U36.74.

Table 6. Chemical composition from EDX analysis of synthesized slow-release urea

Sample code		C K	N K	O K	Br K	Si K
MS/APTMS	Weight (%)	18.68	3.81	51.21	1.20	25.11
	Atomic (%)	26.19	4.58	53.92	0.25	15.06
MS/APTMS/U6.74	Weight (%)	25.93	4.02	47.91	1.06	21.07
	Atomic (%)	34.80	4.63	48.26	0.21	12.09
MS/APTMS/U16.74	Weight (%)	14.90	4.63	46.71	0.36	33.40
	Atomic (%)	21.82	5.81	51.36	0.08	20.92
MS/APTMS/U26.74	Weight (%)	21.51	5.17	47.03	0.83	25.82

	Atomic (%)	29.35	6.15	49.00	0.17	15.32
MS/APTMS/U36.74	Weight (%)	25.70	6.36	44.66	0.91	22.37
	Atomic (%)	34.55	7.33	45.08	0.18	12.86

FTIR analysis was performed to examine the formation of interaction bonding of urea in a matrix structure and the effect of APTMS on the synthesized slow-release urea. Figure 9. represents the FTIR spectra of different tested samples at wavenumbers of 4000 – 500 cm^{-1} (Figure 9(a).) and 2300 – 1300 cm^{-1} (Figure 9(b).) ⁴⁹. From Figure 9(a)., it can be found that all tested samples experienced an intense broad peak ranging from 1250 – 900 cm^{-1} , indicating the vibration of Si-O-Si groups ⁴⁹. Figure 9(b). was developed to further analyze the formation of new functional groups upon the application of APTMS and the introduction of urea to the matrix. It can be seen that the application of APTMS to the mesoporous silica generated slightly higher recorded absorbance at 1556 and 1495 cm^{-1} that correspond to the vibrations of N-H and C-N groups, respectively ²⁴. This is explainable by the formation of abundant N-H and C-N groups from APTMS on the mesoporous silica structure during the surface modification process.

On the other hand, the varied concentrations of urea introduction to the MS/APTMS were also found, resulting in higher recorded absorbance intensity at several wavenumbers. Absorption bands at 2100 and 1636 cm^{-1} indicate the stretching vibrations of N=C=O and C=O groups, attributed to the natural composition and cyanate

impurities inside the urea. Intense peaks recorded at 1556, 1495, and 1340 cm^{-1} are related to the vibrations of N-H, C-N, and C-H groups ^{49,50}. By comparing the relative absorbance intensity of the tested samples, a sample of MS/APTMS/U26.74 generates the higher intensity of C=O, N-H, C-N, and C-H groups. The higher intensity means the higher content of respective groups in the MS/APTMS/U26.74 than other samples, suggesting the best formulation for the slow-release urea. Figure 9(c). depicts the proposed bonding formations of grafted aminopropyl groups from APTMS to the siloxane groups on the surface of the mesoporous silica resulting in the aminopropyl-functionalized mesoporous silica. This functionalization is needed to effectively adsorb the urea and control its release. The amine groups from urea bonded with amine sites of aminopropyl groups. This amine bonding formation (N-H) was recorded and explained on FTIR spectra. Furthermore, hydrogen bonding as another attractive intermolecular force can occur due to the abundance of highly electronegative atoms such as oxygen (O), nitrogen (N), and hydrogen (H). Therefore, it can provide a stronger bonding of urea groups on the surface of the functionalized mesoporous silica thus, resulting in the effective slow-release property.

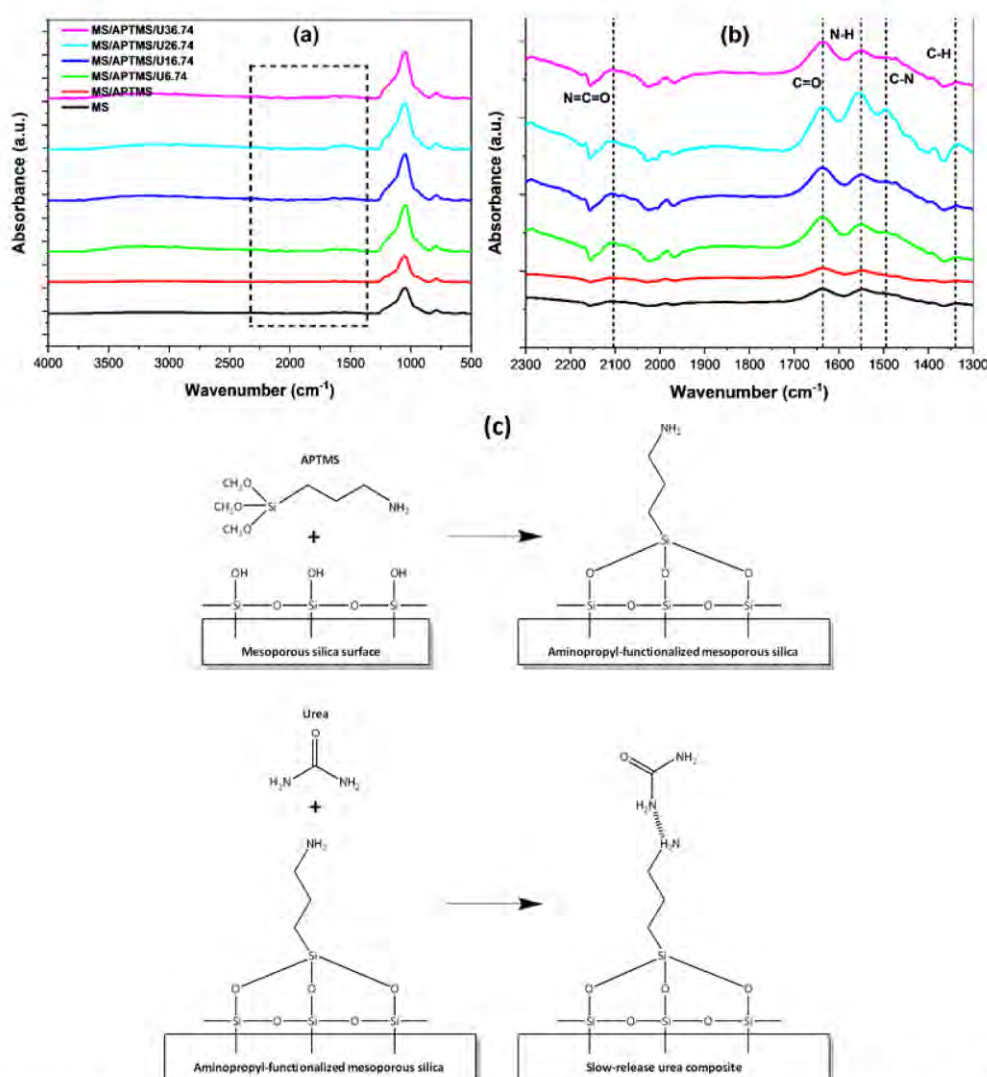


Figure 9. FTIR results of slow-release urea with different formulations (a) FTIR results with wavenumber 4000-500 cm⁻¹, (b) Further evaluation of FTIR spectra at wavenumber 2300-1300 cm⁻¹, and (c) Proposed bonding formation mechanisms of aminopropyl and urea groups on synthesized slow-release urea.

Study of release kinetics of synthesized slow-release urea

The performance of slow-release urea was executed by measuring urea content in overflow liquid (see section 2.2.4.). The observed samples were MS/APTMS/U26.74 as the best formulation for slow-release urea previously discussed and the commercial silica as the control variable. **Initial urea content in each sample was set to be 200 ppm.** Figure 10(a). depicts the amount (ppm) of urea released during seven days of observation from the sample to the overflow liquid.

The highest overflow urea concentration was recorded on the second day for MS/APTMS/U26.74 with a value of 28.55 ppm, and nearly constant on the next days. On the other hand, the highest overflow urea content was found on the third day with a value of 52.65 ppm and gradually decreased on the next few days. Subsequently, the performance of synthesized slow-release urea was also evaluated by measuring the cumulative urea release, as presented in Figure 10(b). MS/APTMS/U26.74 shows the linear trend of cumulative urea release profile with total release urea of 124.6 ppm

(64.4%) on the last day. In contrast, the commercial urea shows an exponential trend of cumulative urea release profile with a value of 184.5 ppm (92.4%) in total. This result indicates that APTMS/U26.74 can release the urea slower than the commercial urea. It can be partially due to the abundance of solid interaction bonding between urea molecules and the MS/APTMS as the matrix of this slow-release urea resulting in a relatively slower release of urea molecules.

To further understand the behavior of urea release, kinetic modeling of urea release was evaluated using several models, i.e., pseudo-first order (Figure 10(c).), pseudo-second order (Figure 10(d).), Higuchi (Figure 10(e).), and Hixson-Crowell (Figure 10(f).). The fitted kinetic parameters and the correlation coefficients are completely listed in Table 7. The pseudo-first order model provided a reasonably good fit for commercial urea and MS/APTMS/U26.74 with R^2 values of 0.8528 and 0.8395, respectively. The pseudo-first order rate kinetic constant values were 0.3502 day^{-1} for commercial urea and 0.2654 day^{-1} for MS/APTMS/U26.74. In addition, the k_i value of commercial urea was recorded higher than MS/APTMS/U26.74, indicating that the commercial urea has a higher urea release per day than MS/APTMS/U26.74. This result indicates that the modified slow-release urea had a significant impact on reducing its release rate. On the other hand, in this study, the pseudo-second order kinetic model was seemingly unsuitable for modeling the urea release behavior. It is evident with the low number of correlation coefficients with just only 0.3258 for commercial

urea and 0.5703 for MS/APTMS/U26.74. The low value of R^2 indicates that the model is less capable of being used for data predictions. The Higuchi kinetic model performed the best fit of urea release among other fitted models, which had the highest R^2 values of 0.9901 for commercial urea and 0.9979 for MS/APTMS/U26.74. The Higuchi constants were measured $54.0668 \text{ \% day}^{1/2}$ for commercial urea and $24.4964 \text{ \% day}^{1/2}$ for MS/APTMS/U26.74. The higher Higuchi constant represents the higher diffusion rate of urea release from the sample⁶³. Thus, the modification of MS/APTMS as the matrix medium has significantly improved the urea release rate by reducing the diffusivity of urea release from the slow-release urea due to solid interaction bonding between modified mesoporous silica and the urea molecules. The Hixson-Crowell model was also showed the excellent urea release fit for both samples with R^2 values of 0.9617 and 0.9772 for commercial urea and MS/APTMS/U26.74, respectively, with Hixson-Crowell constants of $4.8308 \text{ \%}^{1/3} \text{ day}^1$ and $2.3678 \text{ \%}^{1/3} \text{ day}^1$ for commercial urea and MS/APTMS/U26.74, respectively. This result suggests that the primary mechanism of urea release is a diffusion-controlled mechanism⁶⁷, a similar indication from the Higuchi model previously discussed. Based on the studies and results, it can be reasonably suggested that the modification of mesoporous silica with APTMS has a significant impact on reducing urea release rate by lowering the diffusivity of urea from the slow-release urea. Based on the findings and explanation, it can be reasonably concluded that the slow-release urea has been successfully synthesized.

Table 7. Model parameter and correlation coefficient of commercial urea and MS/APTMS/U26.74 to evaluate urea release kinetics using pseudo-first order, Higuchi, and Hixson-Crowell models

Sample	Kinetic models							
	Pseudo-first order		Pseudo-second order		Higuchi		Hixson-Crowell	
	k_1 (day^{-1})	R^2	k_2 (\% day^{-1})	R^2	K_H ($\text{\%}^{1/2} \text{ day}$)	R^2	K_{HC} ($\text{\%}^{1/3} \text{ day}^1$)	R^2
Commercial urea	0.3502	0.8528	0.0037	0.3286	54.0668	0.9901	4.8308	0.9617
MS/APTMS/U26.74	0.2654	0.8395	0.0046	0.5703	24.4964	0.9979	2.3678	0.9772

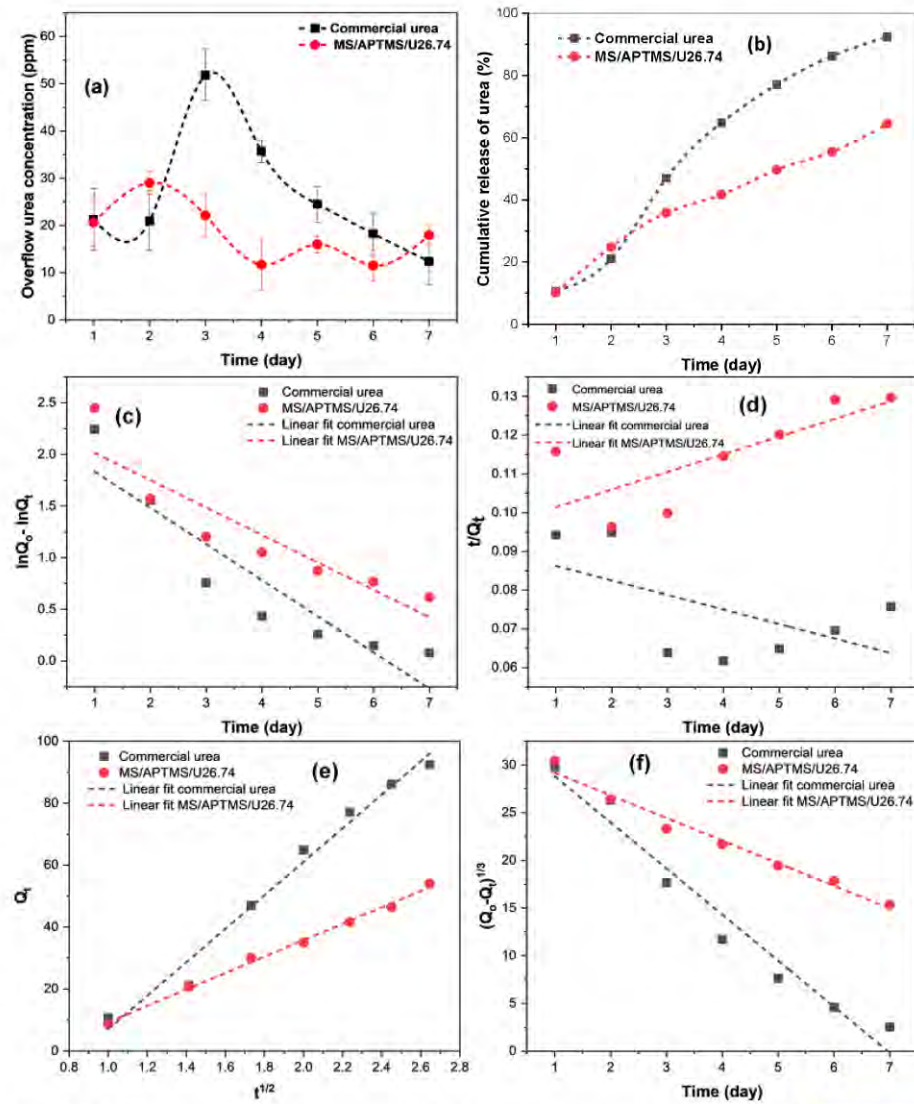


Figure 10. Performance test results of slow-release urea: (a) Result of measured urea concentration in overflow liquid and (b) Cumulative release of urea for commercial urea and MS/APTMS/U26.74. Curve fittings of urea release kinetics for commercial urea and MS/APTMS/U26.74 using (c) Pseudo-first order model, (d) Pseudo-second order model, (e) Higuchi model, and (f) Hixson-Crowell model.

CONCLUSION

In this work, a prominent slow-release urea fertilizer was developed with aminopropyl-functionalized mesoporous silica as the matrix to enhance the urea adsorption and slow-release property. It was developed by utilizing geothermal silica as the silica source, CTAB

as the surfactant, and APTMS as the surface modification agent. The acid leaching treatment using H_2SO_4 was conducted to purify the geothermal silica sample and increase SiO_2 content from 86.30% to 96.00%, which is feasible for mesoporous silica synthesis. The synthesized mesoporous silica was formulated with different mole amounts of CTAB. It showed the most desirable mesoporous silica

with fairly uniform surface micromorphology containing particles with 38.55 %wt of silica content, surface area of **668.849 m²/g**, adsorption-desorption range of 149.33 – 353.28 mL/g, and adsorption pore volume of 0.26 mL/g were achieved with addition of 0.05 mole of CTAB. All synthesized mesoporous silicas showed type IV hysteresis which correspond to mesoporous type material, signaling the successful development of the mesoporous structure. The DSC results showed that the mesoporous silica becomes more reactive with recorded enthalpies of 69.2175 J/g and -10.0796 J/g at temperatures of 82.3 °C and 159.5 °C due to the addition of CTAB in the synthesis process. TGA thermograms showed that the mesoporous silica has quite good thermal stability and only experienced 17.61% of weight loss at a temperature of up to 124 °C. These findings suggest the excellent potential of the synthesized mesoporous silica for prominent matrix material. Further, the functionalization of the aminopropyl group to the mesoporous silica using APTMS was done. SEM results showed that the functionalization process and the adsorption of urea to the mesoporous silica resulted in no significant changes in the **morphology** of mesoporous silica. Meanwhile, significant changes were observed in generated chemical functional groups after the APTMS functionalization resulting in some new groups including C=O, N-H, and C-N. From the FTIR spectra, MS/APTMS/U26.74 was observed to have a relatively higher intensity of C=O, N-H, C-N, and C-H groups among the other samples, suggesting the higher content of respective groups in the MS/APTMS/U26.74. The comparison experiment and the kinetic study regarding the release property and kinetic between MS/APTMS/U26.74 as the best slow-release urea and the commercial urea was investigated. The cumulative urea release during seven days of observation was **184.5 ppm (92.4%)** for commercial urea and **124.6 ppm (64.6%)** for MS/APTMS/U26.74. The abundance of strong interaction bonding between urea molecules and the MS/APTMS as the matrix of relatively slower release of urea molecules. The Higuchi kinetic model performed the best fit among the other models to predict the release kinetics of MS/APTMS/U26.74 with generated R² of 0.9979 and Higuchi constant of 24.4964 % day^{-1/2}. The Higuchi constant of MS/APTMS/U26.74 was smaller than commercial urea (54.0668 % day^{-1/2}), indicating the synthesized slow-release urea has a lower urea diffusivity out from the sample, thus resulting in the slower and controllable urea release. Finally, the synthesized MS/APTMS/U26.74 by utilizing geothermal silica, CTAB, and APTMS can be noted as a potential composition for the slow-release urea fertilizer to enhance the usage efficiency of urea.

Author Contributions

S. Silviana: Conceptualization, Methodology, Supervision, Funding acquisition, Resources, Writing – original draft. Atikah Ayu Janitra: Methodology, Investigation, Writing – original draft. Afriza Ni'matus Sa'adah: Project administration, Software, Formal analysis. Febio Dalanta: Data curation, Software, Visualization, Formal analysis, Writing – review and editing.

Funding Sources

This project was financially supported by the Ministry of Education, Culture, Research and Technology of the Republic of Indonesia through grant No. 225-S4/UN7.6.1/PP/2020.

ACKNOWLEDGMENT

The authors would also like to show their gratitude to the community of AMaL (Advanced Material Laboratory) of Diponegoro University for all support and discussion throughout the research.

ABBREVIATIONS

SRU, slow-release urea; MS, mesoporous silica; CTAB, Cetyltrimethylammonium bromide; APTMS, (3-Aminopropyl)trimethoxysilane; SEM: scanning electron microscopy; XRF: x-ray fluorescence; XRD: x-ray diffraction; FTIR: fourier-transform infrared; BET-BJH: barrett-joyner-halenda; TGA: thermogravimetric analysis; DSC: differential scanning calorimetry; HCl: hydrochloric acid; U6.74: urea 6.74 %wt; U16.74: urea 16.74 %wt; U26.74: urea 26.74 %wt; U36.74: urea 36.74 %wt.

REFERENCES

- (1) Kay-Shoemaker, J. L.; Watwood, M. E.; Kilpatrick, L.; Harris, K. Exchangeable Ammonium and Nitrate from Different Nitrogen Fertilizer Preparations in Polyacrylamide-Treated and Untreated Agricultural Soils. *Biol. Fertil. Soils* **2000**, *31* (3–4), 245–248. <https://doi.org/10.1007/s003740050652>.
- (2) Saha, B. K.; Rose, M. T.; Wong, V.; Cavagnaro, T. R.; Patti, A. F. Hybrid Brown Coal-Urea Fertiliser Reduces Nitrogen Loss Compared to Urea Alone. *Sci. Total Environ.* **2017**, *601–602*, 1496–1504. <https://doi.org/10.1016/j.scitotenv.2017.05.270>.
- (3) Getahun, D.; Alemneh, T.; Akebergn, D.; Getabalew, M.; Zewdie, D. Urea Metabolism and Recycling in Ruminants. *Biomed. J. Sci. Tech. Res.* **2019**, *20* (1). <https://doi.org/10.26717/BJSTR.2019.20.003401>.
- (4) Hailemariam, S.; Zhao, S.; He, Y.; Wang, J. Urea Transport and Hydrolysis in the Rumen: A Review. *Anim. Nutr.* **2021**, *7* (4), 989–996. <https://doi.org/10.1016/j.aninu.2021.07.002>.
- (5) Mehta, R.; Brahmabhatt, H.; Saha, N. K.; Bhattacharya, A. Removal of Substituted Phenyl Urea Pesticides by Reverse Osmosis Membranes: Laboratory Scale Study for Field Water Application. *Desalination* **2015**, *358*, 69–75. <https://doi.org/10.1016/j.desal.2014.12.019>.
- (6) Berrada, H.; Font, G.; Moltó, J. C. Determination of Urea Pesticide Residues in Vegetable, Soil, and Water Samples. *Crit. Rev. Anal. Chem.* **2003**, *33* (1), 19–41. <https://doi.org/10.1080/713609152>.
- (7) Sasmal, S.; Roy Chowdhury, S.; Podder, D.; Haldar, D. Urea-Appended Amino Acid To Vitalize Yeast Growth, Enhance Fermentation, and Promote Ethanol Production. *ACS Omega* **2019**, *4* (8), 13172–13179. <https://doi.org/10.1021/acsomega.9b01260>.
- (8) Santos, A. S.; Ferreira, L. M. M.; Martin-Rosset, W.; Cotovio, M.; Silva, F.; Bennett, R. N.; Cone, J. W.; Bessa, R. J. B.; Rodrigues, M. A. M. The Influence of Casein and Urea as Nitrogen Sources on in Vitro Equine Caecal Fermentation. *Animal* **2012**, *6* (7), 1096–1102. <https://doi.org/10.1017/S1751731111002527>.
- (9) Li, Y.; Huang, L.; Zhang, H.; Wang, M.; Liang, Z. Assessment of Ammonia Volatilization Losses and Nitrogen Utilization during the Rice Growing Season in Alkaline Salt-Affected Soils. *Sustainability* **2017**, *9* (1), 132. <https://doi.org/10.3390/su9010132>.
- (10) Azeem, B.; KuShaari, K.; Man, Z. B.; Basit, A.; Thanh, T. H. Review on Materials & Methods to Produce Controlled Release Coated Urea Fertilizer. *J. Control. Release* **2014**, *181* (12), 11–21. <https://doi.org/10.1016/j.jconrel.2014.02.020>.
- (11) Jie, C.; Jing-zhang, C.; Man-zhi, T.; Zi-tong, G. Soil Degradation: A Global Problem Endangering Sustainable Development. *J. Geogr. Sci.* **2002**, *12* (2), 243–252. <https://doi.org/10.1007/BF02837480>.
- (12) Liu, L.; Kost, J.; Fishman, M. L.; Hicks, K. B. A Review: Controlled Release Systems for Agricultural and Food Applications; 2008; pp 265–281. <https://doi.org/10.1021/bk-2008-0992.ch014>.
- (13) Espézie Bueno, S. C.; Filho, M. B.; de Almeida, P. S. G.; Polidoro, J. C.; Olivares, F. L.; Stel, M. S.; Vargas, H.; Mota, L.; da Silva, M. G. Cuban Zeolite as Ammonium Carrier in Urea-Based Fertilizer Pellets: Photoacoustic-Based Sensor for Monitoring N-Ammonia Losses by Volatilization in Aqueous Solutions. *Sensors Actuators B Chem.* **2015**, *212*, 35–40. <https://doi.org/10.1016/j.snb.2015.01.114>.

- (14) Míhok, F.; Macko, J.; Oriňák, A.; Oriňáková, R.; Kovaľ, K.; Sisáková, K.; Petruš, O.; Kostecká, Z. Controlled Nitrogen Release Fertilizer Based on Zeolite Clinoptilolite: Study of Preparation Process and Release Properties Using Molecular Dynamics. *Curr. Res. Green Sustain. Chem.* **2020**, *3*, 100030. <https://doi.org/10.1016/j.crgsc.2020.100030>.
- (15) Maghsoodi, M. R.; Najafi, N.; Reyhanitabar, A.; Oustan, S. Hydroxyapatite Nanorods, Hydrochar, Biochar, and Zeolite for Controlled-Release Urea Fertilizers. *Geoderma* **2020**, *379*, 114644. <https://doi.org/10.1016/j.geoderma.2020.114644>.
- (16) Pereira, E. I.; da Cruz, C. C. T.; Solomon, A.; Le, A.; Cavigelli, M. A.; Ribeiro, C. Novel Slow-Release Nanocomposite Nitrogen Fertilizers: The Impact of Polymers on Nanocomposite Properties and Function. *Ind. Eng. Chem. Res.* **2015**, *54* (14), 3717–3725. <https://doi.org/10.1021/acs.iecr.5b00176>.
- (17) Yamamoto, C. F.; Pereira, E. I.; Mattoso, L. H. C.; Matsunaka, T.; Ribeiro, C. Slow Release Fertilizers Based on Urea/Urea-Formaldehyde Polymer Nanocomposites. *Chem. Eng. J.* **2016**, *287*, 390–397. <https://doi.org/10.1016/j.cej.2015.11.023>.
- (18) Shen, Y.; Zhou, J.; Du, C.; Zhou, Z. Hydrophobic Modification of Waterborne Polymer Slows Urea Release and Improves Nitrogen Use Efficiency in Rice. *Sci. Total Environ.* **2021**, *794*, 148612. <https://doi.org/10.1016/j.scitotenv.2021.148612>.
- (19) Bortolin, A.; Aouada, F. A.; de Moura, M. R.; Ribeiro, C.; Longo, E.; Mattoso, L. H. C. Application of Polysaccharide Hydrogels in Adsorption and Controlled-Extended Release of Fertilizers Processes. *J. Appl. Polym. Sci.* **2012**, *123* (4), 2291–2298. <https://doi.org/10.1002/app.34742>.
- (20) Li, L.; Sun, Y.; Cao, B.; Song, H.; Xiao, Q.; Yi, W. Preparation and Performance of Polyurethane/Mesoporous Silica Composites for Coated Urea. *Mater. Des.* **2016**, *99*, 21–25. <https://doi.org/10.1016/j.matdes.2016.03.043>.
- (21) de Silva, M.; Siriwardena, D. P.; Sandaruwan, C.; Priyadarshana, G.; Karunaratne, V.; Kottegoda, N. Urea-Silica Nanohybrids with Potential Applications for Slow and Precise Release of Nitrogen. *Mater. Lett.* **2020**, *272*, 127839. <https://doi.org/10.1016/j.matlet.2020.127839>.
- (22) Elhassani, C. E.; Essamlali, Y.; Aqil, M.; Nzenguet, A. M.; Ganetri, I.; Zahouily, M. Urea-Impregnated HAP Encapsulated by Lignocellulosic Biomass-Extruded Composites: A Novel Slow-Release Fertilizer. *Environ. Technol. Innov.* **2019**, *15*, 100403. <https://doi.org/10.1016/j.eti.2019.100403>.
- (23) Vanichvattanadecha, C.; Singhapong, W.; Jaroenworarluck, A. Different Sources of Silicon Precursors Influencing on Surface Characteristics and Pore Morphologies of Mesoporous Silica Nanoparticles. *Appl. Surf. Sci.* **2020**, *513*, 145568. <https://doi.org/10.1016/j.apsusc.2020.145568>.
- (24) Yang, Y.; Wang, J.; Qian, X.; Shan, Y.; Zhang, H. Aminopropyl-Functionalized Mesoporous Carbon (APTMS-CMK-3) as Effective Phosphate Adsorbent. *Appl. Surf. Sci.* **2018**, *427*, 206–214. <https://doi.org/10.1016/j.apsusc.2017.08.213>.
- (25) Ghobashy, M. M.; Mousaa, I. M.; El-Sayyad, G. S. Radiation Synthesis of Urea/Hydrogel Core Shells Coated with Three Different Natural Oils via a Layer-by-Layer Approach: An Investigation of Their Slow Release and Effects on Plant Growth-Promoting Rhizobacteria. *Prog. Org. Coatings* **2021**, *151*, 106022. <https://doi.org/10.1016/j.porgcoat.2020.106022>.
- (26) Guo; Liu; Zhan; Wu, L. Preparation and Properties of a Slow-Release Membrane-Encapsulated Urea Fertilizer with Superabsorbent and Moisture Preservation. *Ind. Eng. Chem. Res.* **2005**, *44* (12), 4206–4211. <https://doi.org/10.1021/ie0489406>.
- (27) Abdelghany, A. M.; Meikhal, M. S.; Asker, N. Synthesis and Structural-Biological Correlation of PVC/PVAc Polymer Blends. *J. Mater. Res. Technol.* **2019**, *8* (5), 3908–3916. <https://doi.org/10.1016/j.jmrt.2019.06.053>.
- (28) Cui, Y.; Xiang, Y.; Xu, Y.; Wei, J.; Zhang, Z.; Li, L.; Li, J. Poly-Acrylic Acid Grafted Natural Rubber for Multi-Coated Slow Release Compound Fertilizer: Preparation, Properties and Slow-Release Characteristics. *Int. J. Biol. Macromol.* **2020**, *146*, 540–548. <https://doi.org/10.1016/j.ijbiomac.2020.01.051>.
- (29) dos Santos, A. C. S.; Henrique, H. M.; Cardoso, V. L.; Reis, M. H. M. Slow Release Fertilizer Prepared with Lignin and Poly(Vinyl Acetate) Bioblend. *Int. J. Biol. Macromol.* **2021**, *185*, 543–550. <https://doi.org/10.1016/j.ijbiomac.2021.06.169>.
- (30) Liu, J.; Yang, Y.; Gao, B.; Li, Y. C.; Xie, J. Bio-Based Elastic Polyurethane for Controlled-Release Urea Fertilizer: Fabrication, Properties, Swelling and Nitrogen Release Characteristics. *J. Clean. Prod.* **2019**, *209*, 528–537. <https://doi.org/10.1016/j.jclepro.2018.10.263>.
- (31) Ni, B.; Liu, M.; Lü, S.; Xie, L.; Wang, Y. Multifunctional Slow-Release Organic-Inorganic Compound Fertilizer. *J. Agric. Food Chem.* **2010**, *58* (23), 12373–12378. <https://doi.org/10.1021/jf1029306>.
- (32) Ni, B.; Liu, M.; Lü, S.; Xie, L.; Wang, Y. Environmentally Friendly Slow-Release Nitrogen Fertilizer. *J. Agric. Food Chem.* **2011**, *59* (18), 10169–10175. <https://doi.org/10.1021/jf202131z>.
- (33) Pang, L.; Gao, Z.; Zhang, S.; Li, Y.; Hu, S.; Ren, X. Preparation and Anti-UV Property of Modified Cellulose Membranes for Biopesticides Controlled Release. *Ind. Crops Prod.* **2016**, *89*, 176–181. <https://doi.org/10.1016/j.indcrop.2016.05.014>.
- (34) Sathisaran, I.; Balasubramanian, M. Physical Characterization of Chitosan/Gelatin-Alginate Composite Beads for Controlled Release of Urea. *Heliyon* **2020**, *6* (11), e05495. <https://doi.org/10.1016/j.heliyon.2020.e05495>.
- (35) Shan, L.; Gao, Y.; Zhang, Y.; Yu, W.; Yang, Y.; Shen, S.; Zhang, S.; Zhu, L.; Xu, L.; Tian, B.; Yun, J. Fabrication and Use of Alginate-Based Cryogel Delivery Beads Loaded with Urea and Phosphates as Potential Carriers for Bioremediation. *Ind. Eng. Chem. Res.* **2016**, *55* (28), 7655–7660. <https://doi.org/10.1021/acs.iecr.6b01256>.
- (36) Wang, Y.; Liu, M.; Ni, B.; Xie, L. κ -Carrageenan–Sodium Alginate Beads and Superabsorbent Coated Nitrogen Fertilizer with Slow-Release, Water-Retention, and Anticompaction Properties. *Ind. Eng. Chem. Res.* **2012**, *51* (3), 1413–1422. <https://doi.org/10.1021/ie2020526>.
- (37) Qiao, D.; Liu, H.; Yu, L.; Bao, X.; Simon, G. P.; Petinakis, E.; Chen, L. Preparation and Characterization of Slow-Release Fertilizer Encapsulated by Starch-Based Superabsorbent Polymer. *Carbohydr. Polym.* **2016**, *147*, 146–154. <https://doi.org/10.1016/j.carbpol.2016.04.010>.
- (38) Wanyika, H.; Gatebe, E.; Kioni, P.; Tang, Z.; Gao, Y. Mesoporous Silica Nanoparticles Carrier for Urea: Potential Applications in Agrochemical Delivery Systems. *J. Nanosci. Nanotechnol.* **2012**, *12* (3), 2221–2228. <https://doi.org/10.1166/jnn.2012.5801>.
- (39) He, H.; Xiao, H.; Kuang, H.; Xie, Z.; Chen, X.; Jing, X.; Huang, Y. Synthesis of Mesoporous Silica Nanoparticle–Oxaliplatin Conjugates for Improved Anticancer Drug Delivery. *Colloids Surfaces B Biointerfaces* **2014**, *117*, 75–81. <https://doi.org/10.1016/j.colsurfb.2014.02.014>.
- (40) Yan, E.; Ding, Y.; Chen, C.; Li, R.; Hu, Y.; Jiang, X. Polymer/Silica Hybrid Hollow Nanospheres with pH-Sensitive Drug Release in Physiological and Intracellular Environments. *Chem. Commun.* **2009**, No. 19, 2718. <https://doi.org/10.1039/b900751b>.
- (41) Yang, D.; Fan, R.; Luo, F.; Chen, Z.; Gerson, A. R. Facile and Green Fabrication of Efficient Au Nanoparticles Catalysts Using Plant Extract via a Mesoporous Silica-Assisted Strategy. *Colloids Surfaces A Physicochem. Eng. Asp.* **2021**, *621*, 126580. <https://doi.org/10.1016/j.colsurfa.2021.126580>.
- (42) Yin, F.; Xu, F.; Zhang, K.; Yuan, M.; Cao, H.; Ye, T.; Wu, X.; Xu, F. Synthesis and Evaluation of Mesoporous Silica/Mesoporous Molecularly Imprinted Nanoparticles as Adsorbents for Detection and Selective Removal of Imidacloprid in Food Samples. *Food Chem.* **2021**, *364*, 130216. <https://doi.org/10.1016/j.foodchem.2021.130216>.
- (43) Huang, R.; Shen, Y.-W.; Guan, Y.-Y.; Jiang, Y.-X.; Wu, Y.; Rahman, K.; Zhang, L.-J.; Liu, H.-J.; Luan, X. Mesoporous Silica Nanoparticles: Facile Surface Functionalization and Versatile Biomedical Applications in Oncology. *Acta Biomater.* **2020**, *116*, 1–15. <https://doi.org/10.1016/j.actbio.2020.09.009>.
- (44) Kaya, S.; Cresswell, M.; Bocaccini, A. R. Mesoporous Silica-Based

- Bioactive Glasses for Antibiotic-Free Antibacterial Applications. *Mater. Sci. Eng. C* **2018**, *83*, 99–107. <https://doi.org/10.1016/j.msec.2017.11.003>.
- (45) dos Santos, S. M. L.; Nogueira, K. A. B.; de Souza Gama, M.; Lima, J. D. F.; da Silva Júnior, I. J.; de Azevedo, D. C. S. Synthesis and Characterization of Ordered Mesoporous Silica (SBA-15 and SBA-16) for Adsorption of Biomolecules. *Microporous Mesoporous Mater.* **2013**, *180*, 284–292. <https://doi.org/10.1016/j.micromeso.2013.06.043>.
- (46) Policicchio, A.; Conte, G.; Stelitano, S.; Bonaventura, C. P.; Putz, A.-M.; Ianăși, C.; Almásy, L.; Horváth, Z. E.; Agostino, R. G. Hydrogen Storage Performances for Mesoporous Silica Synthesized with Mixed Tetraethoxysilane and Methyltriethoxysilane Precursors in Acidic Condition. *Colloids Surfaces A Physicochem. Eng. Asp.* **2020**, *601*, 125040. <https://doi.org/10.1016/j.colsurfa.2020.125040>.
- (47) Gil-Ortiz, R.; Naranjo, M. A.; Ruiz-Navarro, A.; Caballero-Molada, M.; Añares, S.; García, C.; Vicente, O. New Eco-Friendly Polymeric-Coated Urea Fertilizers Enhanced Crop Yield in Wheat. *Agronomy* **2020**, *10* (3), 438. <https://doi.org/10.3390/agronomy10030438>.
- (48) Cheah, W.-K.; Sim, Y.-L.; Yeoh, F.-Y. Amine-Functionalized Mesoporous Silica for Urea Adsorption. *Mater. Chem. Phys.* **2016**, *175*, 151–157. <https://doi.org/10.1016/j.matchemphys.2016.03.007>.
- (49) Luechinger, M.; Prins, R.; Pirngruber, G. D. Functionalization of Silica Surfaces with Mixtures of 3-Aminopropyl and Methyl Groups. *Microporous Mesoporous Mater.* **2005**, *85* (1–2), 111–118. <https://doi.org/10.1016/j.micromeso.2005.05.031>.
- (50) Hicks, J. C.; Dabestani, R.; Buchanan, A. C.; Jones, C. W. Assessing Site Isolation of Amine Groups on Aminopropyl-Functionalized SBA-15 Silica Materials via Spectroscopic and Reactivity Probes. *Inorganica Chim. Acta* **2008**, *361* (11), 3024–3032. <https://doi.org/10.1016/j.ica.2008.01.002>.
- (51) Burkett, S. L.; Sims, S. D.; Mann, S. Synthesis of Hybrid Inorganic–Organic Mesoporous Silica by Co-Condensation of Siloxane and Organosiloxane Precursors. *Chem. Commun.* **1996**, No. 11, 1367–1368. <https://doi.org/10.1039/CC9960001367>.
- (52) Purnomo, A.; Dalanta, F.; Oktaviani, A. D.; Silviana, S. Superhydrophobic Coatings and Self-Cleaning through the Use of Geothermal Scaling Silica in Improvement of Material Resistance; 2018; p 020077. <https://doi.org/10.1063/1.5065037>.
- (53) Silviana, S.; Darmawan, A.; Subagio, A.; Dalanta, F. Statistical Approaching for Superhydrophobic Coating Preparation Using Silica Derived from Geothermal Solid Waste. *ASEAN J. Chem. Eng.* **2020**, *19* (2), 91. <https://doi.org/10.22146/ajche.51178>.
- (54) Silviana, S.; Darmawan, A.; Dalanta, F.; Subagio, A.; Hermawan, F.; Milen Santoso, H. Superhydrophobic Coating Derived from Geothermal Silica to Enhance Material Durability of Bamboo Using Hexadimethylsilazane (HMDS) and Trimethylchlorosilane (TMCS). *Materials (Basel)*. **2021**, *14* (3), 530. <https://doi.org/10.3390/ma14030530>.
- (55) Silviana, S.; Darmawan, A.; Janitra, A. A.; Ma'ruf, A.; Triesty, I. Silicon Preparation Derived from Geothermal Silica by Reduction Using Magnesium. *Int. J. Emerg. Trends Eng. Res.* **2020**, *8* (8), 4861–4866. <https://doi.org/10.30534/ijeter/2020/126882020>.
- (56) Silviana, S.; Sanyoto, G. J.; Darmawan, A. Preparation of Geothermal Silica Glass Coating Film Through Multi-Factor Optimization. *J. Teknol.* **2021**, *83* (4), 41–49. <https://doi.org/10.11113/jurnalteknologi.v83.16377>.
- (57) Tut Hakkıdır, F. S.; Şengün, R.; Aydın, H. Characterization and Comparison of Geothermal Fluids Geochemistry within the Kızıldere Geothermal Field in Turkey: New Findings with Power Capacity Expanding Studies. *Geothermics* **2021**, *94*, 102110. <https://doi.org/10.1016/j.geothermics.2021.102110>.
- (58) Silviana, S.; Anggoro, D. D.; Salsabila, C. A.; Aprilio, K. Utilization of Geothermal Waste as a Silica Adsorbent for Biodiesel Purification. *Korean J. Chem. Eng.* **2021**, *38* (10), 2091–2105. <https://doi.org/10.1007/s11814-021-0827-z>.
- (59) Silviana, S.; Bayu, W. J. Silicon Conversion From Bamboo Leaf Silica By Magnesiothermic Reduction for Development of Li-Ion Battery Anode. *MATEC Web Conf.* **2018**, *156*, 05021. <https://doi.org/10.1051/mateconf/201815605021>.
- (60) Silviana, S.; Purbasari, A.; Siregar, A.; Rochyati, A. F.; Papra, T. Synthesis of Mesoporous Silica Derived from Geothermal Waste with Cetyl Trimethyl Ammonium Bromide (CTAB) Surfactant as Drug Delivery Carrier. *AIP Conf. Proc.* **2020**, *2296*, 020007. <https://doi.org/10.1063/5.0030487>.
- (61) Silviana, S.; Sagala, E. A. P. P.; Sari, S. E.; Siagian, C. T. M. Preparation of Mesoporous Silica Derived from Geothermal Silica as Precursor with a Surfactant of Cetyltrimethylammonium Bromide; 2019; p 020070. <https://doi.org/10.1063/1.5141683>.
- (62) Silviana, S.; Sanyoto, G. J.; Darmawan, A.; Sutanto, H. GEOTHERMAL SILICA WASTE AS SUSTAINABLE AMORPHOUS SILICA SOURCE FOR THE SYNTHESIS OF SILICA XEROGELS. *Rasayan J. Chem.* **2020**, *13* (03), 1692–1700. <https://doi.org/10.31788/RJC.2020.1335701>.
- (63) Silviana, S.; Dalanta, F.; Sanyoto, G. J. Utilization of Bamboo Leaf Silica as a Superhydrophobic Coating Using Trimethylchlorosilane as a Surface Modification Agent. *J. Phys. Conf. Ser.* **2021**, *1943* (1), 012180. <https://doi.org/10.1088/1742-6596/1943/1/012180>.
- (64) Silviana, S.; Ma'ruf, A. Synthesized Silica Mesoporous from Silica Geothermal Assisted with CTAB and Modified by APTMS. *Int. J. Emerg. Trends Eng. Res.* **2020**, *8* (8), 4854–4860. <https://doi.org/10.30534/ijeter/2020/125882020>.
- (65) Travaglini, L.; Picchetti, P.; Del Giudice, A.; Galantini, L.; De Cola, L. Tuning and Controlling the Shape of Mesoporous Silica Particles with CTAB/Sodium Deoxycholate Catanionic Mixtures. *Microporous Mesoporous Mater.* **2019**, *279*, 423–431. <https://doi.org/10.1016/j.micromeso.2019.01.030>.
- (66) Che Ismail, N. H.; Ahmad Bakhtiar, N. S. A.; Md. Akil, H. Effects of Cetyltrimethylammonium Bromide (CTAB) on the Structural Characteristic of Non-Expandable Muscovite. *Mater. Chem. Phys.* **2017**, *196*, 324–332. <https://doi.org/10.1016/j.matchemphys.2017.05.007>.
- (67) Khoeini, M.; Najafi, A.; Rastegar, H.; Amani, M. Improvement of Hollow Mesoporous Silica Nanoparticles Synthesis by Hard-Templating Method via CTAB Surfactant. *Ceram. Int.* **2019**, *45* (10), 12700–12707. <https://doi.org/10.1016/j.ceramint.2019.03.125>.

Ready for Acceptance (25 Mei 2022)

9/2/22, 12:25 PM

Department of Chemical Engineering, Diponegoro University Mail - Ready for Acceptance - Additional Information Needed fo...



Silviana Silviana <silviana@che.undip.ac.id>

Ready for Acceptance - Additional Information Needed for Manuscript ID ie-2022-004247.R1

Industrial & Engineering Chemistry Research <onbehalfof@manuscriptcentral.com> Wed, May 25, 2022 at 3:34 AM
Reply-To: nenoff-office@iecr.acs.org
To: silviana@che.undip.ac.id

24-May-2022

Journal: Industrial & Engineering Chemistry Research

Manuscript ID: ie-2022-004247.R1

Title: "Synthesis of aminopropyl-functionalized mesoporous silica derived from geothermal silica for effective slow-release urea carrier"

Author(s): Silviana, S.; Janitra, Atikah; Sa'adah, Afriza; Dalanta, Febio

COVID-19 Support: Please visit the following website to access important information for ACS authors and reviewers during the COVID-19 crisis: <https://axial.acs.org/2020/03/25/chemists-covid-19-coronavirus/>

We are flexible in these unprecedented times affecting the global research community. If you need more time to complete authoring or reviewing tasks, please contact the editorial office and request an extension.

Dear Dr. Silviana:

Your manuscript is ready to be accepted for publication in ACS Industrial & Engineering Chemistry Research. However, the following issues must be addressed prior to acceptance. Please do not include any highlighting or marking on the manuscript. We would like to receive your revision as soon as possible, by 14-Jun-2022 at the latest.

- 1) Please upload a clean, unmarked copy of your manuscript, without any highlighting or tracked changes.
- 2) An email address is required for each corresponding author identified on the manuscript file. Please add the corresponding author email(s) to any page of the manuscript.
- 3) Please include author names, article titles, journal name, publication year, and at least the first page for each reference citation for the following incomplete journal references: 3.
- 4) A Table of Contents graphic must be included on the last page of your manuscript file. Guidelines for creating a successful graphic can be found at: http://pubs.acs.org/paragonplus/submission/toc_abstract_graphics_guidelines.pdf

To revise your manuscript, log into ACS Paragon Plus with your ACS ID at <http://acsparagonplus.acs.org/> and select "My Authoring Activity". There you will find your manuscript title listed under "Revisions Requested by Editorial Office." With the exception of your main text file, all of your original files will be available to you for review or replacement during the revision process. If you need to replace a file, please be sure to remove the original before uploading a new one. In all circumstances you must upload a new manuscript text file.

Prior to submitting the manuscript, ensure that the manuscript addresses the following points:

Format: Your revised manuscript must adhere to ACS format, especially references. For your convenience I have provided a link at the bottom of this message to the Industrial & Engineering Chemistry Research guidelines for authors. Note that in ACS Paragon Plus, authors have the option of embedding graphics into the manuscript or supplying graphics separately.

Supporting Information: If the manuscript is accompanied by any supporting information for publication, a brief description of the supplementary material is required in the manuscript. The appropriate format is: Supporting Information. Brief statement in nonsentence format listing the contents of the material supplied as Supporting Information.

Table of Contents (TOC) Graphic: If you have not already prepared a TOC Graphic, please include one in your revision submission. We feature all TOC graphics online when a manuscript is accepted for publication and select a few compelling TOC graphics for the cover of each issue of the journal. For information on how to prepare an effective TOC Graphic, please read the ACS Guidelines for Table of Contents/Abstract Graphics (http://pubs.acs.org/paragonplus/submission/toc_abstract_graphics_guidelines.pdf).

<https://mail.google.com/mail/u/0/?ik=ae189121fa&view=pt&search=all&permmsgid=msg-f%3A1733741225749324179&siml=msg-f%3A1733741...> 1/2

Funding Sources: Authors are required to report ALL funding sources and grant/award numbers relevant to this manuscript. Enter all sources of funding for ALL authors relevant to this manuscript in BOTH the Open Funder Registry tool in ACS Paragon Plus and in the manuscript to meet this requirement. See http://pubs.acs.org/page/4authors/funder_options.html for complete instructions.

ORCID: Authors submitting manuscript revisions are required to provide their own validated ORCID iDs before completing the submission, if an ORCID iD is not already associated with their ACS Paragon Plus user profiles. This iD may be provided during original manuscript submission or when submitting the manuscript revision. You can provide only your own ORCID iD, a unique researcher identifier. If your ORCID iD is not already validated and associated with your ACS Paragon Plus user profile, you may do so by following the ORCID-related links in the Email/Name section of your ACS Paragon Plus account. All authors are encouraged to register for and associate their own ORCID iDs with their ACS Paragon Plus profiles. The ORCID iD will be displayed in the published article for any author on a manuscript who has a validated ORCID iD associated with ACS Paragon Plus when the manuscript is accepted. Learn more at <http://www.orcid.org>.

We look forward to seeing your paper in Industrial & Engineering Chemistry Research.

Sincerely,

Dr. Tina M. Nenoff
Associate Editor
Industrial & Engineering Chemistry Research
Sandia National Laboratories
Phone: 919-967-7730
Email: nenoff-office@iecr.acs.org

Please click the link below to view the Industrial & Engineering Chemistry Research Author Guidelines:
<http://pubs.acs.org/page/iecred/submission/index.html>

FOR ASSISTANCE WITH YOUR MANUSCRIPT SUBMISSION PLEASE CONTACT:

ACS Publications Customer Services & Information (CSI)
Email: support@services.acs.org
Phone: 202-872-4357
Toll Free Phone: 800-227-9919 (USA/Canada only)

PLEASE NOTE: This email message, including any attachments, contains confidential information related to peer review and is intended solely for the personal use of the recipient(s) named above. No part of this communication or any related attachments may be shared with or disclosed to any third party or organization without the explicit prior written consent of the journal Editor and ACS. If the reader of this message is not the intended recipient or is not responsible for delivering it to the intended recipient, you have received this communication in error. Please notify the sender immediately by e-mail, and delete the original message.

As an author or reviewer for ACS Publications, we may send you communications about related journals, topics or products and services from the American Chemical Society. Please email us at pubs-comms-unsub@acs.org if you do not want to receive these. Note, you will still receive updates about your manuscripts, reviews, or future invitations to review.

Thank you.

Supplementary Journal Cover Invitation (25 Mei 2022)

9/2/22, 12:21 PM

Department of Chemical Engineering, Diponegoro University Mail - Supplementary Journal Cover Invitation ie-2022-004247.R1



Silviana Silviana <silviana@che.undip.ac.id>

Supplementary Journal Cover Invitation ie-2022-004247.R1

Industrial & Engineering Chemistry Research <onbehalfof@manuscriptcentral.com> Wed, May 25, 2022 at 3:34 AM

Reply-To: support@services.acs.org

To: silviana@che.undip.ac.id

24-May-2022

Manuscript ID: ie-2022-004247.R1

Manuscript Type: Article

Title: "Synthesis of aminopropyl-functionalized mesoporous silica derived from geothermal silica for effective slow-release urea carrier"

Author(s): Silviana, S.; Janitra, Atikah; Sa'adah, Afriza; Dalanta, Febio

Dear Dr. Silviana:

Did you know that we now offer a great way to promote your work on a supplementary journal cover? When you submit your revised manuscript, you can also submit cover art to be considered for one of Industrial & Engineering Chemistry Research's supplementary covers. Supplementary covers are featured on the Industrial & Engineering Chemistry Research website and corresponding article pages. ACS Publications will provide additional promotional support for your work via social media. You will also receive a complimentary 18 x 24 inch (45.7 x 61.0 cm) printed poster for display and a high-resolution file to include in your scientific talks, for use on your blog or website, or to post on social media.

If you are interested in participating, include your proposed supplementary cover art when you submit your revised manuscript. Here's how you do it:

1. Respond "Yes" to the Cover Art question when you submit your revised manuscript.
2. Upload your image and caption text in ACS Paragon Plus during the File Upload step. Use the Cover Art and Cover Art Caption file designations, respectively. To be considered, you must submit the image and caption at the same time as the revised manuscript.

Submission of a cover does not guarantee selection. All authors have the opportunity to submit Cover Art while submitting a revision, and your cover image will be evaluated among the submissions we receive. You will be notified if your supplementary cover art is selected for publication. You are responsible for obtaining and providing any needed permissions if you (or another author) did not create any portion of the image. Artwork must be included with the submission of your revised manuscript to be considered.

If your supplementary cover art is selected, we do ask that you contribute to the production costs. Full details about program costs, including the discount available to ACS Premium Members, can be found at <http://pubs.acs.org/page/4authors/promotion/journal-cover-image.html>.

Please note that the artwork you submit for supplementary covers may also be under consideration for our front cover, which is offered with no charge to authors. If you want to be considered only for the front cover, and not a supplementary cover, please respond NO accordingly to the Supplementary Cover Art question and consult the Author Guidelines for further instruction.

For more information on the Industrial & Engineering Chemistry Research's supplementary cover art program, please visit <http://pubs.acs.org/page/4authors/promotion/journal-cover-image.html> or contact our Publications Support team at support@services.acs.org to answer any questions.

ACS Publications is proud to support you throughout the publication of your research, and we are delighted that you have chosen us as your partner.

With best wishes,

ACS Publications
American Chemical Society

FOR ASSISTANCE WITH YOUR MANUSCRIPT SUBMISSION PLEASE CONTACT:

<https://mail.google.com/mail/u/0/?ik=ae189121fa&view=pt&search=all&permmsgid=msg-f%3A1733741225815233941&simpl=msg-f%3A1733741...> 1/2

ACS Publications Customer Services & Information (CSI)

Email: support@services.acs.org

Phone: 202-872-4357

Toll Free Phone: 800-227-9919 (USA/Canada only)

PLEASE NOTE: This email message, including any attachments, contains confidential information related to peer review and is intended solely for the personal use of the recipient(s) named above. No part of this communication or any related attachments may be shared with or disclosed to any third party or organization without the explicit prior written consent of the journal Editor and ACS. If the reader of this message is not the intended recipient or is not responsible for delivering it to the intended recipient, you have received this communication in error. Please notify the sender immediately by e-mail, and delete the original message.

As an author or reviewer for ACS Publications, we may send you communications about related journals, topics or products and services from the American Chemical Society. Please email us at pubs-comms-unsub@acs.org if you do not want to receive these. Note, you will still receive updates about your manuscripts, reviews, or future invitations to review.

Thank you.

Manuscript assigned to Editor (28 Mei 2022)

9/2/22, 12:23 PM

Department of Chemical Engineering, Diponegoro University Mail - Manuscript ie-2022-004247.R2 assigned to Editor



Silviana Silviana <silviana@che.undip.ac.id>

Manuscript ie-2022-004247.R2 assigned to Editor

Industrial & Engineering Chemistry Research <onbehalf@manuscriptcentral.com> Sat, May 28, 2022 at 8:02 PM

Reply-To: savage-office@iecr.acs.org

To: silviana@che.undip.ac.id

Cc: silviana@che.undip.ac.id, atikahayujanitra@gmail.com, afr312000@gmail.com, dalanta@student.undip.ac.id

28-May-2022

Journal: Industrial & Engineering Chemistry Research

Manuscript ID: ie-2022-004247.R2

Title: "Synthesis of aminopropyl-functionalized mesoporous silica derived from geothermal silica for effective slow-release urea carrier"

Author(s): Silviana, S.; Janitra, Atikah; Sa'adah, Afriza; Dalanta, Febio

Manuscript Status: Associate Editor Assigned

Dear Dr. Silviana:

Your manuscript entitled "Synthesis of aminopropyl-functionalized mesoporous silica derived from geothermal silica for effective slow-release urea carrier" has been assigned to the following editor:

Dr. Tina M. Nenoff
Associate Editor
Industrial & Engineering Chemistry Research
Sandia National Laboratories
Phone: 919-967-7730
Email: nenoff-office@iecr.acs.org

Please address all future correspondence regarding this manuscript to the above editor.

Submission of a manuscript to Industrial & Engineering Chemistry Research implies that the work reported therein has not received prior publication and is not under consideration for publication elsewhere in any medium, including electronic journals and computer databases of a public nature. This manuscript is being considered with the understanding that it is submitted on an exclusive basis. If otherwise, please advise.

Also please note that according to ACS Ethical Guidelines to Publication of Chemical Research, all authors must have reviewed and approved the submission of their manuscript. If you are a coauthor and approve its submission, no action is necessary. Similarly coauthors must approve the appointment of a Corresponding Author to select and execute the appropriate ACS publishing agreement, and should be informed by the Corresponding Author of the terms and conditions of that agreement. If you do not approve its submission to Industrial & Engineering Chemistry Research or the selection of Corresponding Author, please let us know as soon as possible. Refer to the manuscript number listed above in any correspondence, or you may simply reply to this message leaving the subject line intact. For more information on ethical responsibilities of authors, see the Ethical Guidelines to Publication of Chemical Research at <http://pubs.acs.org/page/policy/ethics/index.html>.

ACS Publications uses Crossref Similarity Check Powered by iThenticate to detect instances of similarity in submitted manuscripts. In publishing only original research, ACS is committed to deterring plagiarism, including self-plagiarism. Your manuscript may be screened for similarity to published material.

Sincerely,

Prof. Phillip E. Savage
Editor-in-Chief
Industrial & Engineering Chemistry Research
Phone: (919) 869-7650
Fax: (919) 929-9494
Email: eic@iecr.acs.org; savage-office@iecr.acs.org

<https://mail.google.com/mail/u/0/?ik=ae189121fa&view=pt&search=all&permmsgid=msg-f%3A1734075195133205162&simpl=msg-f%3A1734075...> 1/2

9/2/22, 12:23 PM

Department of Chemical Engineering, Diponegoro University Mail - Manuscript ie-2022-004247.R2 assigned to Editor

PLEASE NOTE: This email message, including any attachments, contains confidential information related to peer review and is intended solely for the personal use of the recipient(s) named above. No part of this communication or any related attachments may be shared with or disclosed to any third party or organization without the explicit prior written consent of the journal Editor and ACS. If the reader of this message is not the intended recipient or is not responsible for delivering it to the intended recipient, you have received this communication in error. Please notify the sender immediately by e-mail, and delete the original message.

As an author or reviewer for ACS Publications, we may send you communications about related journals, topics or products and services from the American Chemical Society. Please email us at pubs-comms-unsub@acs.org if you do not want to receive these. Note, you will still receive updates about your manuscripts, reviews, or future invitations to review.

Thank you.

<https://mail.google.com/mail/u/0/?ik=ae189121fa&view=pt&search=all&permmsgid=msg-f%3A1734075195133205162&simpl=msg-f%3A1734075...> 2/2

Resubmission of the Revised Manuscript 2 (28 Mei 2022)

9/2/22, 12:24 PM

Department of Chemical Engineering, Diponegoro University Mail - Industrial & Engineering Chemistry Research - Manuscript...



Silviana Silviana <silviana@che.undip.ac.id>

Industrial & Engineering Chemistry Research - Manuscript ID ie-2022-004247.R2

Industrial & Engineering Chemistry Research <onbehalf@manuscriptcentral.com> Sat, May 28, 2022 at 8:03 PM

Reply-To: support@services.acs.org

To: silviana@che.undip.ac.id

Cc: nenoff-office@lecr.acs.org, silviana@che.undip.ac.id, atikahayujanita@gmail.com, afr312000@gmail.com, dalanta@student.undip.ac.id

28-May-2022

Title: "Synthesis of aminopropyl-functionalized mesoporous silica derived from geothermal silica for effective slow-release urea carrier"

Authors: Silviana, S.; Janitra, Atikah; Sa'adah, Afriza; Dalanta, Febio

Manuscript ID: ie-2022-004247.R2

Materials and Interfaces

Manuscript Status: Submitted

Dear Dr. Silviana:

Your manuscript has been successfully submitted to Industrial & Engineering Chemistry Research.

Please reference the above manuscript ID in all future correspondence or when calling the office for questions. If there are any changes in your contact information, please log in to ACS Paragon Plus with your ACS ID at <http://acsparagonplus.acs.org/> and select "Edit Your Profile" to update that information.

You can view the status of your manuscript by checking your "Authoring Activity" tab on ACS Paragon Plus after logging in to <http://acsparagonplus.acs.org/>.

ACS Authoring Services

Did you know that ACS provides authoring services to help scientists prepare their manuscripts and communicate their research more effectively? Trained chemists with field-specific expertise are available to edit your manuscript for grammar, spelling, and other language errors, and our figure services can help you increase the visual impact of your research.

Visit <https://authoringservices.acs.org> to see how we can help you! Please note that the use of these services does not guarantee that your manuscript will be accepted for publication.

Thank you for submitting your manuscript to Industrial & Engineering Chemistry Research.

Sincerely,

Industrial & Engineering Chemistry Research

PLEASE NOTE: This email message, including any attachments, contains confidential information related to peer review and is intended solely for the personal use of the recipient(s) named above. No part of this communication or any related attachments may be shared with or disclosed to any third party or organization without the explicit prior written consent of the journal Editor and ACS. If the reader of this message is not the intended recipient or is not responsible for delivering it to the intended recipient, you have received this communication in error. Please notify the sender immediately by e-mail, and delete the original message.

As an author or reviewer for ACS Publications, we may send you communications about related journals, topics or products and services from the American Chemical Society. Please email us at pubs-comms-unsub@acs.org if you do not want to receive these. Note, you will still receive updates about your manuscripts, reviews, or future invitations to review.

Thank you.

<https://mail.google.com/mail/u/0/?ik=ae189121fa&view=pt&search=all&permmsgid=msg-f%3A1734075216120119771&simpl=msg-f%3A1734075...> 1/1

Synthesis of Aminopropyl-Functionalized Mesoporous Silica Derived from Geothermal Silica for an Effective Slow-Release Urea Carrier

S. Silviana,* Atikah A. Janitra, Afriza N. Sa'adah, and Febio Dalanta

Cite This: <https://doi.org/10.1021/acs.iecr.2c00424>

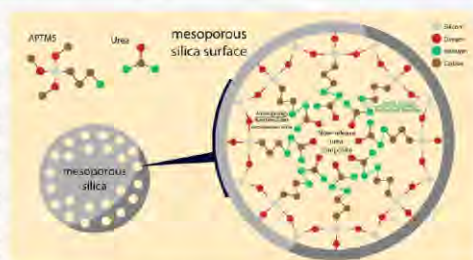
Read Online

ACCESS |

Metrics & More

Article Recommendations

ABSTRACT: An effective method to prepare slow-release urea was developed with aminopropyl-functionalized mesoporous silica (MS) to achieve enhanced urea adsorption and slow-release properties. As a novel study, mesoporous silica was developed using treated geothermal silica as the silica source, cetyltrimethylammonium bromide (CTAB) as the surfactant, and 3-aminopropyl trimethoxy silane (APTMS) as the surface modification agent. Mesoporous silica with the most desirable properties of uniform micro-morphology containing 38.55 wt % silica particles, 668.849 m²/g surface area, 149.33–353.28 mL/g adsorption–desorption range, and 0.26 mL/g adsorption pore volume was achieved using 0.05 mol of CTAB. The synthesized mesoporous silica showed type-IV hysteresis, which corresponds to mesoporous materials. Differential scanning calorimetry (DSC)—thermogravimetric analysis (TGA) thermograms showed that mesoporous silica is more reactive, with peaks at 82.3 and 159.5 °C, has good thermal stability, and undergoes only 17.61% weight loss until 124 °C. Scanning electron microscopy (SEM) showed that functionalization and urea adsorption to mesoporous silica resulted in no significant morphological changes. In the Fourier transform infrared (FTIR) spectra, MS/APTMS/U26.74 was observed to have higher intensities of C=O, N–H, C–N, and C–H groups compared with other samples. The cumulative urea release during 7 days was 184.5 ppm (92.4%) for commercial urea and 124.6 ppm (64.4%) for MS/APTMS/U26.74. The Higuchi kinetic model yielded the best fit predicting MS/APTMS/U26.74 release kinetics, with an R^2 of 0.9979 and a Higuchi constant of 24.4964%/day. Finally, MS/APTMS/U26.74 synthesized using geothermal silica, CTAB, and APTMS was noted to possess a potential composition for slow-release urea with enhanced efficiency.



INTRODUCTION

Nowadays, urea is being widely used in fertilizers,^{1,2} as a source of nitrogen in ruminants,^{3,4} in pesticides,^{5,6} for microbial growth,⁷ and for various agriculture activities due to its rich nitrogen content, abundance, and cost-effectiveness. However, several studies reported that a high content of urea fertilizers is lost due to leaching and ammonia volatilization⁸ upon application in soil, eventually generating severe environmental pollution, especially in soil and water sources.^{10–12} Therefore, slow-release urea (SRU) development serves as a means to improve urea efficiency, enhance controllable usage, and minimize environmental pollution. Currently, SRU is commonly prepared by encapsulating or adsorbing a saturated urea solution to porous matrix media such as zeolites,^{13–15} porous polymer composites,^{16–18} or mesoporous materials^{19–24} to control the urea release. Several polymers have been used as SRU matrix media, such as polyacrylonitrile,^{25,26} polysulfone,¹⁰ poly(vinyl chloride),²⁷ polyacrylic-rubber,²⁸ poly(vinyl acetate),²⁹ and polyurethane.³⁰ Sulfur-only-coated urea releases

83% urea after 7 days,¹⁰ whereas impregnation on hydroxypapatite yields a release rate of 88% after 460 s.¹⁴ Another study found that the use of bentonite in polycaprolactone or polyacrylamide hydrogel yields 75% urea release after 30 or 60 h.¹⁵ Slow-release membrane-encapsulated urea yields 90% nitrogen release after the 5th day²⁵ and double-coated slow-release fertilizers using ethyl cellulose (EC and starch-based superabsorbent polymer) yield 70% urea release at 96 h.²³ However, these polymers generate additional environmental issues due to the remaining nonbiodegradable polymer waste after they are used. Therefore, the application of biodegradable polymers has been carried out to solve the environmental

Received: February 4, 2022

Revised: May 28, 2022

Accepted: May 31, 2022

issues associated with the use of conventional polymers on SRU. Natural polymers have been applied as the matrix medium for SRU, including inorganics such as attapulgite^{31,32} and organics such as cellulose,³³ chitosan,³⁴ alginate,^{35,36} starch,³⁷ and lignin.³⁹ Nevertheless, due to their natural characteristics, these natural polymers are easily attacked by fungi, bacteria, and other microorganisms, causing a lack of performance. Therefore, further investigations to develop a prominent matrix material for enhancing SRU characteristics and performance are still needed, and it remains a vast area of research.

Mesoporous silica (MS) has gained considerable attention because of its potential in various fields, including drug delivery,^{38–40} catalysis,⁴¹ adsorbents,⁴² sensing,⁴³ and antibiotic-free antibacterial applications.⁴⁴ Due to the chemistry of silica, functionalizing and controllable tailoring of MS is easy, which allows it to be designed for the desired applications, including as the matrix medium for SRU. Many works have been conducted to synthesize MS with different structures, compositions, and pore properties to achieve desired and tunable characteristics.^{25,41,45,46} The type of precursor, pH, reaction time, temperature, type and concentration of catalyst, cosolvent, and surfactant are the main influencers of the final properties of the synthesized MS.^{38,41,43} Several synthesis procedures have been reported to develop MS with tunable and controllable properties, which are generally carried out in acidic and basic media.^{38,45,47} Under both conditions, the effects of the reaction temperature, surfactant, cosolvent, and additive concentrations were observed, and numerous MS properties have been clearly explained.^{38,45,47} A high specific surface area, high porosity, and tunable network framework structure can enable the generation of massive binding sites for urea in this matrix medium. However, it has also been reported that the thickness, hydrophilicity, and layer structure of the matrix medium strongly affect the release rate of SRU.^{28,30,34,47} Consequently, to achieve a maintainable rate of urea release from the slow-release urea, further modification and/or functionalization of the SRU matrix medium is highly required.

Aminopropyl-functionalized materials have gained considerable interest due to their stronger absorption capability compared with several chemicals such as amines, phosphates, and nitrates. The presence of an amine group on aminopropyl-functionalized silica, which has an amine functional group similar to that of urea, causes the crystallization of urea by hydrogen bonding with other amine groups. This acts as a seed to initiate the crystallization of the urea network, thus enhancing the absorption of urea on the surface of aminopropyl-functionalized silica.^{24,48,49} Various organometallic groups have been utilized to functionalize adsorption-based materials and enhance the capacity of adsorption and produce controllable kinetics.^{50,51} Currently, the most investigated aminopropyl-functionalized material is biochar or activated carbon. Nevertheless, these materials preferably have well-developed surface morphology, but the micropore domination alters the adsorbate diffusion into the pores, causing a decrease in the adsorption capacity. Compared with biochar or activated carbon, MS has a high specific surface area, ordered pores, and relatively high pore volumes, indicating that it is a potential material for adsorbents with a controllable diffusion behavior.^{23,38} Therefore, we was hypothesized the functionalization of MS as the SRU matrix medium to enhance the performance of SRU in terms of a high urea adsorption capacity and

controllable diffusion of urea from the synthesized SRU into the soil.

In this study, SRU with MS as the matrix medium was prepared from geothermal silica. Geothermal silica can be applied as the silica source to synthesize MS due to its high content of SiO₂, which has been utilized in numerous applications.^{52–57} The geothermal silica was purified using acid-leaching treatment before it was used. The purified silica was converted to sodium silicate as the precursor of silica source in MS preparation. Cetyltrimethylammonium bromide (CTAB) was used as the surfactant, and the mole amount of CTAB was varied to investigate its impact on the properties of the synthesized MS. The synthesized MS was further functionalized by covalently grafting aminopropyl groups on the MS surface using a 10% 3-aminopropyl trimethoxy silane (APTMS) solution to enhance the sorption capacity and slow-release properties of the synthesized slow-release urea. The essential analyses, including morphology, chemical groups and compositions, surface area involving gas sorption, hysteresis behaviors, pore characteristics, and thermal properties, were comprehensively characterized using scanning electron microscopy (SEM), energy-dispersive X-ray (EDX) spectrometry, X-ray fluorescence (XRF), X-ray diffraction (XRD), Fourier transform infrared (FTIR) spectroscopy, Brunauer–Emmett–Teller and Barrett–Joyner–Halenda (BET–BJH) analyses, thermogravimetric analysis (TGA), and differential scanning calorimetry (DSC). The synthesized slow-release urea was experimentally tested in the soil to investigate the release characteristics and compared with commercial urea. The release kinetics of the synthesized slow-release urea were also studied by applying several appropriate kinetic models. Such a novel study of slow-release urea synthesis using aminopropyl-functionalized MS as the matrix, derived from geothermal silica as the silica source, and CTAB as the surfactant has not yet been reported.

■ MATERIALS AND METHODS

Materials. The geothermal silica sample as the primary raw material for mesoporous silica synthesis was supplied by the geothermal power plant of PT Geo Dipa Energi, Dieng, Indonesia. Cetyltrimethylammonium bromide (CTAB, 99–101%) and 3-aminopropyl trimethoxy silane (APTMS, 99.8%) were purchased from Himedia and Sigma-Aldrich, Germany, respectively. Sulfuric acid (H₂SO₄, 98%), sodium hydroxide (NaOH, 95%), and hydrochloric acid (HCl, 36.5–38%) used in purification treatments of geothermal silica were supplied by Mallinckrodt. Aqueous ammonia (NH₄OH, 25%) and ethanol (C₂H₅OH, 96%) utilized in the preparation were purchased from Merck, Germany. Commercial urea (nitrogen ≥46%) was supplied by PT Petrokimia Gresik, Indonesia. Distilled (DI) water was utilized in all experiments.

Methods. Purification Treatments of Geothermal Silica Samples. Geothermal silica contains contaminants. Therefore, it required a purification treatment to produce high-purity silica as the primary material to synthesize mesoporous silica.^{58–62} There were two steps in the purification treatment, i.e., acid-leaching and a sodium silicate process. First, 250 g of the geothermal silica sample was dried in an oven at 110 °C for 12 h to reduce its moisture content. Then, the dried sample was crushed into a fine powder. This sample was then examined by X-ray fluorescence (XRF, Thermo Fisher Scientific) and X-ray diffraction (XRD, Thermo Fisher Scientific) to reveal its chemical composition and amorphous

structure. Next, acid-leaching treatment was conducted based on the methods reported recently.^{58,59} The treated geothermal silica (125 g) was carefully dispersed and constantly mixed in 500 mL of 20% H_2SO_4 solution at 100 °C for 105 min. The acid processing by H_2SO_4 is intended to remove the residual impurities on the sample, specifically the metal oxide content. After that, repeated washing and rinsing of the residue were performed to remove any unspent acid until a neutral pH was achieved. The residue was then placed in an oven at a temperature of 110 °C until completely dry. The treated silica from this step was analyzed using XRF and XRD.

The second purification step was conducted by filtering out the sodium silicate to further purify the treated silica of insoluble impurities. This procedure was conducted based on a method reported previously.^{55,59} It was started by mixing 125 g of the treated silica sample with 600 mL of 4 M NaOH solution and was stirred and maintained at 90 °C for 60 min. After that, the mixture was filtered through a filter paper (Whatman No. 42) using a vacuum filter. The generated filtrate was sodium silicate, which was further applied as the precursor to synthesize mesoporous silica.

Synthesis of Mesoporous Silica. This step followed the modified Stöber method that was reported previously.^{59–61} First, the primary solution was composed of 10 mol of ethanol, 22.4 mol of water, and 5.2 mol of NH_4OH . The solution was constantly mixed at low speed (80–100 rpm) for 15 min. After that, CTAB as a surfactant was slowly added into the solution at concentrations of 0.015, 0.03, and 0.05 mol. Sodium silicate was prepared by dissolving 10 g of treated silica in 82.5 mL of 4 M NaOH. Next, 100 mL of the prepared sodium silicate solution was slowly added to the above solution. The solution turned opaque immediately, indicating that the reaction has started. The solution was continuously mixed and maintained for 2 h under room temperature conditions. After that, the solution was filtered to separate the solids as the generated mesoporous silica from the mixture through a filter paper (Whatman No. 42) using a vacuum filter. Subsequently, the solids were washed to remove any unspent solution. The solid was then calcined in a furnace burner at 550 °C to remove the remaining organic compounds, creating a mesoporous structure throughout the surface of the silica. The prepared mesoporous silica was characterized by scanning electron microscopy–energy-dispersive X-ray spectroscopy (Thermo Fisher Scientific), Brunauer–Emmett–Teller and Barrett–Joyner–Halenda (BET–BJH) analyses (autosorb IQ Quantachrome Instruments from Anton Paar Switzerland AG), thermal analysis of TG/DTA/DSC (Linseis STA 1600 Premium Series), and Fourier transform infrared spectroscopy (IRPrestige21, Shimadzu, Japan, by the transmittance mode of acquisition).

Purification Treatments of Geothermal Silica Samples. This procedure was based on previously reported studies.^{49,50} In this method, APTMS was utilized as a silane coupling agent to modify the surface characteristics of mesoporous silica. First, calcined mesoporous silica was carefully mixed at 150 rpm with 10% APTMS solution at room temperature for 8 h. This step was performed to allow the surface modification reaction of mesoporous silica to yield the slow-release urea. It was then dried under atmospheric pressure at 40 °C. Finally, the modified mesoporous silica with APTMS was characterized using BET–BJH analysis and FTIR spectroscopy.

Next, 1 g of modified mesoporous silica/APTMS was added to the urea solution (U) at certain concentrations (6.74, 16.74,

26.74, and 36.74 wt %) with respect to 100 mL of aquadest. The mesoporous silica/APTMS with different urea compositions is presented in Table 1. The mixture was constantly

Table 1. Contents of CTAB, APTMS, and Urea in the Preparation of the Slow-Release Urea

sample code	CTAB (mol)	APTMS solution (%)	urea solution (wt %)
MS	0.05	0	0
MS/APTMS	0.05	10	0
MS/APTMS/U6.74	0.05	10	6.74
MS/APTMS/U16.74	0.05	10	16.74
MS/APTMS/U26.74	0.05	10	26.74
MS/APTMS/U36.74	0.05	10	36.74

stirred for 24 h at room temperature to allow the adsorption of urea into the mesoporous silica by hydrogen bonding.³⁸ Afterward, it was filtered, and the solids were dried in an oven at a temperature of 40 °C. Finally, the generated solids were characterized using FTIR spectroscopy.

Performance Test of the Prepared Slow-Release Urea. The slow-release urea performance was experimentally assessed by measuring the amount of urea present in the overflow liquid. The dissolved urea content in the groundwater was determined. Figure 1 depicts a schematic illustration of the

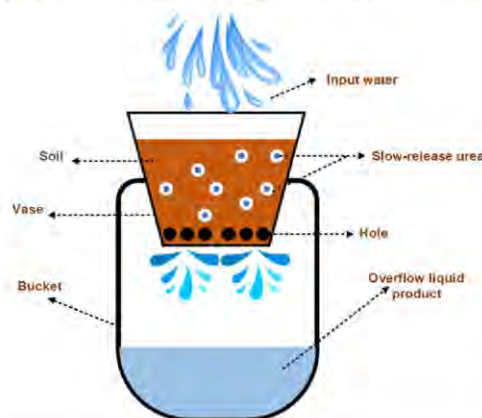


Figure 1. Schematic illustration of the apparatus for the slow-release urea performance test.

respective experiment. Initially, 1 g of slow-release urea was immersed in 25 g of soil in a plastic vase. Subsequently, 25 mL of DI water was used for watering the sample every day during 7 days of observation, and the overflow water from the vase was carefully collected. This test was repeated for three replications. The urea content in the overflow liquid was measured using a UV–vis spectrophotometer (Thermo Scientific GENESYS 10S). The measurement was performed at an optimum wavelength of 195 nm, which is close to the wavelength of 190 nm used in a previous research.⁶²

C

<https://doi.org/10.1021/acs.iecr.2c00424>
Ind. Eng. Chem. Res. XXXX, XXX, XXX–XXX

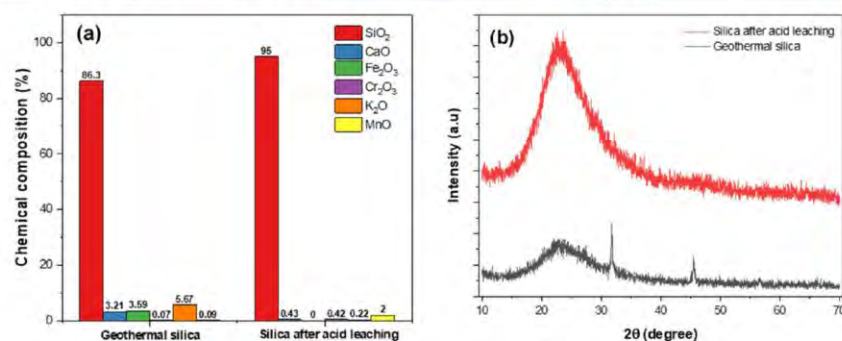


Figure 2. (a) XRF results of the geothermal silica sample and purified silica after acid-leaching and (b) XRD patterns of geothermal silica and purified silica after acid-leaching.

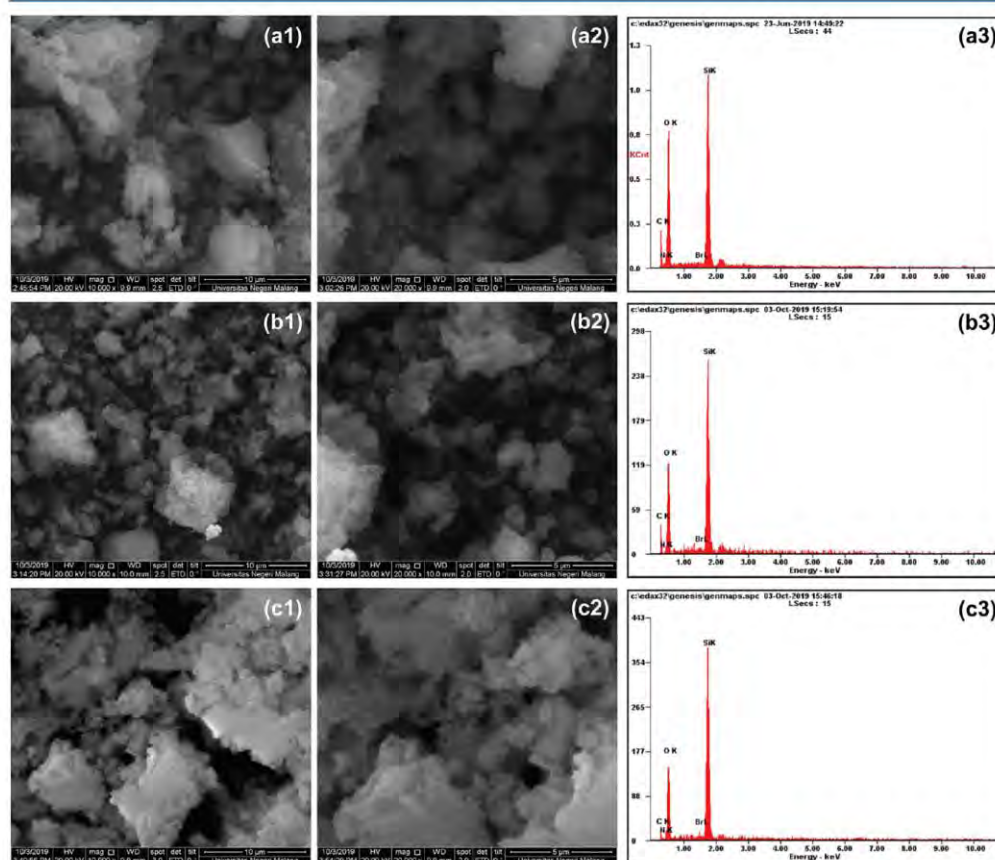


Figure 3. SEM-EDX micrographs of the modified mesoporous silica using (a) 0.015 mol, (b) 0.03 mol, and (c) 0.05 mol of CTAB.

Study of Urea Release Kinetics. The mechanism of urea release from the slow-release urea was theoretically evaluated

by applying some kinetic models, such as the pseudo-first-order, pseudo-second-order, Higuchi, and Hixson-Crowell

D

<https://doi.org/10.1021/acs.iecr.2c00424>
Ind. Eng. Chem. Res. XXXX, XXX, XXX-XXX

Table 2. Chemical Composition Data Extracted from EDX Spectra for Mesoporous Silica Using Three Different Amounts of CTAB

element	EDX recorded	MS-0.015 ^a		MS-0.03 ^b		MS-0.05 ^c	
		weight (%)	atomic (%)	weight (%)	atomic (%)	weight (%)	atomic (%)
carbon	C K	25.16	33.59	27.94	27.66	11.42	17.36
nitrogen	N K	4.08	4.67	2.59	3.00	2.72	3.54
oxygen	O K	50.02	50.13	44.99	45.52	48.60	55.45
bromine	Br K	0.64	0.13	0.78	0.16	1.38	0.32
silicon	Si K	20.11	11.48	23.70	13.66	35.88	23.32

^aMS-0.015 represents the mesoporous silica with 0.015 mol of CTAB. ^bMS-0.03 represents the mesoporous silica with 0.03 mol of CTAB. ^cMS-0.05 represents the mesoporous silica with 0.05 mol of CTAB.

models; the mathematical expressions of these models are represented by eqs 1–4.

Pseudo-first-order model⁶³

$$\ln Q_t = \ln Q_0 - k_1 t \quad (1)$$

Pseudo-second-order model⁶⁴

$$\frac{t}{Q_t} = \frac{1}{k_2 Q_0^2} - \frac{t}{Q_0} \quad (2)$$

Higuchi model⁶⁵

$$Q_t = K_H t^{1/2} \quad (3)$$

Hixson–Crowell model⁶³

$$Q_0^{1/3} - Q_t^{1/3} = K_{HC} t \quad (4)$$

where Q_t is the amount of urea released at a certain time (%), Q_0 is the initial amount of urea in the slow-release urea (%), k_1 is the pseudo-first-order rate constant, k_2 is the pseudo-second-order rate constant, K_H is the Higuchi constant, K_{HC} is the Hixson–Crowell constant, and t is time (day).

RESULTS AND DISCUSSION

Properties of Purified Silica after Acid-Leaching Treatment. The sample of geothermal silica was subjected to acid-leaching treatment to remove the impurities, especially metal oxides. Figure 2a depicts the XRF results of geothermal silica and the purified silica after acid-leaching. The geothermal silica was found to consist of 86.3 wt % SiO_2 , with a fairly high content of metal oxides including CaO, Fe_2O_3 , Cr_2O_3 , K_2O , and MnO with concentrations of 3.21, 3.59, 0.07, 5.67, and 0.09 wt %, respectively. The presence of Cr_2O_3 is a drawback of geothermal silica because it is not very reactive but dissolves in acid as hydrated chromium ions $[\text{Cr}(\text{H}_2\text{O})_6]^{3+}$. This sample of geothermal silica was treated in 500 mL of 20% H_2SO_4 solution at 100 °C for 105 min to dissolve the metal oxides into the sulfuric acid. The XRF analysis of the silica product after acid-leaching revealed that the sample consists of 95 wt % SiO_2 , leaving small amounts of metal oxides such as CaO, Cr_2O_3 , K_2O , and MnO with concentrations of 0.43, 0.42, 0.22, and 2.00 wt %, respectively. Based on this analysis, the acid-leaching process significantly removed the metal oxides from the geothermal silica, resulting in a higher purity of the silica. The influence of the acid-leaching treatment was further evaluated by an XRD analysis.

Figure 2b represents the XRD patterns of geothermal silica and the purified silica after acid-leaching. The diffractogram pattern of geothermal silica shows a broad peak ranging from a 2θ of 15–30°, indicating the existence of amorphous SiO_2 .

Three significant sharp peaks were found at 32.5, 46.3, and 49.8°, which correspond to Fe_2O_3 , K_2O , and Cr_2O_3 in the sample, respectively.³⁸ The purified silica after acid-leaching was also evaluated by XRD analysis. It can be clearly observed that the purified silica has a more significant broad peak at a 2θ of 15–30°, which indicates a higher amount of amorphous SiO_2 than that in the geothermal silica sample. Also, there are no other metal oxide peaks appearing in the diffractogram of the purified silica. Therefore, it can be reasonably concluded that the acid-leaching treatment successfully removed the metal oxides in the geothermal silica. Silica with higher purity ($\geq 95\%$) can be utilized as the main material for synthesizing mesoporous silica with a higher Si content on its surface to react with surface-modifying agents.

Characterization of the Synthesized Mesoporous Silica. *Surface Micrographs and Chemical Composition of the Synthesized Mesoporous Silica.* In this study, the modified Stöber method was adapted for the synthesis of mesoporous silica. The reaction was conducted at room temperature using CTAB as the surfactant, aqueous NH_4OH as the catalyst, ethanol as the cosolvent, and sodium silicate derived from geothermal silica as the silica source. For different formulations of material synthesis, the amount of NH_4OH , ethanol, and sodium silicate were kept fixed, whereas the amount of CTAB was varied to 0.015, 0.03, and 0.05 mol. Hence, the effects of the mole amount of CTAB on mesoporous silica synthesis were experimentally investigated. It was found that different amounts of CTAB as a surfactant during synthesis have a significant effect on the micro-morphology of the synthesized mesoporous silica, as clearly revealed by the SEM–EDX analysis shown in Figure 3 (with 10.000× and 20.000× magnifications). Figure 3a–c depicts the surface morphology images of mesoporous silica with 0.015, 0.03, and 0.05 mol of CTAB, respectively.

Different mole amounts of CTAB resulted in different shapes of mesoporous silica particles. When using 0.015 mol of CTAB (Figure 3a), the synthesized mesoporous silica had a randomized shape, fairly similar to that obtained with 0.03 mol of CTAB (Figure 3b), and showed a small increase in the number of mesoporous silica particles. Meanwhile, when using 0.05 mol of CTAB, the synthesized mesoporous silica had a more uniform particle shape. These findings suggest that the addition of CTAB tends to produce mesoporous silica particles. This phenomenon is in agreement with a previous study that an increasing amount of surfactant produces abundant interaction of two counter-charged surfactants, resulting in the growth of silicate particles.⁶¹

Further, an SEM–EDX analysis was carried out to reveal the chemical composition of the synthesized mesoporous silica with different loaded amounts of CTAB. Figure 3 shows the

E

<https://doi.org/10.1021/acs.iecr.2c00424>
Ind. Eng. Chem. Res. XXXX, XXX, XXX–XXX

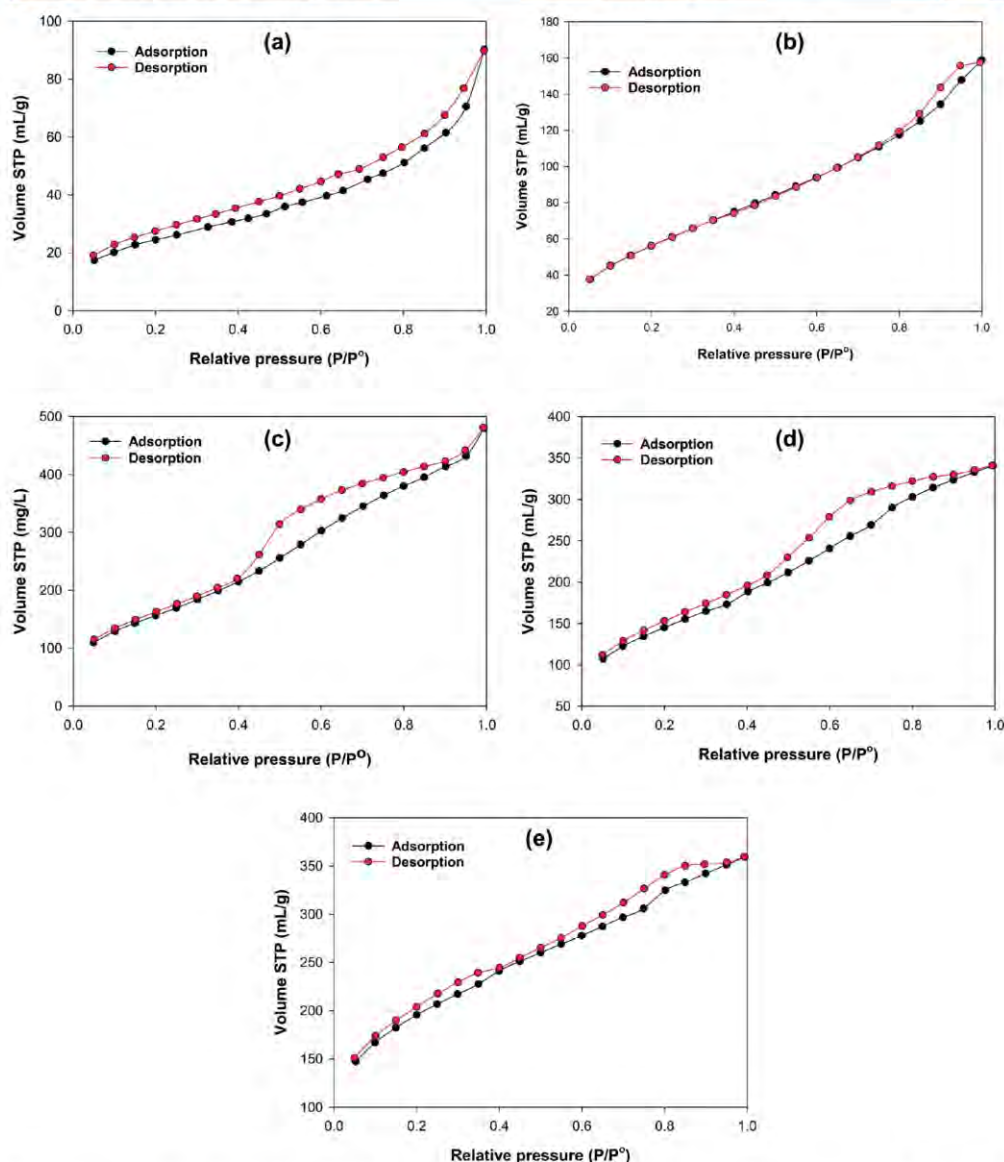


Figure 4. Sorption isotherm of (a) geothermal silica, (b) purified silica after acid-leaching, and mesoporous silica products with CTAB variations of (c) 0.015 mol, (d) 0.03 mol⁶⁸, and (e) 0.05 mol.

EDX spectra of the synthesized mesoporous silica with 0.015 mol (Figure 3a3), 0.03 mol (Figure 3b3), and 0.05 mol of CTAB (Figure 3c3). The quantification results of EDX are shown in Table 2, providing information about the chemical composition of the tested samples. The mesoporous silica synthesized with 0.015, 0.03, and 0.05 mol of CTAB were

found to consist of 20.11, 23.70, and 35.88 wt % Si, respectively. In the micrograph analysis, the mesoporous silica from 0.05 mol of CTAB was visualized as a white solid. According to previous research,⁶⁶ the CTAB surfactant undergoes a polar interaction with the silica precursor. It was observed that the hydrophilic head of CTAB was attached to

F

<https://doi.org/10.1021/acs.iecr.2c00424>
Ind. Eng. Chem. Res. XXXX, XXX, XXX–XXX

the surface of the silica, whereas the tail was oriented toward the polymer matrix. This phenomenon may be assumed to result from an interaction between the OH^- ion on the silica surface and the N^+ ion of CTAB. In this step, ion exchange and aggregate formation can occur simultaneously. Furthermore, more mesoporous silica aggregates are released with a higher CTAB content. The aggregation of mesoporous silica is likely rectangular, as detected by the SEM analysis. Based on the BET–BJH analysis, a higher amount of CTAB resulted in a higher quality of mesoporous silica in terms of physical properties such as specific surface area, pore volume, and pore radius. Moreover, the Si content of mesoporous silica was detected to be higher at higher CTAB contents. Meanwhile, the components of C, N, and Br in EDX results were found to be from the residual amount of CTAB in the synthesized mesoporous silica after calcination to remove the CTAB. It can be assumed that the calcination operation conditions (at 550 °C for 3 h) did not completely decompose all of the CTAB. It can be concluded that using 0.05 mol of CTAB provided the best mesoporous silica with a high content of Si and a lower content of unreacted CTAB (based on the C content). These findings from EDX results are confirmed with SEM micrographs, as discussed previously.

Sorption Isotherm and Pore Properties of the Synthesized Mesoporous Silica. The pore properties and sorption isotherm of several samples were analyzed by a BET–BJH analysis of the N_2 adsorption/desorption patterns. Figure 4 represents the sorption isotherm of geothermal silica (Figure 4a), silica purified by acid-leaching (Figure 4b), and mesoporous silica synthesized with 0.015 mol (Figure 4c), 0.03 mol (Figure 4d), and 0.05 mol (Figure 4e) of CTAB. A type-IV sorption isotherm was developed for all samples, indicating mesoporous materials.⁶⁷

A complete summary of the values of specific surface area, adsorbed–desorbed volume range, pore volume, and pore radius is presented in Table 3, and the pore size distribution of

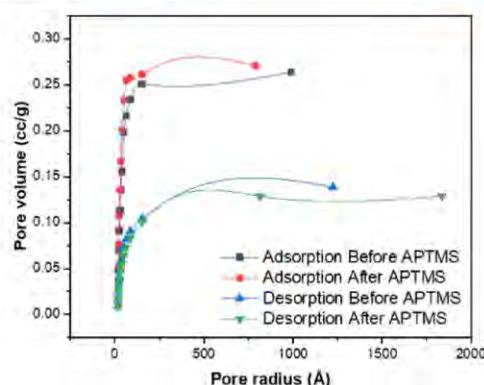


Figure 5. BJH pore size distribution of mesoporous silica products with 0.05 mol of CTAB before and after treatment with APTMS.

oxides from the bulk body of silica, which produces more empty sites resulting in a higher measured surface area and higher adsorption ability. It was also found that the specific surface area considerably increased upon an increase in the mole contents of CTAB, which are 582.454, 511.946, and 668.849 m^2/g for mesoporous silica synthesized with CTAB amounts of 0.015, 0.03, and 0.05 mol, respectively. This phenomenon indicates the greater generation of mesoporous structures upon an increase in the CTAB loading, resulting in a higher estimated surface area. This is in agreement with the SEM results showing that an increased loading of CTAB produces a more uniformly shaped particle, which possibly generates a higher surface area. At the same time, the initial intake adsorption–desorption volume was also found to increase from 18.61 mL/g (geothermal silica) to 102.35, 103.47, and 149.33 mL/g for mesoporous silica synthesized with CTAB contents of 0.015, 0.03, and 0.05 mol, respectively. However, the observed adsorption pore volume decreased upon the addition of CTAB from 0.62 mL/g for purified silica to 0.62, 0.39, and 0.26 mL/g for mesoporous silica synthesized with CTAB contents of 0.015, 0.03, and 0.05 mol, respectively. This can be explained by the increased growth of particles when a higher amount of CTAB was introduced, as evident from the SEM images. The uniform particle distribution can possibly produce a smaller void volume in the bulk body due to the smaller gaps between particles. Further, the measured pore radii were 19.83, 17.07, 19.11, 15.31, and 17.04 Å for geothermal silica, purified silica, and mesoporous silica with 0.015, 0.03, and 0.05 mol of CTAB, respectively. These pore radius values indicate that all of them can be classified as mesoporous materials.⁶⁷ Therefore, from these findings, synthesized mesoporous silica with 0.05 mol of CTAB showed the most desirable characteristics in terms of the adsorption isotherm specific surface area, adsorbed–desorbed volume, and pore radius, suggesting that it is a preferable matrix material for slow-release urea.

Thermal Analysis of the Synthesized Mesoporous Silica. To investigate the thermal characteristics of the synthesized mesoporous silica, DSC and TGA analyses were performed using an inert gas (nitrogen). Figure 6 shows DSC thermograms of three different samples, i.e., geothermal silica, mesoporous silica (best formulation using 0.05 mol of

Table 3. BET Analysis Results, Including Specific Surface Area, Pore Volume, and Pore Radius (Adsorption Isotherm) of Geothermal Silica, Purified Silica after Acid-Leaching, and Modified Mesoporous Silica with Different Amounts of CTAB⁶⁸

sample	specific surface area (m^2/g)	adsorbed–desorbed volume range (mL/g)	pore volume (mL/g)	pore radius (Å)
geothermal silica	40.899	18.61–86.79	0.11	19.83
purified silica after acid-leaching	178.063	37.62–158.62	0.62	17.07
mesoporous silica with CTAB 0.015 mol	582.454	102.35–485.75	0.62	19.11
mesoporous silica with CTAB 0.03 mol	511.946	103.47–346.11	0.39	15.31
mesoporous silica with CTAB 0.05 mol	668.849	149.33–353.28	0.26	17.04

the mesoporous silica product before and after APTMS introduction is shown in Figure 5. They show the variations of measured values upon an increased CTAB content. The specific surface area of geothermal silica was significantly increased from 40.899 to 178.063 m^2/g in purified silica after acid-leaching. It could be possibly due to the removal of metal

G

<https://doi.org/10.1021/acs.iecr.2c00424>
Ind. Eng. Chem. Res. XXXX, XXX, XXX–XXX

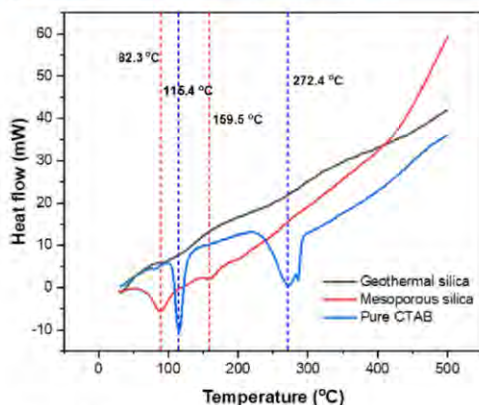


Figure 6. DSC thermogram of geothermal silica, mesoporous silica, and pure CTAB.

CTAB), and pure CTAB. The DSC thermogram of geothermal silica shows no significant peaks that indicate the melting behavior of the sample. DSC was carried out by comparing the temperatures of the sample and reference material during temperature changes. The temperature of the reference material will be the same if there are no changes. Thermal phenomena such as melting can cause decomposition or changes in the amorphous structure of the sample. The DSC curve in Figure 6 shows two endothermic steps in mesoporous silica. The enthalpies measured were -69.2175 J/g (at 82.3 °C) and -10.0796 J/g (at 159.5 °C). The measured enthalpies in pure CTAB were -141.8772 J/g (at 115.4 °C) and -19.6368 J/g (at 272.4 °C).

The TGA analysis confirmed the weight loss behavior of geothermal silica, mesoporous silica, and pure CTAB at temperatures ranging from 30 to 500 °C. TGA thermograms of the three samples and a summary of the weight loss and degradation temperatures are shown in Figure 7 and Table 4, respectively. All samples experienced a gradual weight loss as a function of temperature. Generally, the degradation occurred in four steps for geothermal silica and mesoporous silica and in three steps for pure CTAB. The most significant weight loss in geothermal silica (Figure 7a) occurred at temperatures ranging from 30 to 135 °C, with 11.59% weight loss. This condition is possibly due to the evaporation of trapped and bonded water in the sample. Meanwhile, based on the TGA thermogram, mesoporous silica (Figure 7b) shows four regions of weight loss, which were 17.61% at 30 – 124 °C, 45.56% at 125 – 227 °C, 14.40% at 228 – 294 °C, and 5.72% at 295 – 500 °C. These are attributable to the evaporation of trapped water molecules in the first step, the degradation of organic compounds in the second step, degradation of CTAB in the third step, and degradation of the remaining long-chain organic compounds in the last step. In addition, the TGA thermogram of pure CTAB shows a significant weight loss of 87.45% at 227 – 287 °C, which was due to the degradation of organic chains in CTAB. A similar pattern was also observed in the TGA thermogram of mesoporous silica. This finding explains that the presence of CTAB in mesoporous silica interfered with the intermolecular interaction of CTAB and silica, and this interaction led to a

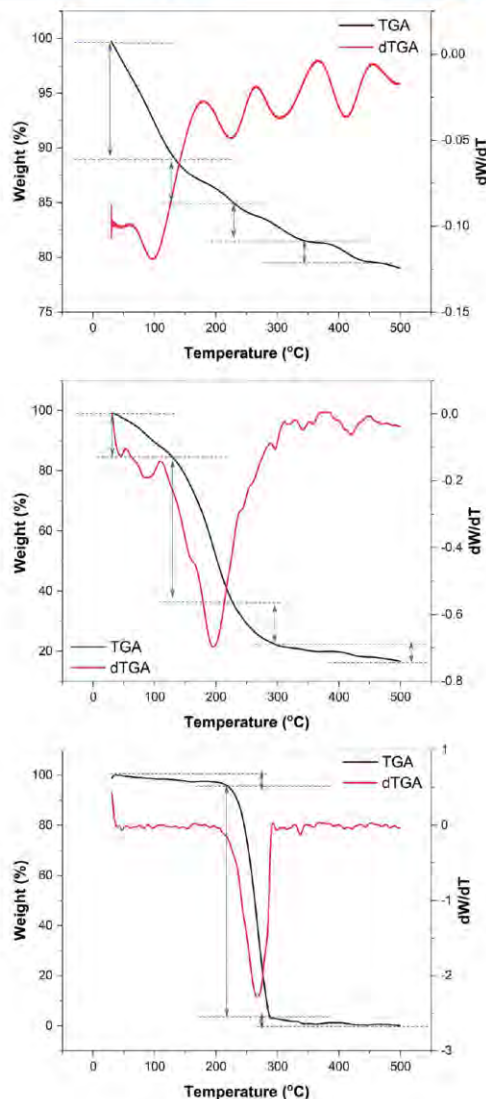


Figure 7. TGA thermograms of (a) geothermal silica, (b) mesoporous silica, (c) pure CTAB.

change in the thermal degradation behavior of the synthesized mesoporous silica.

Characteristics of Slow-Release Urea with APTMS as a Surface-Modifying Agent. Based on previous discussions, synthesized mesoporous silica with 0.05 mol of CTAB shows the most suitable characteristics to be utilized as the matrix material for slow-release urea. Furthermore, to develop the desirable slow-release characteristic, surface modification of mesoporous silica was performed using a solution containing

H

<https://doi.org/10.1021/acs.iecr.2c00424>
Ind. Eng. Chem. Res. XXXX, XXX, XXX–XXX

Table 4. TGA Data Including Weight Losses at Certain Temperatures of Geothermal Silica, Mesoporous Silica, and Pure CTAB

sample	temperature range (°C)	weight loss (%)
geothermal silica	30–135	11.59
	136–236	4.32
	237–347	1.86
	348–453	1.05
mesoporous silica	30–124	17.61
	125–227	45.56
	228–294	14.40
	295–500	5.72
pure CTAB	30–226	6.75
	227–287	87.45
	288–500	5.45

10% 3-aminopropyl trimethoxy silane (APTMS). APTMS possibly undergoes an intermolecular interaction with the molecules of urea.⁴⁸ This interaction leads to a strong bonding between urea and the matrix of mesoporous silica; therefore, they can be combined to produce slow-release urea. However, the introduction of APTMS also created cross-linking between the APTMS molecules, which led to vertical polymerization and possibly pore blocking. This phenomenon affected the properties of mesoporous silica, especially its porosity, resulting in a lower value of the surface area, pore volume, and pore radius, as shown in Table 5.

Table 5. BET Analysis Results, Including Specific Surface Area, Pore Volume, and Pore Radius (Adsorption Isotherm) of Modified Mesoporous Silica Using 0.05 mol of CTAB before and after the Introduction of APTMS

sample	specific surface area (m ² /g)	adsorbed–desorbed volume range (mL/g)	pore volume (mL/g)	pore radius (Å)
mesoporous silica with CTAB 0.05 mol before the introduction of APTMS	668.849	149.33–353.28	0.26	17.04
mesoporous silica with CTAB 0.05 mol after the introduction of APTMS	103.049	4.62–93.18	0.14	15.30

Figure 8 represents the SEM micrographs and EDX spectra of the synthesized slow-release urea. Based on Figure 8, it can be observed that all samples had a surface micromorphology similar to that of MS/APTMS. No significant changes in terms of the morphology occurred upon an increase in urea introduction to the slow-release urea. It can be reasonably concluded that the introduction of urea to MS/APTMS as the matrix did not influence the morphology of the generated slow-release urea. In addition, EDX results in Figure 8 reveal the spectra of the elements recorded in the tested samples. It was found that the major elements that appeared in all samples were Si, C, and O. A complete summary of the chemical composition of the synthesized slow-release urea is presented in Table 6. According to Table 6, introducing an increasing concentration of urea into the slow-release urea generates a higher content of N, corresponding to the quantity of urea in the slow-release urea. MS/APTMS has 3.81 wt % nitrogen, which gradually increased upon increasing the amount of urea introduced, which are 4.02, 4.63, 5.17, and 6.36 wt % for MS/

APTMS/U6.74, MS/APTMS/U16.74, MS/APTMS/U26.74, and MS/APTMS/U36.74, respectively. Therefore, the initial concentration of urea introduced significantly influenced the generated urea concentration in the synthesized slow-release urea.

FTIR analysis was performed to examine the bond interaction of urea in the matrix structure and the effect of APTMS on the synthesized slow-release urea. Figure 9 represents the FTIR spectra of different tested samples at wavenumbers of 4000–500 cm^{−1} (Figure 9a) and 2300–1300 cm^{−1} (Figure 9b).⁵⁰ From Figure 9a, it can be found that all tested samples displayed an intensely broad peak ranging from 1250 to 900 cm^{−1}, indicating the vibration of Si–O–Si groups.⁴⁹ As shown in Figure 9b, further analysis of the formation of new functional groups upon the application of APTMS and the introduction of urea to the matrix was performed. It can be seen that the application of APTMS to the mesoporous silica generated a slightly higher recorded absorbance at 1556 and 1495 cm^{−1}, which correspond to the vibrations of N–H and C–N groups, respectively.²⁴ This is explained by the formation of abundant N–H and C–N groups of APTMS on the mesoporous silica structure during the surface modification process.

On the other hand, the varied concentrations of urea introduced into MS/APTMS were also found to result in higher recorded absorbance intensities at several wavenumbers. Absorption bands at 2100 and 1636 cm^{−1} indicate the stretching vibrations of N=C=O and C=O groups, attributed to the natural composition of urea and its cyanate impurities. Intense peaks recorded at 1556, 1495, and 1340 cm^{−1} are related to the vibrations of N–H, C–N, and C–H groups, respectively.^{49,50} On comparing the relative absorbance intensities of the tested samples, MS/APTMS/U26.74 was found to generate a higher intensity of C=O, N–H, C–N, and C–H groups. A higher intensity implies a higher content of the respective groups in MS/APTMS/U26.74 compared with other samples, suggesting the best formulation for the slow-release urea. Figure 9c depicts the proposed bond formations of the aminopropyl groups grafted from APTMS to the siloxane groups on the surface of the mesoporous silica, resulting in the aminopropyl-functionalized mesoporous silica. This functionalization is needed to effectively adsorb the urea and control its release. The amine groups from urea bonded with the amine sites of aminopropyl groups. This amine bond formation (N–H) was recorded and displayed on FTIR spectra. Furthermore, hydrogen bonding as another attractive intermolecular force can occur due to the abundance of highly electronegative atoms such as oxygen (O), nitrogen (N), and hydrogen (H). Therefore, it can allow a stronger bonding of urea groups on the surface of the functionalized mesoporous silica, thus resulting in an effective slow-release property.

Study of Release Kinetics of the Synthesized Slow-Release Urea. The performance of slow-release urea was determined by measuring the urea content in the overflow liquid (Performance Test of the Prepared Slow-Release Urea). The observed samples were MS/APTMS/U26.74, as the best formulation for slow-release urea discussed previously, and commercial silica, as the control variable. The initial urea content in each sample was set to 200 ppm. Figure 10a depicts the amount (ppm) of urea released during 7 days of observation from the sample to the overflow liquid. The highest overflow urea concentration was recorded on the second day for MS/APTMS/U26.74, with a value of 28.55 ppm, which was nearly constant on the

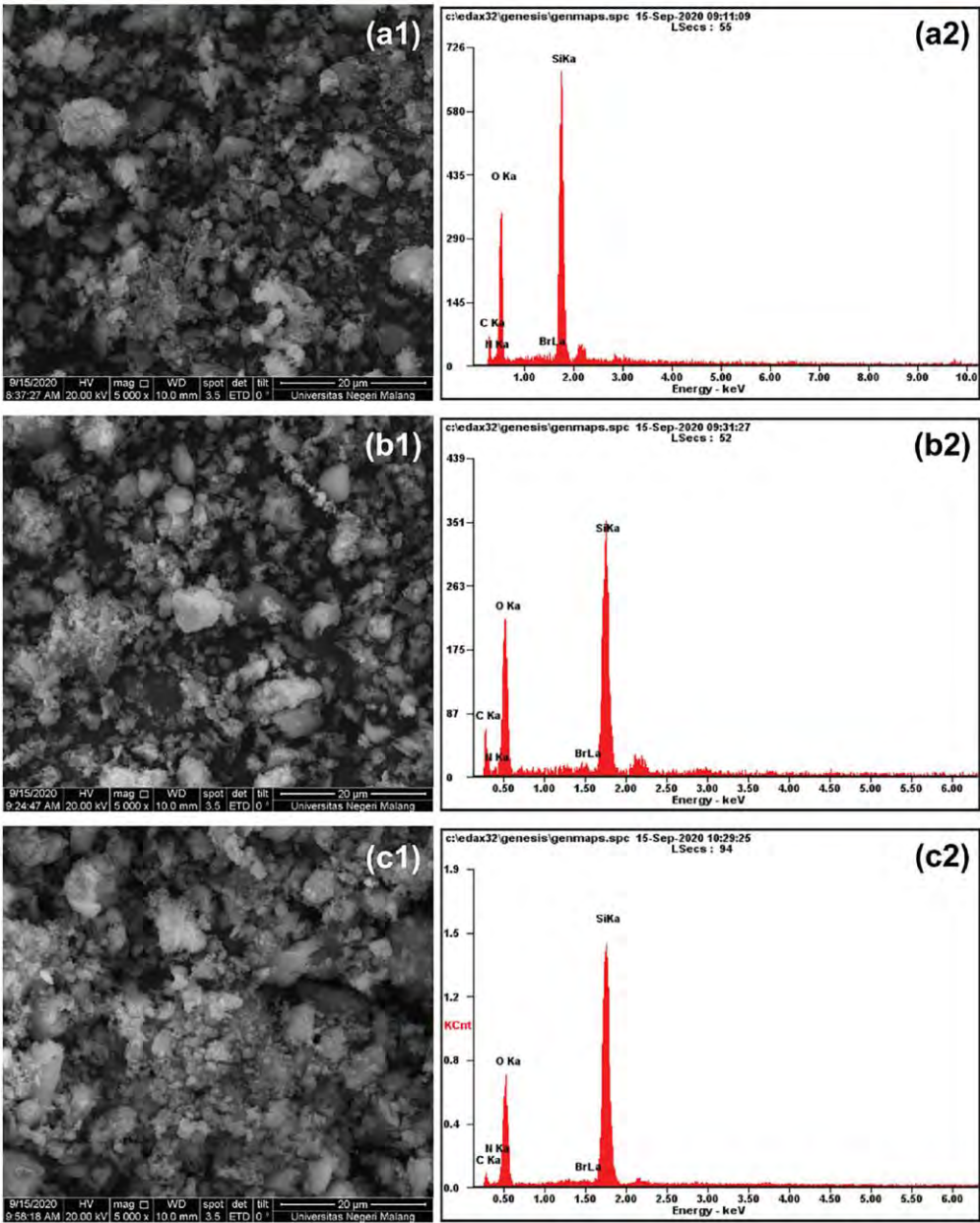


Figure 8. continued

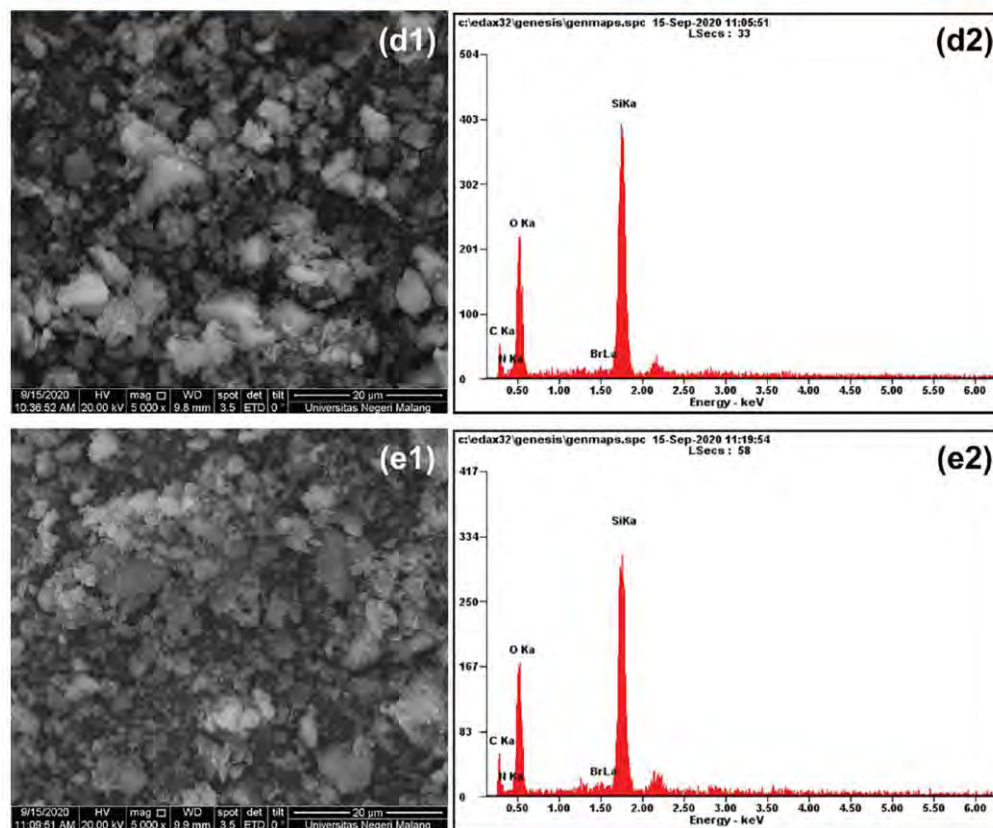


Figure 8. SEM-EDX micrographs and spectra of (a) MS/APTMS and the synthesized slow-release urea: (b) MS/APTMS/U6.74, (c) MS/APTMS/U16.74, (d) MS/APTMS/U26.74, and (e) MS/APTMS/U36.74.

Table 6. Chemical Composition from EDX Analysis of the Synthesized Slow-Release Urea

sample code		C K	N K	O K	Br K	Si K
MS/APTMS	weight (%)	18.68	3.81	51.21	1.20	25.11
	atomic (%)	26.19	4.58	53.92	0.25	15.06
MS/APTMS/U6.74	weight (%)	25.93	4.02	47.91	1.06	21.07
	atomic (%)	34.80	4.63	48.26	0.21	12.09
MS/APTMS/U16.74	weight (%)	14.90	4.63	46.71	0.36	33.40
	atomic (%)	21.82	5.81	51.36	0.08	20.92
MS/APTMS/U26.74	weight (%)	21.51	5.17	47.03	0.83	25.82
	atomic (%)	29.35	6.15	49.00	0.17	15.32
MS/APTMS/U36.74	weight (%)	25.70	6.36	44.66	0.91	22.37
	atomic (%)	34.55	7.33	45.08	0.18	12.86

subsequent days. On the other hand, the highest overflow urea content was found on the third day, with a value of 52.65 ppm, which gradually decreased over the next few days. Subsequently, the performance of the synthesized slow-release urea was also evaluated by measuring the cumulative urea release, as presented in Figure 10b. MS/APTMS/U26.74 shows a linear trend of the cumulative urea release profile, with a total urea release of 124.6 ppm (64.4%) on the last day. In contrast, the commercial urea shows an exponential trend of the cumulative urea release profile, with a value of 184.5 ppm (92.4%) in total. This result indicates that APTMS/U26.74 can release urea more slowly than commercial urea. This can be partially due to the abundance of solid bonding interaction between urea molecules and MS/APTMS as the matrix of this slow-release urea, resulting in a relatively slower release of urea molecules.

To further understand the behavior of urea release, the kinetics of urea release was evaluated using several models, i.e., pseudo-first order (Figure 10c), pseudo-second order (Figure 10d), Higuchi (Figure 10e), and Hixson–Crowell (Figure 10f) models. Complete details of the fitted kinetic parameters and

K

<https://doi.org/10.1021/acs.iecr.2c00424>
Ind. Eng. Chem. Res. XXXX, XXX, XXX–XXX

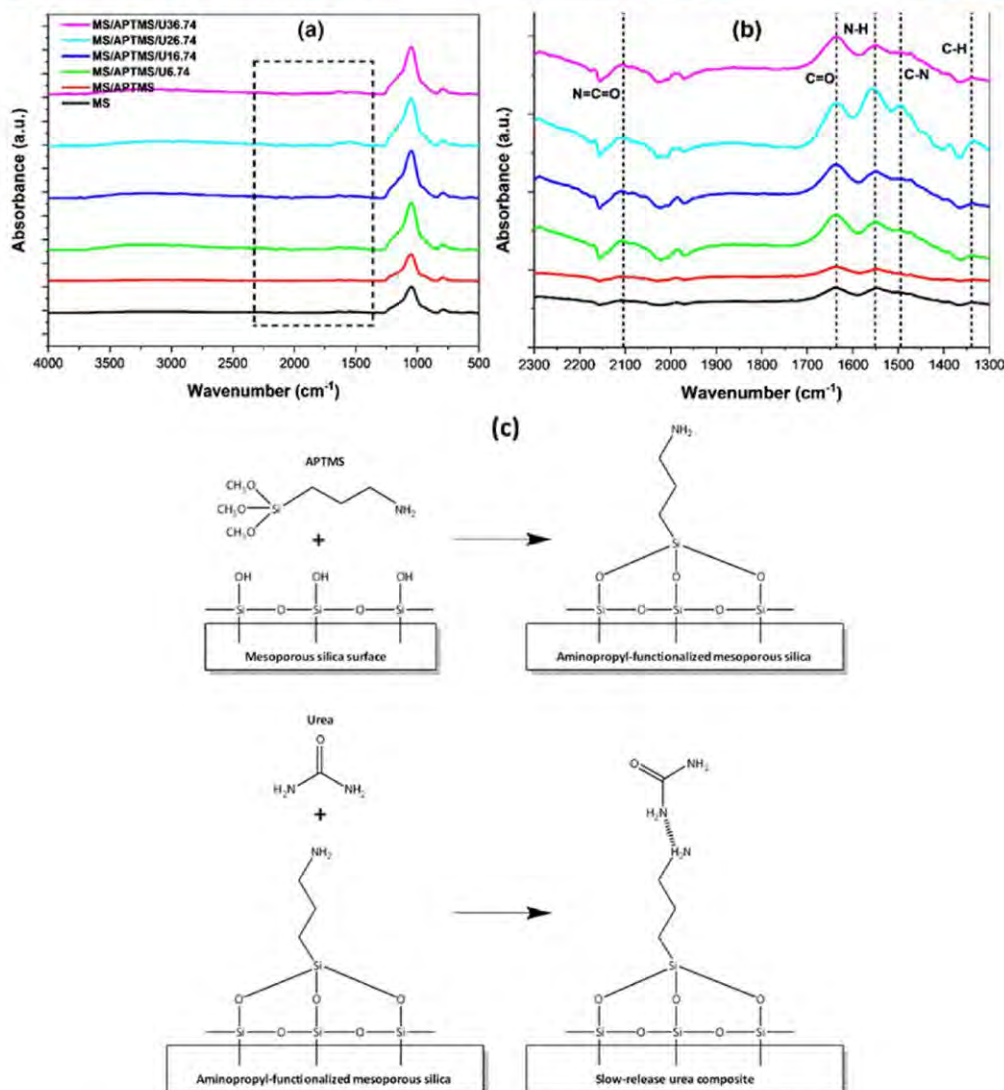


Figure 9. FTIR results of the slow-release urea with different formulations: (a) FTIR results at a wavenumber of 4000–500 cm^{-1} ; (b) further evaluation of FTIR spectra at a wavenumber of 2300–1300 cm^{-1} ; and (c) proposed bond formation mechanisms of aminopropyl and urea groups on the synthesized slow-release urea.

the correlation coefficients are provided in Table 7. The pseudo-first-order model provided a reasonably good fit for commercial urea and MS/APTMS/U26.74, with R^2 values of 0.8528 and 0.8395, respectively. The pseudo-first-order rate kinetic constant values were 0.3502 day^{-1} for commercial urea and 0.2654 day^{-1} for MS/APTMS/U26.74. In addition, the k_1 value of commercial urea was recorded to be higher than that of MS/APTMS/U26.74, indicating that commercial urea has a

higher urea release rate per day than MS/APTMS/U26.74. This result indicates that the modified slow-release urea had a significantly reduced release rate. On the other hand, in this study, the pseudo-second-order kinetic model was seemingly unsuitable for modeling the urea release behavior, which is evident from the low correlation coefficients of only 0.3258 for commercial urea and 0.5703 for MS/APTMS/U26.74. The low value of R^2 indicates that the model is less capable of being

L

<https://doi.org/10.1021/acs.iecr.2c00424>
Ind. Eng. Chem. Res. XXXX, XXX, XXX–XXX

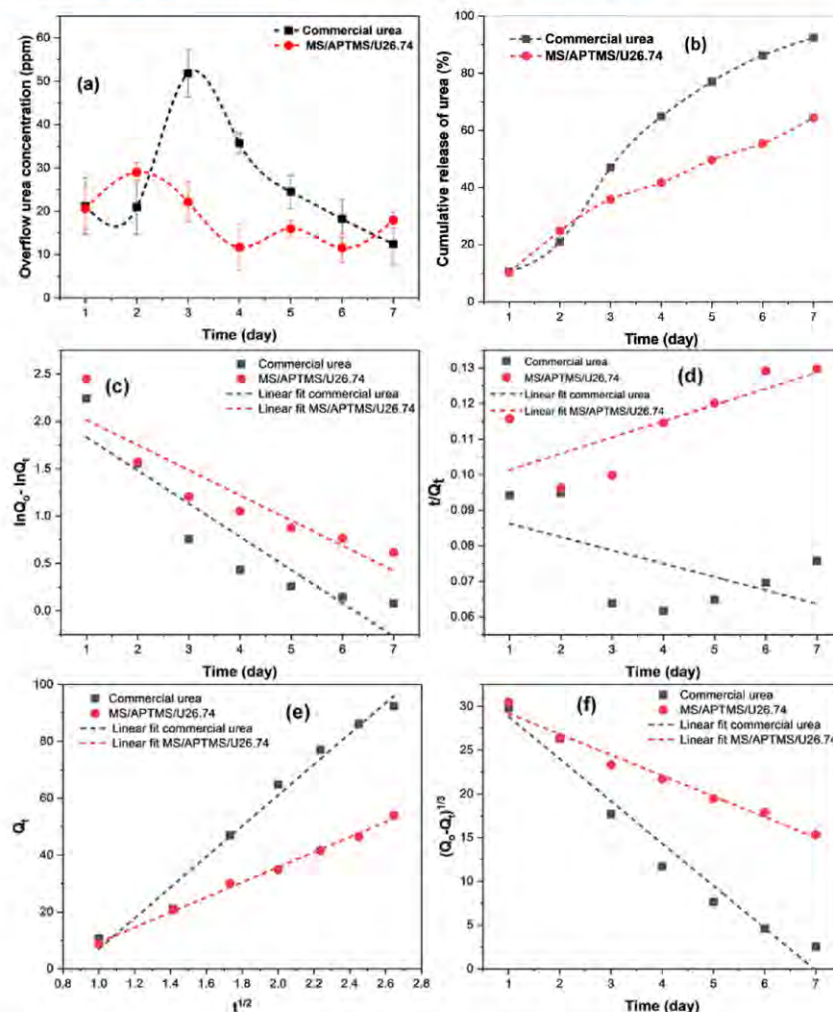


Figure 10. Performance test results of the slow-release urea: (a) result of the measured urea concentration in the overflow liquid and (b) cumulative release of urea from commercial urea and MS/APTMS/U26.74. Curve fittings of the urea release kinetics for commercial urea and MS/APTMS/U26.74 using (c) pseudo-first-order, (d) pseudo-second-order, (e) Higuchi, and (f) Hixson–Crowell models.

Table 7. Model Parameters and Correlation Coefficients of Commercial Urea and MS/APTMS/U26.74 to Evaluate the Urea Release Kinetics Using Pseudo-First-Order, Pseudo-Second-Order, Higuchi, and Hixson–Crowell Models

sample	kinetic models							
	pseudo-first order		pseudo-second order		Higuchi		Hixson–Crowell	
	k_1 (day ⁻¹)	R^2	k_2 (%/day)	R^2	K_H (%/day ^{1/2})	R^2	K_{HC} (% ^{1/3} /day)	R^2
commercial urea	0.3502	0.8528	0.0037	0.3286	54.0668	0.9901	4.8308	0.9617
MS/APTMS/U26.74	0.2654	0.8395	0.0046	0.5703	24.4964	0.9979	2.3678	0.9772

used for data predictions. The Higuchi kinetic model yielded the best fit of urea release among all of the fitted models, with the highest R^2 values of 0.9901 for commercial urea and 0.9979

for MS/APTMS/U26.74. The Higuchi constants were measured to be 54.0668%/day for commercial urea and 24.4964%/day for MS/APTMS/U26.74. The higher Higuchi

M

<https://doi.org/10.1021/acs.iecr.2c00424>
Ind. Eng. Chem. Res. XXXX, XXX, XXX–XXX

constant represents the higher diffusion rate of urea release from the sample.⁶³ Thus, the modification of MS/APTMS as the matrix medium has significantly improved the urea release rate by reducing the diffusivity of urea from the slow-release urea due to solid bonding interaction between the modified mesoporous silica and the urea molecules. The Hixson–Crowell model also showed an excellent urea release fit for both samples, with R^2 values of 0.9617 and 0.9772 and Hixson–Crowell constants of 4.8308 and 2.3678%^{1/3}/day for commercial urea and MS/APTMS/U26.74, respectively. This result suggests that the primary mode of urea release is a diffusion-controlled mechanism,⁶⁷ an indication similar to that of the Higuchi model discussed previously. Based on the studies and results, it can be reasonably suggested that the modification of mesoporous silica with APTMS has a significant impact on reducing the urea release rate by lowering the diffusivity of urea from the slow-release urea. Based on the findings and explanation, it can be reasonably concluded that slow-release urea has been synthesized successfully.

CONCLUSIONS

In this work, a prominent slow-release urea fertilizer was developed with aminopropyl-functionalized mesoporous silica as the matrix to enhance the urea adsorption and slow-release property. It was developed by utilizing geothermal silica as the silica source, CTAB as the surfactant, and APTMS as the surface modification agent. Acid-leaching treatment using H_2SO_4 was conducted to purify the geothermal silica sample and increase the SiO_2 content from 86.30 to 96.00%, which is feasible for mesoporous silica synthesis. The synthesized mesoporous silica was formulated with different mole amounts of CTAB. The mesoporous silica synthesized with the addition of 0.05 mol of CTAB possessed the most desirable properties of a fairly uniform surface micromorphology containing particles with 38.55 wt % silica content, a surface area of 668.849 m^2/g , an adsorption–desorption range of 149.33–353.28 mL/g, and an adsorption pore volume of 0.26 mL/g. All synthesized mesoporous silicas showed a type-IV hysteresis, which corresponds to mesoporous-type materials, signaling the successful development of the mesoporous structure. The DSC results showed that the mesoporous silica becomes more reactive with recorded enthalpies of 69.2175 and -10.0796 J/g at temperatures of 82.3 and 159.5 °C, respectively, due to the addition of CTAB in the synthesis process. TGA thermograms show that the mesoporous silica has very good thermal stability and experienced only 17.61% weight loss at a temperature of up to 124 °C. These findings suggest the excellent potential of the synthesized mesoporous silica as a promising matrix material. Further, the functionalization of the aminopropyl group to the mesoporous silica using APTMS was performed. SEM results showed that the functionalization process and the adsorption of urea to the mesoporous silica resulted in no significant changes in the morphology of mesoporous silica. Meanwhile, significant changes were observed in the chemical functional groups generated after APTMS functionalization, resulting in some new groups including C=O, N–H, and C–N. From the FTIR spectra, MS/APTMS/U26.74 was observed to have a relatively higher intensity of C=O, N–H, C–N, and C–H groups among other samples, suggesting the higher content of the respective groups in MS/APTMS/U26.74. A comparative experiment and the kinetic study regarding the release property and kinetics between MS/APTMS/U26.74 as the best slow-release urea and commercial urea was conducted.

The cumulative urea release during 7 days of observation was 184.5 ppm (92.4%) for commercial urea and 124.6 ppm (64.6%) for MS/APTMS/U26.74. The abundance of strong bonding interaction between urea molecules and MS/APTMS as the matrix led to a relatively slower release of urea molecules. The Higuchi kinetic model yielded the best fit among the other models to predict the release kinetics of MS/APTMS/U26.74 with an R^2 value of 0.9979 and a Higuchi constant of 24.4964%/day^{1/2}. The Higuchi constant of MS/APTMS/U26.74 was smaller than that of commercial urea (54.0668%/day), indicating that the synthesized slow-release urea has a lower urea diffusivity out of the sample, thus resulting in a slower and controllable urea release. Finally, MS/APTMS/U26.74 synthesized by utilizing geothermal silica, CTAB, and APTMS can be noted to have a potential composition for slow-release urea fertilizers to enhance the usage efficiency of urea.

AUTHOR INFORMATION

Corresponding Author

S. Silviana – Department of Chemical Engineering, Faculty of Engineering, Diponegoro University, Semarang 50275, Indonesia; orcid.org/0000-0002-8831-0147; Email: silviana@che.undip.ac.id

Authors

Atikah A. Janitra – Department of Chemical Engineering, Faculty of Engineering, Diponegoro University, Semarang 50275, Indonesia

Afriza N. Sa'adah – Department of Chemical Engineering, Faculty of Engineering, Diponegoro University, Semarang 50275, Indonesia

Febio Dalanta – Department of Chemical Engineering, Faculty of Engineering, Diponegoro University, Semarang 50275, Indonesia

Complete contact information is available at:
<https://pubs.acs.org/10.1021/acs.iecr.2c00424>

Author Contributions

S.S.: Conceptualization, methodology, supervision, funding acquisition, resources, and writing—original draft; A.A.J.: Methodology, investigation, and writing—original draft. A.N.S.: Project administration, software, and formal analysis. F.D.: Data curation, software, visualization, formal analysis, and writing—review and editing.

Funding

This project was financially supported by the Ministry of Education, Culture, Research and Technology of the Republic of Indonesia through grant No. 225-S4/UN7.6.1/PP/2020.

Notes

The authors declare no competing financial interest.

ACKNOWLEDGMENTS

The authors are grateful to the community of Advanced Material Laboratory (AMaL) of Diponegoro University for all their support and discussion throughout the research.

ABBREVIATIONS

SRU	slow-release urea
MS	mesoporous silica
CTAB	cetyltrimethylammonium bromide
APTMS	(3-aminopropyl)trimethoxysilane

N

<https://doi.org/10.1021/acs.iecr.2c00424>
Ind. Eng. Chem. Res. XXXX, XXX, XXX–XXX

SEM	scanning electron microscopy
XRF	X-ray fluorescence
XRD	X-ray diffraction
FTIR	Fourier transform infrared
BET–BJH	Brunauer–Emmett–Teller and Barrett–Joyner–Halenda
TGA	thermogravimetric analysis
DSC	differential scanning calorimetry
HCl	hydrochloric acid
U6.74	urea 6.74 wt %
U16.74	urea 16.74 wt %
U26.74	urea 26.74 wt %
U36.74	urea 36.74 wt %

REFERENCES

- (1) Kay-Shoemaker, J. L.; Watwood, M. E.; Kilpatrick, L.; Harris, K. Exchangeable Ammonium and Nitrate from Different Nitrogen Fertilizer Preparations in Polyacrylamide-Treated and Untreated Agricultural Soils. *Biol. Fertil. Soils* **2000**, *31*, 245–248.
- (2) Saha, B. K.; Rose, M. T.; Wong, V.; Cavagnaro, T. R.; Patti, A. F. Hybrid Brown Coal-Urea Fertiliser Reduces Nitrogen Loss Compared to Urea Alone. *Sci. Total Environ.* **2017**, *601–602*, 1496–1504.
- (3) Getahun, D.; Alemneh, T.; Akebergn, D.; Getabalew, M.; Zewdie, D. Urea Metabolism and Recycling in Ruminants. *Biomed. J. Sci. Tech. Res.* **2019**, *20*, 14790–14796.
- (4) Hailemariam, S.; Zhao, S.; He, Y.; Wang, J. Urea Transport and Hydrolysis in the Rumen: A Review. *Anim. Nutr.* **2021**, *7*, 989–996.
- (5) Mehta, R.; Brahmabhatt, H.; Saha, N. K.; Bhattacharya, A. Removal of Substituted Phenyl Urea Pesticides by Reverse Osmosis Membranes: Laboratory Scale Study for Field Water Application. *Desalination* **2015**, *358*, 69–75.
- (6) Berrada, H.; Font, G.; Moltó, J. C. Determination of Urea Pesticide Residues in Vegetable, Soil, and Water Samples. *Crit. Rev. Anal. Chem.* **2003**, *33*, 19–41.
- (7) Sasmal, S.; Roy Chowdhury, S.; Podder, D.; Haldar, D. Urea-Appended Amino Acid To Vitalize Yeast Growth, Enhance Fermentation, and Promote Ethanol Production. *ACS Omega* **2019**, *4*, 13172–13179.
- (8) Santos, A. S.; Ferreira, L. M. M.; Martin-Rosset, W.; Cotovio, M.; Silva, F.; Bennett, R. N.; Cone, J. W.; Bessa, R. J. B.; Rodrigues, M. A. M. The Influence of Casein and Urea as Nitrogen Sources on in Vitro Equine Caecal Fermentation. *Animal* **2012**, *6*, 1096–1102.
- (9) Li, Y.; Huang, L.; Zhang, H.; Wang, M.; Liang, Z. Assessment of Ammonia Volatilization Losses and Nitrogen Utilization during the Rice Growing Season in Alkaline Salt-Affected Soils. *Sustainability* **2017**, *9*, No. 132.
- (10) Azeem, B.; KuShaari, K.; Man, Z. B.; Basit, A.; Thanh, T. H. Review on Materials & Methods to Produce Controlled Release Coated Urea Fertilizer. *J. Controlled Release* **2014**, *181*, 11–21.
- (11) Jie, C.; Jing-zhang, C.; Man-zhi, T.; Zi-tong, G. Soil Degradation: A Global Problem Endangering Sustainable Development. *J. Geogr. Sci.* **2002**, *12*, 243–252.
- (12) Liu, L.; Kost, J.; Fishman, M. L.; Hicks, K. B. A Review: Controlled Release Systems for Agricultural and Food Applications; American Chemical Society, 2008; pp 265–281.
- (13) Espézie Bueno, S. C.; Filho, M. B.; de Almeida, P. S. G.; Polidoro, J. C.; Olivares, F. L.; Sthel, M. S.; Vargas, H.; Mota, L.; da Silva, M. G. Cuban Zeolite as Ammonium Carrier in Urea-Based Fertilizer Pellets: Photoacoustic-Based Sensor for Monitoring N-Ammonia Losses by Volatilization in Aqueous Solutions. *Sens. Actuators, B* **2015**, *212*, 35–40.
- (14) Mihok, F.; Macko, J.; Oriňák, A.; Oriňáková, R.; Kovář, K.; Sisáková, K.; Petruš, O.; Kostecká, Z. Controlled Nitrogen Release Fertilizer Based on Zeolite Clinoptilolite: Study of Preparation Process and Release Properties Using Molecular Dynamics. *Curr. Res. Green Sustainable Chem.* **2020**, *3*, No. 100030.
- (15) Maghsoodi, M. R.; Najafi, N.; Reyhanitabar, A.; Oustan, S. Hydroxyapatite Nanorods, Hydrochar, Biochar, and Zeolite for Controlled-Release Urea Fertilizers. *Geoderma* **2020**, *379*, No. 114644.
- (16) Pereira, E. I.; da Cruz, C. C. T.; Solomon, A.; Le, A.; Cavigelli, M. A.; Ribeiro, C. Novel Slow-Release Nanocomposite Nitrogen Fertilizers: The Impact of Polymers on Nanocomposite Properties and Function. *Ind. Eng. Chem. Res.* **2015**, *54*, 3717–3725.
- (17) Yamamoto, C. F.; Pereira, E. I.; Mattoso, L. H. C.; Matsunaka, T.; Ribeiro, C. Slow Release Fertilizers Based on Urea/Urea-Formaldehyde Polymer Nanocomposites. *Chem. Eng. J.* **2016**, *287*, 390–397.
- (18) Shen, Y.; Zhou, J.; Du, C.; Zhou, Z. Hydrophobic Modification of Waterborne Polymer Slows Urea Release and Improves Nitrogen Use Efficiency in Rice. *Sci. Total Environ.* **2021**, *794*, No. 148612.
- (19) Bortolin, A.; Aouada, F. A.; de Moura, M. R.; Ribeiro, C.; Longo, E.; Mattoso, L. H. C. Application of Polysaccharide Hydrogels in Adsorption and Controlled-Extended Release of Fertilizers Processes. *J. Appl. Polym. Sci.* **2012**, *123*, 2291–2298.
- (20) Li, L.; Sun, Y.; Cao, B.; Song, H.; Xiao, Q.; Yi, W. Preparation and Performance of Polyurethane/Mesoporous Silica Composites for Coated Urea. *Mater. Des.* **2016**, *99*, 21–25.
- (21) de Silva, M.; Siriwardena, D. P.; Sandaruwan, C.; Priyadarshana, G.; Karunaratne, V.; Kottegoda, N. Urea-Silica Nanohybrids with Potential Applications for Slow and Precise Release of Nitrogen. *Mater. Lett.* **2020**, *272*, No. 127839.
- (22) Elhassani, C. E.; Essamlali, Y.; Aqlil, M.; Nzenguet, A. M.; Ganetri, I.; Zahouily, M. Urea-Impregnated HAP Encapsulated by Lignocellulosic Biomass-Extruded Composites: A Novel Slow-Release Fertilizer. *Environ. Technol. Innovation* **2019**, *15*, No. 100403.
- (23) Vanichvattanadecha, C.; Singhapong, W.; Jaroenworaduck, A. Different Sources of Silicon Precursors Influencing on Surface Characteristics and Pore Morphologies of Mesoporous Silica Nanoparticles. *Appl. Surf. Sci.* **2020**, *513*, No. 145568.
- (24) Yang, Y.; Wang, J.; Qian, X.; Shan, Y.; Zhang, H. Aminopropyl-Functionalized Mesoporous Carbon (APTMS-CMK-3) as Effective Phosphate Adsorbent. *Appl. Surf. Sci.* **2018**, *427*, 206–214.
- (25) Ghobashy, M. M.; Mousaa, I. M.; El-Sayyad, G. S. Radiation Synthesis of Urea/Hydrogel Core Shells Coated with Three Different Natural Oils via a Layer-by-Layer Approach: An Investigation of Their Slow Release and Effects on Plant Growth-Promoting Rhizobacteria. *Prog. Org. Coat.* **2021**, *151*, No. 106022.
- (26) Guo, M.; Liu, M.; Zhan, F.; Wu, L. Preparation and Properties of a Slow-Release Membrane-Encapsulated Urea Fertilizer with Superabsorbent and Moisture Preservation. *Ind. Eng. Chem. Res.* **2005**, *44*, 4206–4211.
- (27) Abdelghany, A. M.; Meikhal, M. S.; Asker, N. Synthesis and Structural-Biological Correlation of PVC/PVAc Polymer Blends. *J. Mater. Res. Technol.* **2019**, *8*, 3908–3916.
- (28) Cui, Y.; Xiang, Y.; Xu, Y.; Wei, J.; Zhang, Z.; Li, L.; Li, J. Poly-Acrylic Acid Grafted Natural Rubber for Multi-Coated Slow Release Compound Fertilizer: Preparation, Properties and Slow-Release Characteristics. *Int. J. Biol. Macromol.* **2020**, *146*, 540–548.
- (29) dos Santos, A. C. S.; Henrique, H. M.; Cardoso, V. L.; Reis, M. H. M. Slow Release Fertilizer Prepared with Lignin and Poly(Vinyl Acetate) Bioblend. *Int. J. Biol. Macromol.* **2021**, *185*, 543–550.
- (30) Liu, J.; Yang, Y.; Gao, B.; Li, Y. C.; Xie, J. Bio-Based Elastic Polyurethane for Controlled-Release Urea Fertilizer: Fabrication, Properties, Swelling and Nitrogen Release Characteristics. *J. Cleaner Prod.* **2019**, *209*, 528–537.
- (31) Ni, B.; Liu, M.; Lü, S.; Xie, L.; Wang, Y. Multifunctional Slow-Release Organic–Inorganic Compound Fertilizer. *J. Agric. Food Chem.* **2010**, *58*, 12373–12378.
- (32) Ni, B.; Liu, M.; Lü, S.; Xie, L.; Wang, Y. Environmentally Friendly Slow-Release Nitrogen Fertilizer. *J. Agric. Food Chem.* **2011**, *59*, 10169–10175.
- (33) Pang, L.; Gao, Z.; Zhang, S.; Li, Y.; Hu, S.; Ren, X. Preparation and Anti-UV Property of Modified Cellulose Membranes for

O

<https://doi.org/10.1021/acs.iecr.2c00424>
Ind. Eng. Chem. Res. XXXX, XXX, XXX–XXX

- Biopesticides Controlled Release. *Ind. Crops Prod.* **2016**, *89*, 176–181.
- (34) Sathisaran, I.; Balasubramanian, M. Physical Characterization of Chitosan/Gelatin-Alginate Composite Beads for Controlled Release of Urea. *Heliyon* **2020**, *6*, No. e05495.
- (35) Shan, L.; Gao, Y.; Zhang, Y.; Yu, W.; Yang, Y.; Shen, S.; Zhang, S.; Zhu, L.; Xu, L.; Tian, B.; Yun, J. Fabrication and Use of Alginate-Based Cryogel Delivery Beads Loaded with Urea and Phosphates as Potential Carriers for Bioremediation. *Ind. Eng. Chem. Res.* **2016**, *55*, 7655–7660.
- (36) Wang, Y.; Liu, M.; Ni, B.; Xie, L. κ -Carrageenan–Sodium Alginate Beads and Superabsorbent Coated Nitrogen Fertilizer with Slow-Release, Water-Retention, and Anticompaction Properties. *Ind. Eng. Chem. Res.* **2012**, *51*, 1413–1422.
- (37) Qiao, D.; Liu, H.; Yu, L.; Bao, X.; Simon, G. P.; Petinakis, E.; Chen, L. Preparation and Characterization of Slow-Release Fertilizer Encapsulated by Starch-Based Superabsorbent Polymer. *Carbohydr. Polym.* **2016**, *147*, 146–154.
- (38) Wanyika, H.; Gatebe, E.; Kioni, P.; Tang, Z.; Gao, Y. Mesoporous Silica Nanoparticles Carrier for Urea: Potential Applications in Agrochemical Delivery Systems. *J. Nanosci. Nanotechnol.* **2012**, *12*, 2221–2228.
- (39) He, H.; Xiao, H.; Kuang, H.; Xie, Z.; Chen, X.; Jing, X.; Huang, Y. Synthesis of Mesoporous Silica Nanoparticle–Oxaliplatin Conjugates for Improved Anticancer Drug Delivery. *Colloids Surf., B* **2014**, *117*, 75–81.
- (40) Yan, E.; Ding, Y.; Chen, C.; Li, R.; Hu, Y.; Jiang, X. Polymer/Silica Hybrid Hollow Nanospheres with PH-Sensitive Drug Release in Physiological and Intracellular Environments. *Chem. Commun.* **2009**, *19*, 2718.
- (41) Yang, D.; Fan, R.; Luo, F.; Chen, Z.; Gerson, A. R. Facile and Green Fabrication of Efficient Au Nanoparticles Catalysts Using Plant Extract via a Mesoporous Silica-Assisted Strategy. *Colloids Surf., A* **2021**, *621*, No. 126580.
- (42) Yin, F.; Xu, F.; Zhang, K.; Yuan, M.; Cao, H.; Ye, T.; Wu, X.; Xu, F. Synthesis and Evaluation of Mesoporous Silica/Mesoporous Molecularly Imprinted Nanoparticles as Adsorbents for Detection and Selective Removal of Imidacloprid in Food Samples. *Food Chem.* **2021**, *364*, No. 130216.
- (43) Huang, R.; Shen, Y.-W.; Guan, Y.-Y.; Jiang, Y.-X.; Wu, Y.; Rahman, K.; Zhang, L.-J.; Liu, H.-J.; Luan, X. Mesoporous Silica Nanoparticles: Facile Surface Functionalization and Versatile Biomedical Applications in Oncology. *Acta Biomater.* **2020**, *116*, 1–15.
- (44) Kaya, S.; Cresswell, M.; Boccacini, A. R. Mesoporous Silica-Based Bioactive Glasses for Antibiotic-Free Antibacterial Applications. *Mater. Sci. Eng., C* **2018**, *83*, 99–107.
- (45) dos Santos, S. M. L.; Nogueira, K. A. B.; de Souza Gama, M.; Lima, J. D. F.; da Silva Júnior, I. J.; de Azevedo, D. C. S. Synthesis and Characterization of Ordered Mesoporous Silica (SBA-15 and SBA-16) for Adsorption of Biomolecules. *Microporous Mesoporous Mater.* **2013**, *180*, 284–292.
- (46) Policicchio, A.; Conte, G.; Stelitano, S.; Bonaventura, C. P.; Putz, A.-M.; Ianiš, C.; Almásy, L.; Horváth, Z. E.; Agostino, R. G. Hydrogen Storage Performances for Mesoporous Silica Synthesized with Mixed Tetraethoxysilane and Methyltriethoxysilane Precursors in Acidic Condition. *Colloids Surf., A* **2020**, *601*, No. 125040.
- (47) Gil-Ortiz, R.; Naranjo, M. Á.; Ruiz-Navarro, A.; Caballero-Molada, M.; Atares, S.; García, C.; Vicente, O. New Eco-Friendly Polymeric-Coated Urea Fertilizers Enhanced Crop Yield in Wheat. *Agronomy* **2020**, *10*, No. 438.
- (48) Cheah, W.-K.; Sim, Y.-L.; Yeoh, F.-Y. Amine-Functionalized Mesoporous Silica for Urea Adsorption. *Mater. Chem. Phys.* **2016**, *175*, 151–157.
- (49) Luechinger, M.; Prins, R.; Rimgruber, G. D. Functionalization of Silica Surfaces with Mixtures of 3-Aminopropyl and Methyl Groups. *Microporous Mesoporous Mater.* **2005**, *85*, 111–118.
- (50) Hicks, J. C.; Dabestani, R.; Buchanan, A. C.; Jones, C. W. Assessing Site-Isolation of Amine Groups on Aminopropyl-Functionalized SBA-15 Silica Materials via Spectroscopic and Reactivity Probes. *Inorg. Chim. Acta* **2008**, *361*, 3024–3032.
- (51) Burkett, S. L.; Sims, S. D.; Mann, S. Synthesis of Hybrid Inorganic–Organic Mesoporous Silica by Co-Condensation of Siloxane and Organosiloxane Precursors. *Chem. Commun.* **1996**, *11*, 1367–1368.
- (52) Purnomo, A.; Dalanta, F.; Oktaviani, A. D.; Silviana, S. Superhydrophobic Coatings and Self-Cleaning through the Use of Geothermal Scaling Silica in Improvement of Material Resistance. *AIP Conf. Proc.* **2018**, No. 020077.
- (53) Silviana, S.; Darmawan, A.; Subagio, A.; Dalanta, F. Statistical Approaching for Superhydrophobic Coating Preparation Using Silica Derived from Geothermal Solid Waste. *ASEAN J. Chem. Eng.* **2020**, *19*, 91.
- (54) Silviana, S.; Darmawan, A.; Dalanta, F.; Subagio, A.; Hermawan, F.; Milen Santoso, H. Superhydrophobic Coating Derived from Geothermal Silica to Enhance Material Durability of Bamboo Using Hexadimethylsilazane (HMDS) and Trimethylchlorosilane (TMCS). *Materials* **2021**, *14*, No. 530.
- (55) Silviana, S.; Ma'ruf, A. Silicon Preparation Derived from Geothermal Silica by Reduction Using Magnesium. *Int. J. Emerging Trends Eng. Res.* **2020**, *8*, 4861–4866.
- (56) Silviana, S.; Sanyoto, G. J.; Darmawan, A. Preparation of Geothermal Silica Glass Coating Film Through Multi-Factor Optimization. *J. Teknol.* **2021**, *83*, 41–49.
- (57) Tut Hahldir, F. S.; Sengün, R.; Aydın, H. Characterization and Comparison of Geothermal Fluids Geochemistry within the Kızıldere Geothermal Field in Turkey: New Findings with Power Capacity Expanding Studies. *Geothermics* **2021**, *94*, No. 102110.
- (58) Silviana, S.; Anggoro, D. D.; Salsabila, C. A.; Aprilio, K. Utilization of Geothermal Waste as a Silica Adsorbent for Biodiesel Purification. *Korean J. Chem. Eng.* **2021**, *38*, 2091–2105.
- (59) Silviana, S.; Bayu, W. J. Silicon Conversion From Bamboo Leaf Silica By Magnesiothermic Reduction for Development of Li-Ion Battery Anode. *MATEC Web Conf.* **2018**, *156*, No. 05021.
- (60) Silviana, S.; Purbasari, A.; Siregar, A.; Rochyati, A. F.; Papra, T. Synthesis of Mesoporous Silica Derived from Geothermal Waste with Cetyl Trimethyl Ammonium Bromide (CTAB) Surfactant as Drug Delivery Carrier. *AIP Conf. Proc.* **2020**, *2296*, No. 020083.
- (61) Silviana, S.; Sagala, E. A. P. P.; Sari, S. E.; Siagian, C. T. M. Preparation of Mesoporous Silica Derived from Geothermal Silica as Precursor with a Surfactant of Cetyltrimethylammonium Bromide. *AIP Conf. Proc.* **2019**, No. 020070.
- (62) Silviana, S.; Sanyoto, G. J.; Darmawan, A.; Sutanto, H. Geothermal Silica Waste as Sustainable Amorphous Silica Source for the Synthesis of Silica Xerogels. *Rasayan J. Chem.* **2020**, *13*, 1692–1700.
- (63) Shoaib, M. H.; Tazeen, J.; Merchant, H. A.; Yousuf, R. I. Evaluation of drug release kinetics from ibuprofen matrix tablets using HPMC. *Pak. J. Pharm. Sci.* **2006**, *19* (2), 119–124.
- (64) Bullen, J. C.; Saleesongsom, S.; Gallagher, K.; Weiss, D. J. A Revised Pseudo-Second-Order Kinetic Model for Adsorption, Sensitive to Changes in Adsorbate and Adsorbent Concentrations. *Langmuir* **2021**, *37* (10), 3189–3201. <https://doi.org/10.1021/acs.langmuir.1c00142>.
- (65) Dash, S.; Murthy, P. N.; Nath, L.; Chowdhury, P. Kinetic modeling on drug release from controlled drug delivery systems. *Acta Pol. Pharm. - Drug Res.* **2010**, *67* (3), 217–223.
- (66) Che Ismail, N. H.; Ahmad Bakhtiar, N. S. A.; Md Akil, H. Effects of Cetyltrimethylammonium Bromide (CTAB) on the Structural Characteristic of Non-Expandable Muscovite. *Mater. Chem. Phys.* **2017**, *196*, 324–332.
- (67) Khoeini, M.; Najafi, A.; Rastegar, H.; Amani, M. Improvement of Hollow Mesoporous Silica Nanoparticles Synthesis by Hard-Templating Method via CTAB Surfactant. *Ceram. Int.* **2019**, *45*, 12700–12707.

(68) Silviana, S.; Darmawan, A.; Janitra, A. A.; Ma'ruf, A.; Triesty, I. Synthesized Silica Mesoporous from Silica Geothermal Assisted with CTAB and Modified by APTMS. *Int. J. Emerg. Trends Eng. Res.* 2020, 8 (8), 4854–4860. <https://doi.org/10.30534/ijeter/2020/125882020>.

O

<https://doi.org/10.1021/acs.iecr.2c00424>
Ind. Eng. Chem. Res. XXXX, XXX, XXX–XXX

Decision on Manuscript (31 Mei 2022)

9/2/22, 12:26 PM

Department of Chemical Engineering, Diponegoro University Mail - Decision on Manuscript ID ie-2022-004247 R2



Silviana Silviana <silviana@che.undip.ac.id>

Decision on Manuscript ID ie-2022-004247.R2

Industrial & Engineering Chemistry Research <onbehalf@manuscriptcentral.com> Tue, May 31, 2022 at 10:56 PM

Reply-To: nenoff-office@iecr.acs.org

To: silviana@che.undip.ac.id

31-May-2022

Journal: Industrial & Engineering Chemistry Research

Manuscript ID: ie-2022-004247.R2

Title: "Synthesis of aminopropyl-functionalized mesoporous silica derived from geothermal silica for effective slow-release urea carrier"

Authors: Silviana, S.; Janitra, Atikah; Sa'adah, Afriza; Dalanta, Febio

Manuscript Status: Accept

Dear Dr. Silviana:

We are pleased to inform you that your manuscript has been accepted for publication in Industrial & Engineering Chemistry Research.

You will soon receive an email invitation from the ACS Journal Publishing Staff that contains a link to the online Journal Publishing Agreement. Please sign and submit the journal publishing agreement within 48 hours.

Your manuscript has been forwarded to the ACS Publications office. You will be contacted in the near future by the ACS Journal Publishing Staff regarding the proofs for your manuscript.

After you approve your proofs, your manuscript will be published on the Web in approximately 48 hours. In view of this fast publication time, it is important to review your proofs carefully. Once a manuscript appears on the Web it is considered published. Any change to the manuscript once it appears on the Web will need to be submitted to the journal office as additions or corrections.

Once your paper is published, you can track downloads and citations of your work by logging into the ACS Publishing Center (<https://pubs.acs.org/publish/dashboard>) and selecting "Published".

Sincerely,

Dr. Tina M. Nenoff
Associate Editor
Industrial & Engineering Chemistry Research
Sandia National Laboratories
Phone: 919-967-7730
Email: nenoff-office@iecr.acs.org

PLEASE NOTE: This email message, including any attachments, contains confidential information related to peer review and is intended solely for the personal use of the recipient(s) named above. No part of this communication or any related attachments may be shared with or disclosed to any third party or organization without the explicit prior written consent of the journal Editor and ACS. If the reader of this message is not the intended recipient or is not responsible for delivering it to the intended recipient, you have received this communication in error. Please notify the sender immediately by e-mail, and delete the original message.

As an author or reviewer for ACS Publications, we may send you communications about related journals, topics or products and services from the American Chemical Society. Please email us at pubs-comms-unsub@acs.org if you do not want to receive these. Note, you will still receive updates about your manuscripts, reviews, or future invitations to review.

Thank you.

<https://mail.google.com/mail/u/0/?ik=ae189121fa&view=pt&search=all&permmsgid=msg-f%3A1734357901404356206&simpl=msg-f%3A1734357...> 1/1